AD-A112 669 LINCOM CORP PASADENA CA F/G 17/2.1
PHASE NOISE STUDY, ATTACHMENT II,(U)
OCT 81 R A MAAG, F DAVARIAN N00014-81-C-2338
UNCLASSIFIED TR-1082-0881 NL

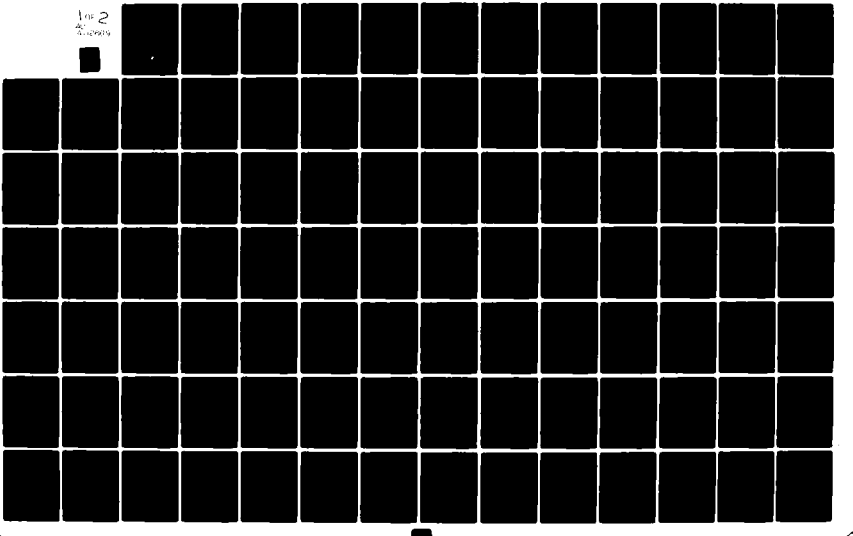

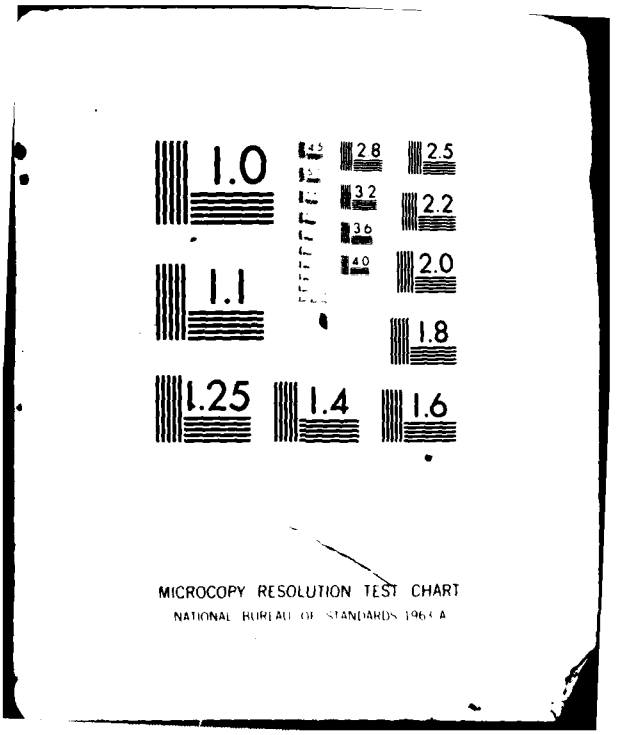
1.0
2.8
2.5
3.2
2.2
3.6
4.0
2.0
1.1
1.8
1.25
1.4
1.6
MICROCOPY RESOLUTION TEST CHART
NATIONAL BUREAU OF STANDARDS 1963 A

(12)

AD A112669

DTIC FILE COPY

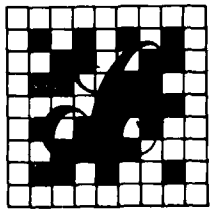

LinCom Corporation
P.O. Box 2793D, Pasadena, Calif 91105

ATTACHMENT II

PHASE NOISE STUDY

PREPARED FOR

NAVAL RESEARCH LABORATORY
WASHINGTON, D.C. 20375

TECHNICAL MONITOR: MR. LEN HEARTON

CONTRACT NO. N00014-81-C-2338, TASK 2

PROGRAM DIRECTOR:

R. A. MAAG

PREPARED BY

R. A MAAG
F. DAVARIAN

LINCOM CORPORATION
P.O. BOX 2793D
PASADENA, CA 91105

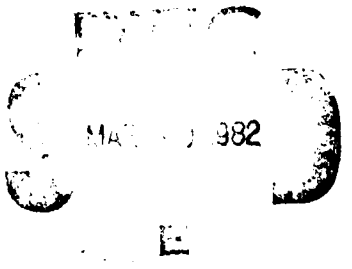

OCTOBER, 1981

TR-1082-0881

TABLE OF CONTENTS

LIST OF FIGURES

LIST OF FIGURES (Continued)

1. Overview of the Phase Noise Study

LinCom has investigated the phase noise requirements of a tracking system receiver when N data links occupy a contiguous system bandwidth and are used to, in addition to transferring data, obtain time transfer between (N/2) platforms. The basic concept of time transfer was investigated under N00014-82-C-2035. In this research effort, the total system phase noise to achieve the required tracking accuracy was investigated. The noise sources which contribute to phase noise are:

- Filter ISI
  - Ideal Filtering
  - Filter Implementation
- Thermal Noise
- Adjacent Channel Interference
- IF Oscillator Instabilities
- Coherent Demodulation VCO
- Data Spectrum Occupancy in the Tracking Bandwidth
- Doppler

The two basic RF receiving system configurations which were studied are shown in Fiugres 1a and 1b. The basic concept of RF filter imperfections is illustrated in Figure 2 and has been defined as asymmetrical filtering. The basic baseband configuration to track the data zero crossing is shown in Figure 3.

Given the above receiving system configuration, the data and time transfer characteristics were investigated for both NRZ and Manchester encoding. A discussion of the overall advantages and disadvantages of these two encoding techniques as well as the advantages of linear vs biphase demodulation are discussed in another document. The effects of adjacent channel interference is shown in Figure 4.

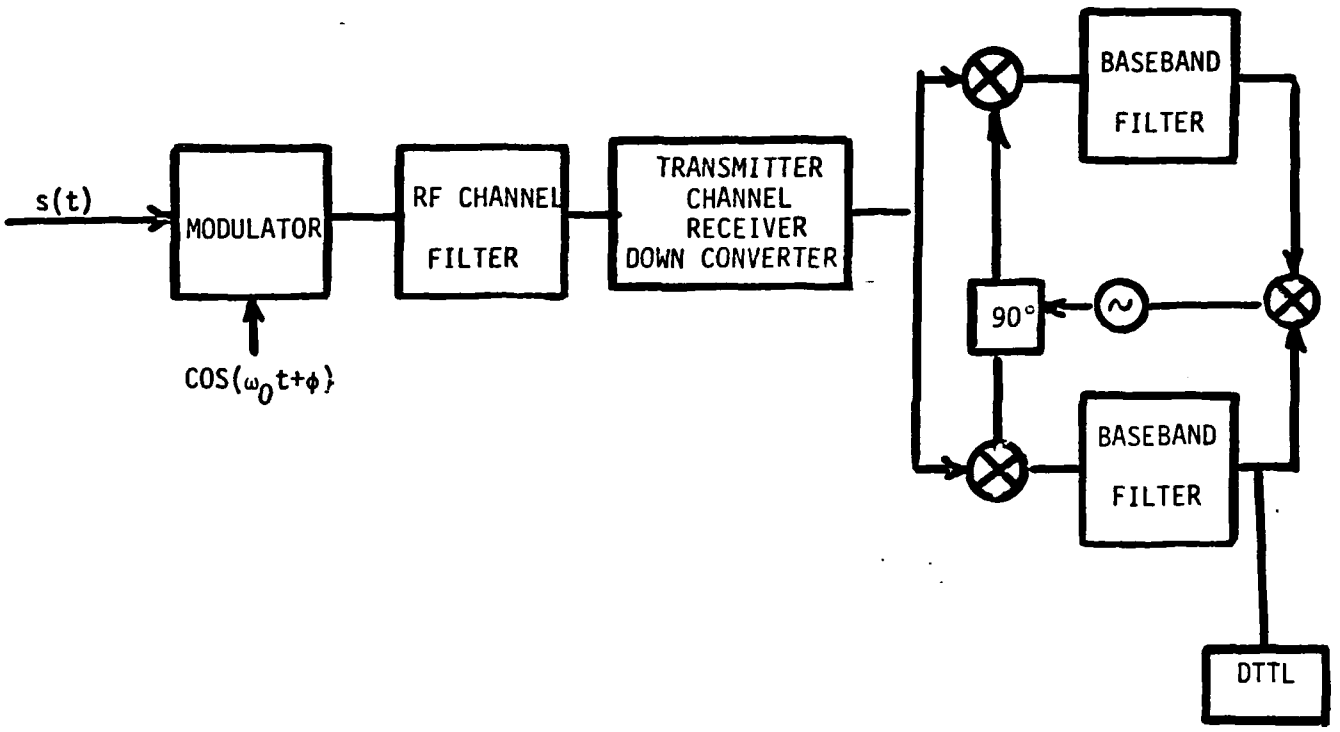

Figure 1a. Costas Demodulation.

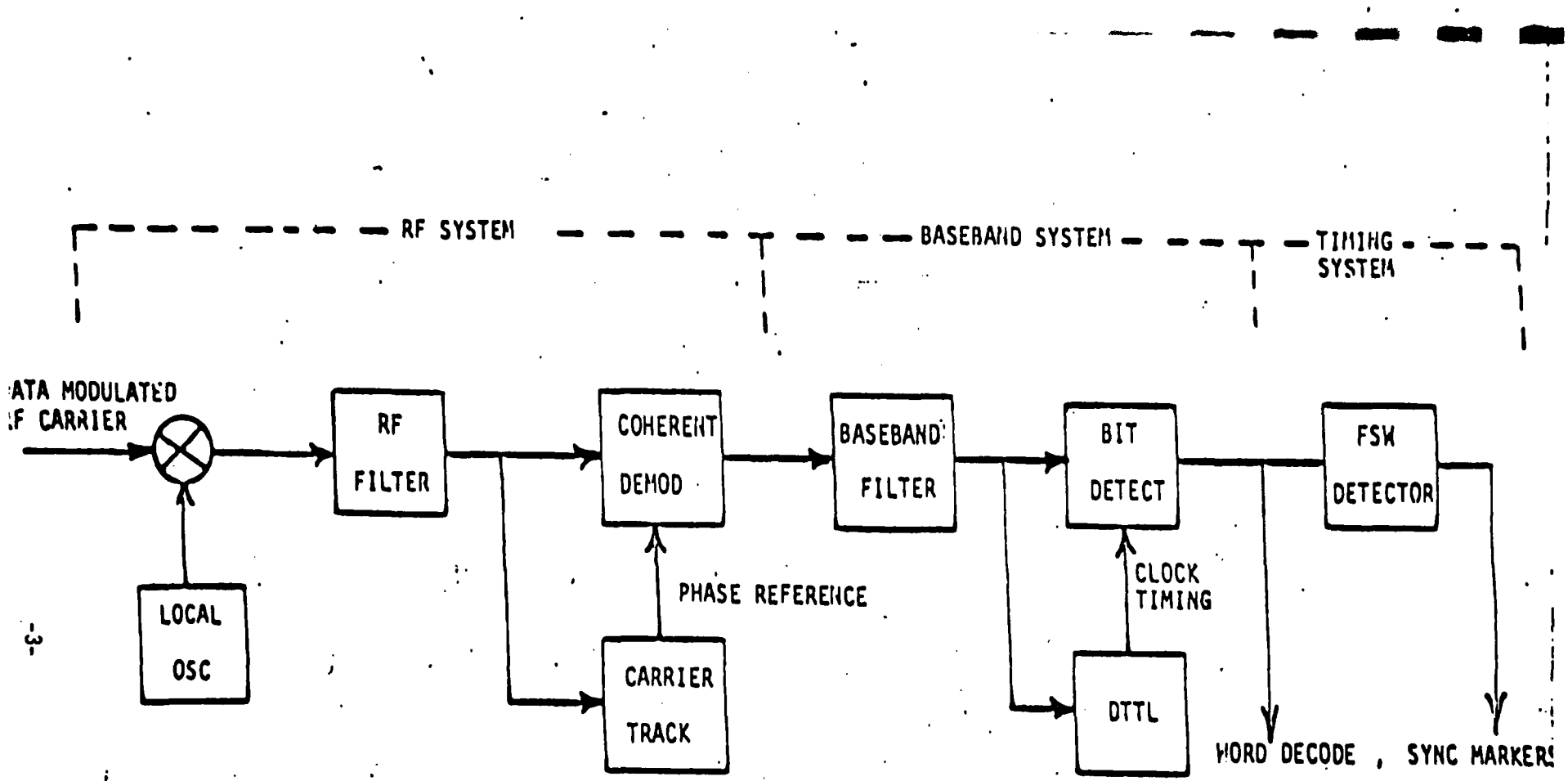

Figure 1b. Partially Coherent Demodulation.

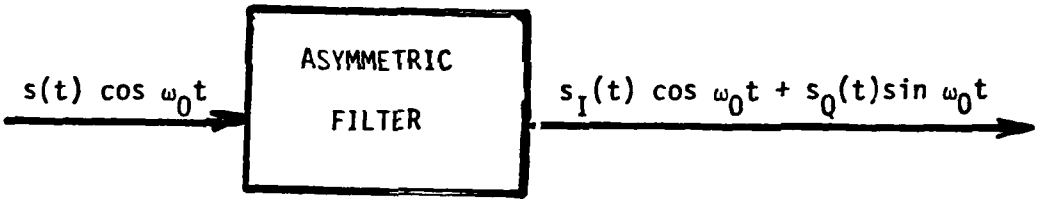

Figure 2. Imperfect Filtering.

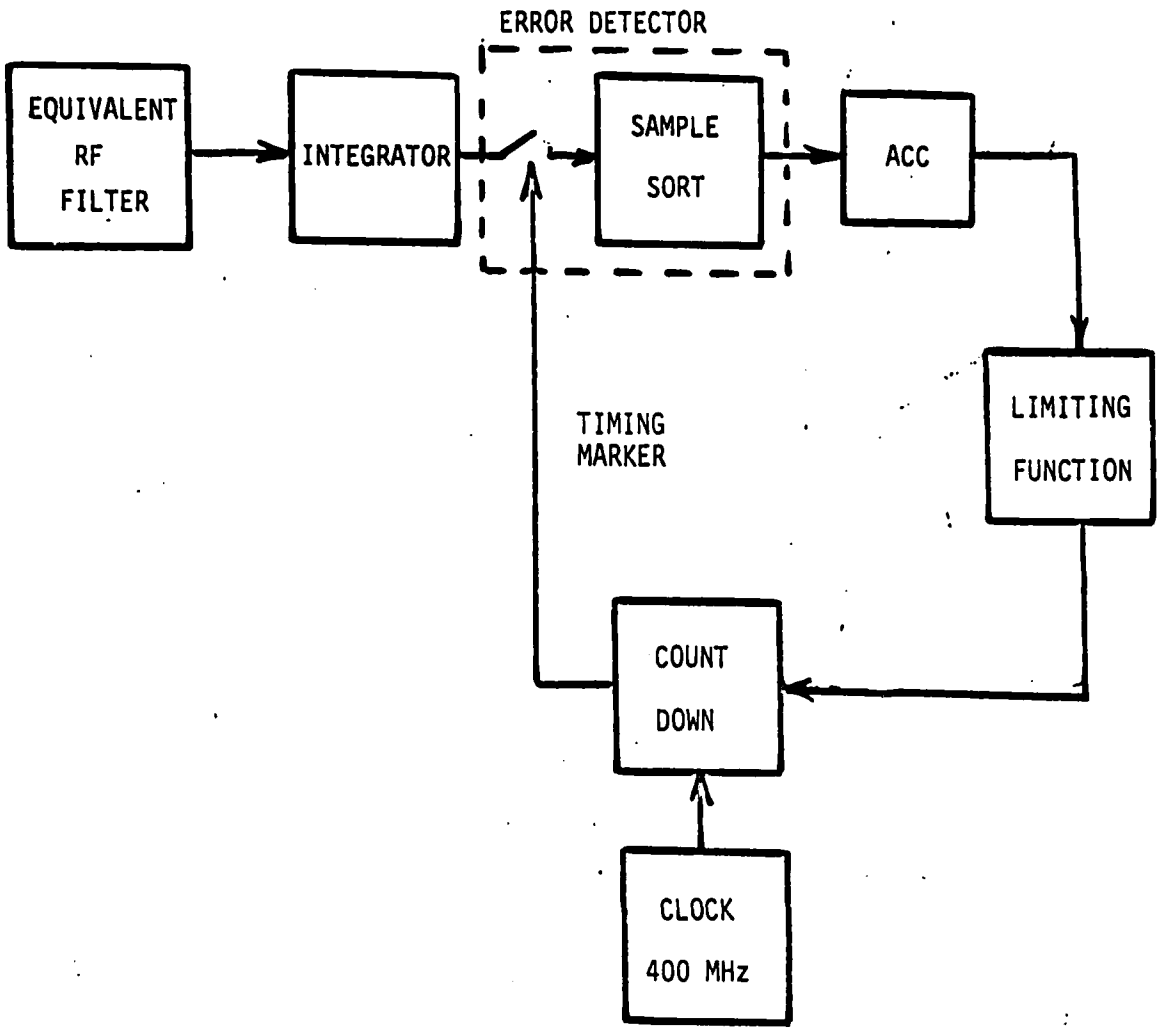

Figure 3. DTTL Block Diagram.

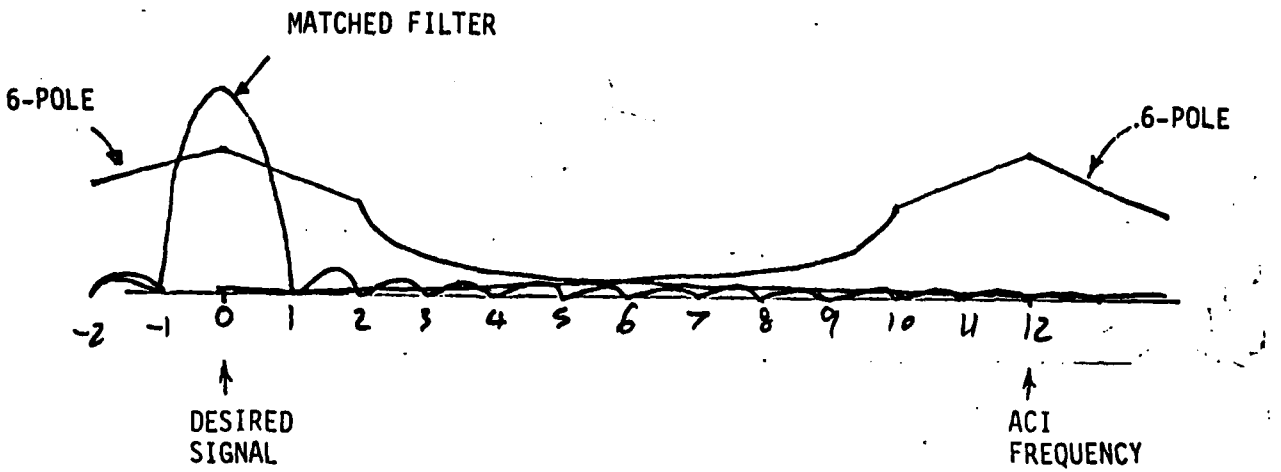

Figure 4. The Desired Signal is Protected From ACI By Two Chebyshev Filters and One Matched Filter.

2. Single Channel Time and Data Transfer Subsystem Phase Noise Mode

The basic block diagram model for the single channel receiving system at either the master or slave is shown in Figure 5. The main goal of this task was to model the total system phase noise. The RF portion of the system is assumed to be composed of an RF mixer and front end filter, followed by a coherent phase demodulator to generate the baseband data waveform. The baseband waveform is then bit decoded using bit timing extracted in the digital transition tracking loop (DTTL). In addition to data recovery, the decoded bits contain frame sync words which are used to establish master-slave timing. Phase demodulation in the RF section is accomplished by carrier phase referencing, and using the carrier reference to coherently demodulate the phase modulated RF carrier. Figure 5 lists the primary design concerns of each subsystem of the overall receiver. Table 1 lists the key parameters in an overall receiver specification. Although system models of this type lack detail for the overall implementation of each block, they do allow initial scoping of key parameter values and spotlight interface problem between subsections. In this section the RF subsystem is examined.

Two types of RF carrier modulations are considered. The first is a standard BPSK waveform with full ($\pm 90^{o}$) modulation index, producing suppressed carrier transmission. The data may be NRZ or Manchester. Phase referencing is accomplished by a balanced Costas loop, in which data decoding is accomplished through one arm of the loop. The second type of carrier is the reduced index ($|\Delta| < 90^{o}$) PSK carrier which maintains a residual carrier component. Phase referencing is achieved by a direct carrier tracking phase lock loop which tracks the residual carrier, using the reference for coherent bit correlation. Again the data may be NRZ or Manchester. The latter requires more RF bandwidth,

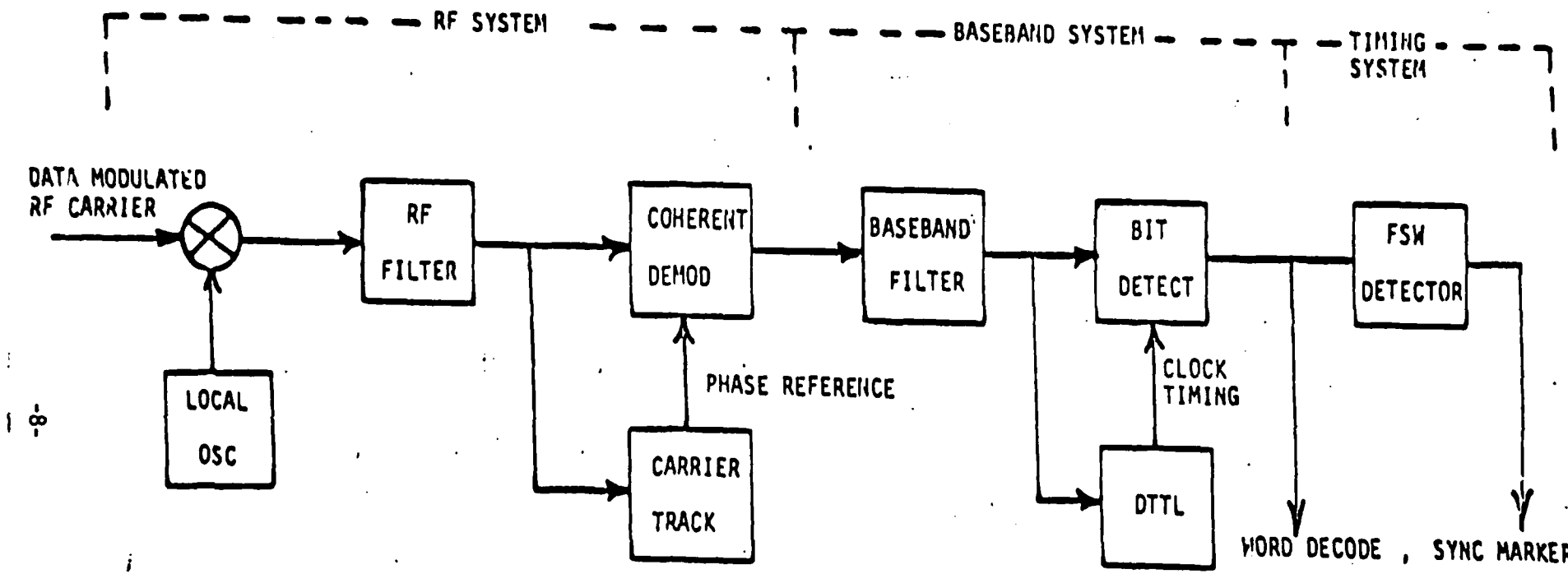

Figure 5. Model of Demodulation System.

but avoids the dc wander and transition density problem of the baseband decoder.

The RF subsystem should be designed to be transparent to the baseband decoding and master-slave timing operations. The primary effects of the RF system on the baseband are:

- Excessive RF filtering that effectively reduces the bandwidth of the baseband waveform. This produces baseband distortion and intersymbol interference.
- Suppression of the baseband power by phase referencing tracking errors.
- Delay bias in passing through the RF section. This delay must be compensated or calibrated.
- Introduction of phase noise or carrier instabilities that add to the phase reference error and cause timing inaccuarcies in the DTTL.

3 Single Channel Parameters

In this section a model of the modem and a channel is given.

3.1 RF Power and Bandwidth Considerations

The ability of the baseband system to data decode and derive bit time depends on the available baseband bit energy to noise level, $(E_b/N_0)_b$. The latter depends on the RF bit energy, and the modulation suppression and phase errors in the RF subsystem. The baseband E_b/N_0 is related to that of the received RF carrier by

$$\left(\frac{E_b}{N_0}\right)_b = \left(\frac{E_b}{N_0}\right)_c \sin^2(\Delta)\cos^2(\theta_e) \qquad (1)$$

where

Δ = RF carrier phase mod index

θ_e = reference loop tracking phase error

Figure 6. BASEBAND SUPPRESSION

$$(E_b/i_0)_b = (E_b/N_0)_c \sin^2(\Delta)\cos^2(\theta_c)$$

$$(E_b/N_0)_b = 10 \text{ dB}$$

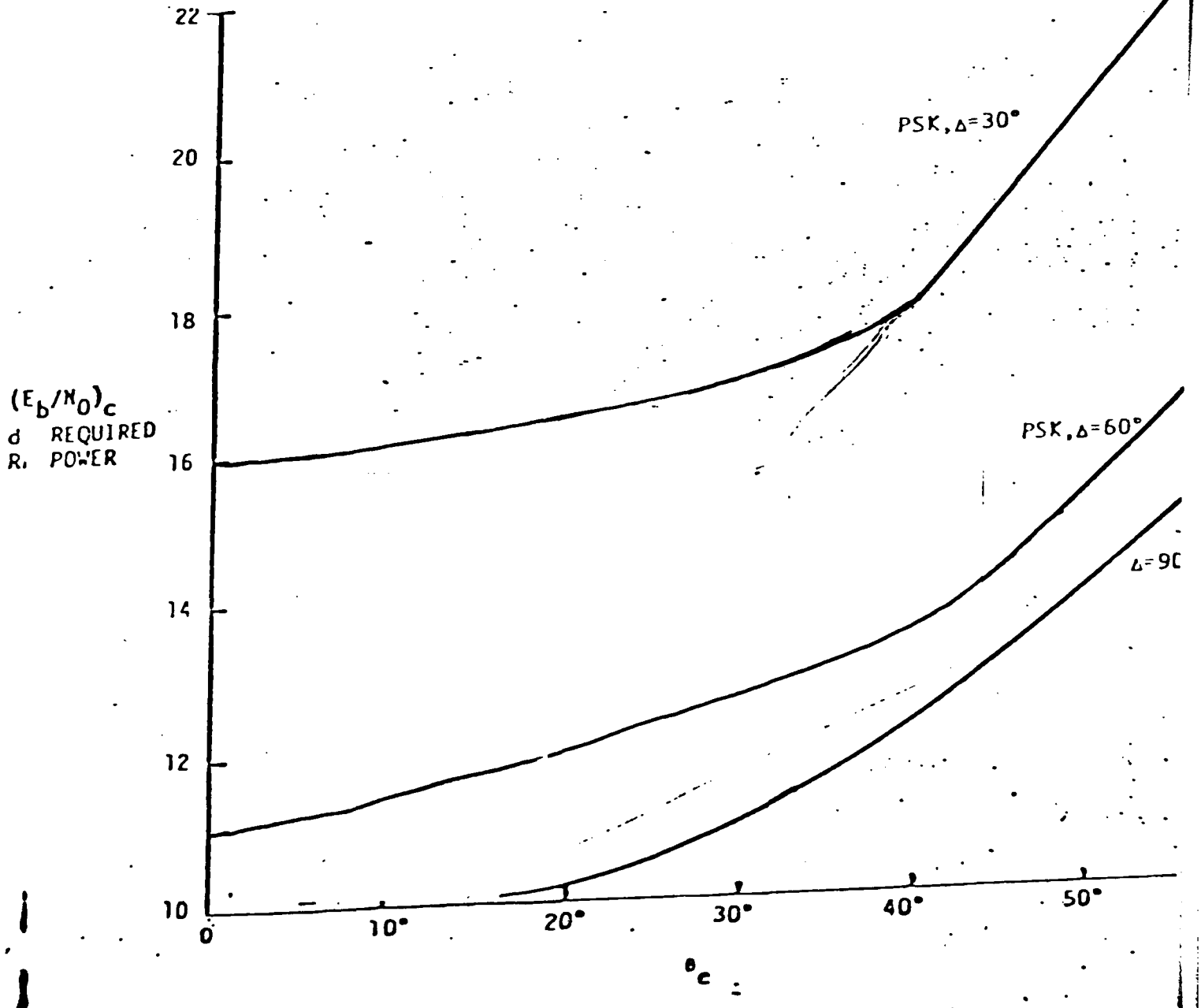

Figure 6 plots the required carrier $(E_b/N_0)_c$ to produce a 10 dB $(E_b/N_0)_b$, for various Δ, as a function of phase error θ_e. Less RF power is required for BPSK with a given θ_e. Note that to produce no more than a 1 dB suppression, a BPSK system can withstand about a 25^o phase error, while PSK carriers require increasingly tighter phase referencing.

Selection of the RF bandwidth can be critical if the filter is too narrow (equal to or less than the RF carrier spectrum). A narrow RF filter will produce intersymbol interference that increases both the RF phase tracking error and the baseband DTTL timing error. Both of these effects have been separately examined to determine the tightest restriction.

The effect of bandwidth reduction of a symmetrical filter on phase referencing was reported by Lindsey and Davidov (National Telecommunications Conference, Houston, Texas, December 1980) for both NRZ and Manchester data. Figure 7 shows a plot of their results, indicating the manner in which the mean squared tracking error increases as the RF filter BT product is reduced. The error is higher for the Manchester data since its spectrum is wider. These results indicate that the intersymbol effect should be negligible at $(E_b/N_0)_b$ values of 10 dB as long as $BT \geq 2$. This corresponds to a RF bandwidth requirement of at least 25 MHz.

The second concern is the effect of narrow RF filtering on the DTTL operation. The intersymbol effect causes waveform spillover on to the subsequent data transitions, which increase the transition tracking errors. This effect is analyzed in Section 2.2.4 using an ideal bandlimited waveform model. A link simulation was also carried out, in which more general waveforms and filter shapes can be analyzed. The principle results of these studies are shown in Figure 8. Here the

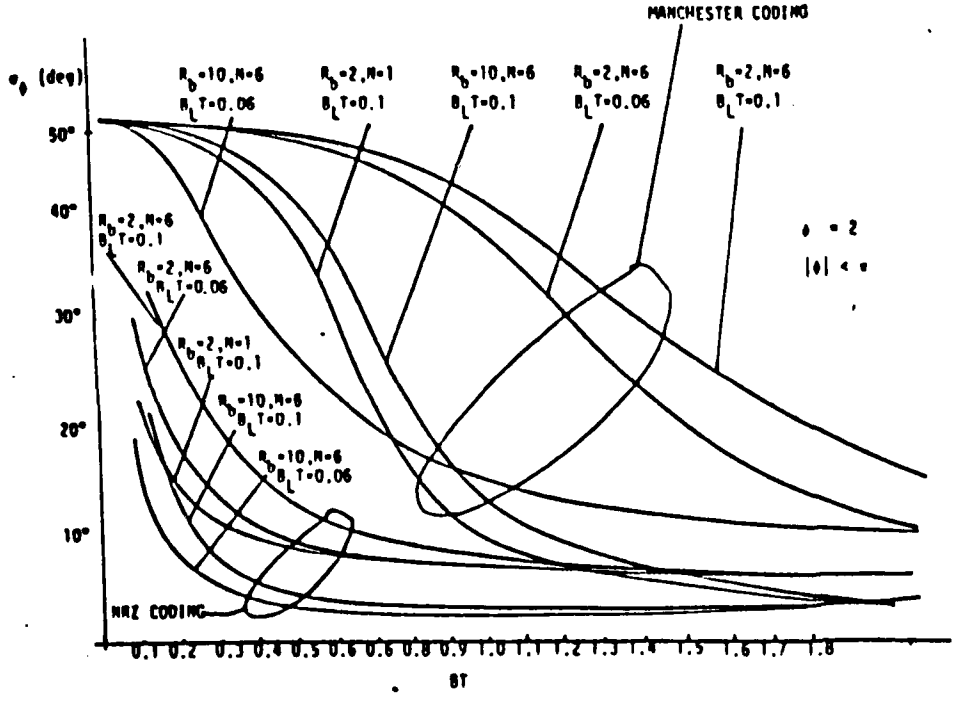

Figure 7. Phase-Error Variance (Manchester Coding).

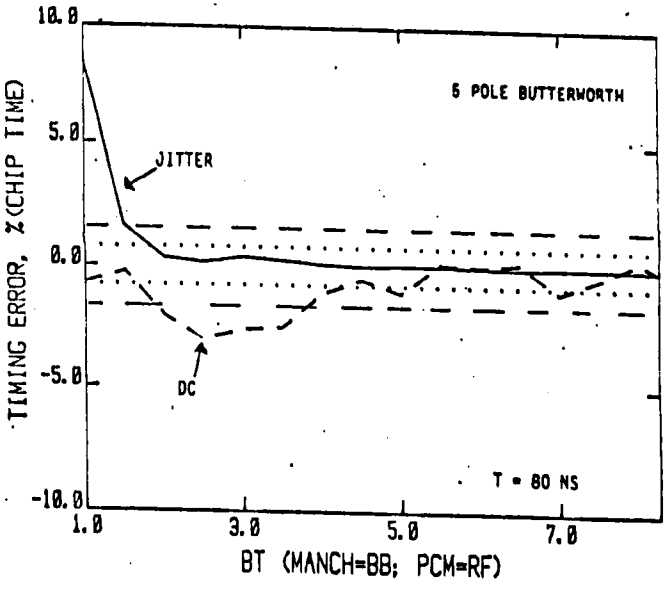

Figure 8. Timing Error in DTTL

rms bit timing error produced by the DTTL is shown as a function of the RF bandwidth directly, for different DTTL tracking bandwidths. As the RF filter band is reduced, the intersymbol interference is increased on the baseband waveform, which increases the transition noise and the DTTL timing error. Because of the extremely tight timing requirement on the bit synchronizer (as opposed to the requirements for phase reference accuracy) the timing effect is more important for setting the RF bandwidth than the phase referencing. As observed in Figure 2-8, an rms timing error on the order of 1 nanosecond requires an RF bandwidth of about 100 MHz for a 1 KHz DTTL bandwidth. Manchester data requires about twice this bandwidth.

3.2 RF Carrier Referencing

Coherent demodulation of the RF carrier requires accurate phase referencing. Phase reference errors will be due primarily to:

- Doppler tracking of the received carrier
- Thermal noise in the loop bandwidth
- Phase noise of the oscillator
- Modulation tracking phase error

The manner in which the phase error is derived from the above effects will depend on whether PSK carrier tracking or BPSK Costas tracking must be used. If f_d is the RF Doppler frequency and $\dot{f}_d$ is the Doppler rate, then the loop phase error is given by

$$\theta_e = \frac{2\pi \dot{f}_d}{\omega_n^2} \qquad (2)$$

f = acceleration component

ω_n = loop natural frequency

The mean squared phase error due to thermal noise of level N_0 at the loop input is given by

$$\sigma^2 = \frac{B_L T}{(E_b/N_0)_c} [\cos^2(\Delta)]^{-1}, \text{ PSK} \qquad (3a)$$

$$\sigma^2 = \frac{B_L T}{(E_b/N_0)_c} [1 + \frac{1}{(E_b/N_0)_c}], \quad \text{Costas BPSK} \qquad (3b)$$

A plot of this rms phase error σ is shown in Figure 2-9 for both the Costas and PSK carriers.

$$B_L \leq 250 \text{ KHz} \qquad (4)$$

This provides an equivalent phase error of about 3° for E_b/N_0 = 10 dB. During a degraded mode of operation, where E_b/N_0 < 10 dB, the bandwidth will be made smaller. The lower bound will be determined by the carrier VCO phase noise.

In addition to thermal noise, the RF tracking design must be concerned with the phase noise infiltrating the loop. The principle contributors are the transmitter oscillator, the RF mixer oscillators, and the VCXO in the reference loop. If we denote the spectrum of each of these sources as

$\phi_0(\omega)$ = phase spectrum of received RF carrier

$\Phi_m(\omega)$ = phase spectrum of RF mixer

$\Phi_0(\omega)$ = phase spectrum of loop VCXO

ω = frequency relative to RF carrier center frequency

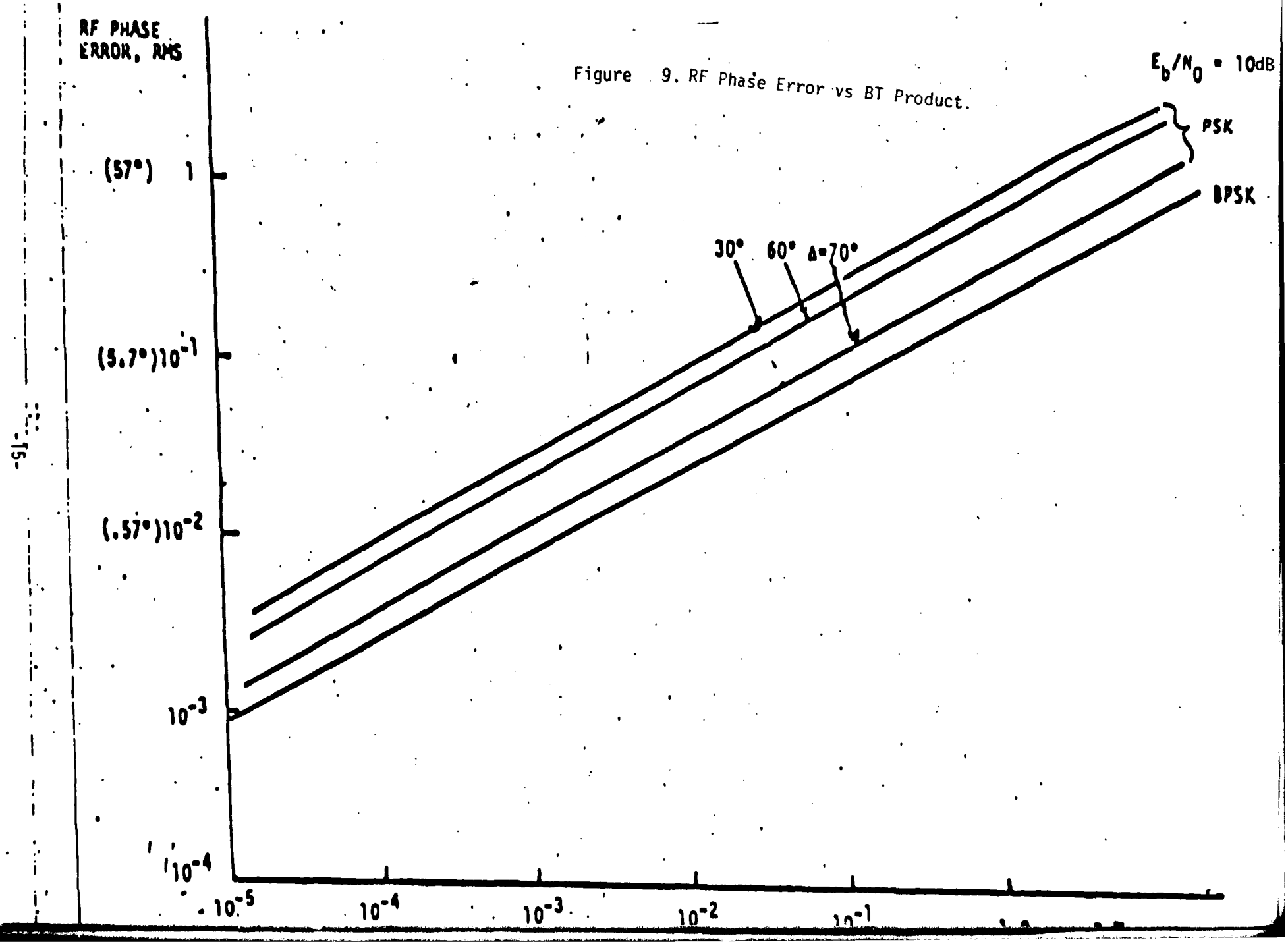

Figure 9. RF Phase Error vs BT Product.

Figure 10. RF CARRIER TRACKING LOOP BANDWIDTH

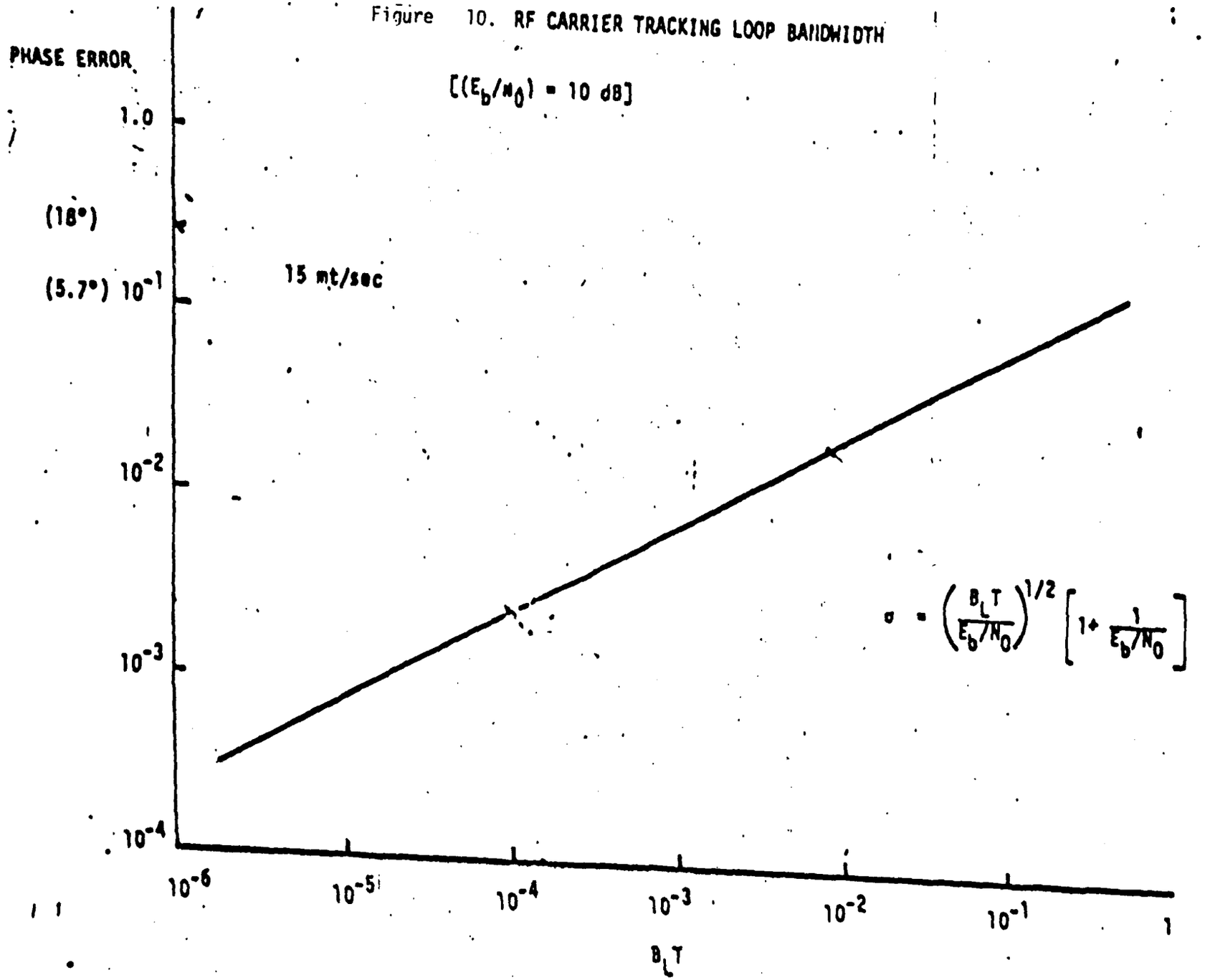

then the mean square phase error contribution by these sources is

$$\sigma^2 = \frac{1}{2\pi}\int_{-\infty}^{\infty}[\phi_0(\omega) + \phi_m(\omega)]|1-H(\omega)|^2 d\omega + \frac{r^2}{2\pi}\int_{-\infty}^{\infty}\phi_0(\omega)|1-H(\omega)|^2 d\omega \quad (5)$$

where

$H(\omega)$ = carrier tracking loop gain function

r = rate of RF to VCXO rest frequency

The r factor accounts for the frequency multiplication of VCXO phase noise to the RF tracking frequency.

To bound the VCO phase noise process specifications for VCO's which have been built will be examined. For example, specify the VCO phase noise power spectrum not to exceed

$$S(f) = \left(\frac{.1}{f}\right)^3$$

for all f. If H(f) denotes the closed loop transfer function of the tracking loop, the VCO phase noise related interference power P_{os} can be computed from Equation 5. To simplify computation of interference, let F_0 denote H(f) cutoff frequency. The VCO phase noise power is approximately given by

$$P_{os} \simeq 2\int_{F_0}^{\infty} S(f)df$$

Therefore

$$P_{os} \simeq 2\int_{F_0}^{\infty}\left(\frac{.1}{f}\right)^3 = .5 \times 10^{-3} \times F_0^{-4}$$

For $F_0 \geq 5$ Hz, we have

$$P_{os} \simeq 0$$

Previous experience in developing the down converter chain indicates that an Allen variance of 2° rms is possible. Numbers on the order of this magnitude do not raise a problem in system operation.

The final error source to be examined is caused by tracking the modulation signal in the single channel case. In Appendix 1, the two cases considered are:

1) Costas loop tracking error for BPSK modulation, and
2) Carrier tracking loop phase error caused by delta modulation.

It is shown that for Manchester coded signals, the tracking error is negligible for a $B_L T$ product much less than the data rate and for NRZ, the $B_L T$ must be less than .01 for acceptable tracking performance.

3.3 Bit Decoding

In addition to accurate bit timing, the baseband subsystem must also provide accurate bit decoding. This is particularly important in the master-slave timing method using coded error transmission, since decoding errors transfer directly to sync errors. The probability of bit error in decoding the data bits following RF carrier demodulation to baseband will depend on the baseband $(E_b/N_0)_b$ and the RF carrier tracking accuracy. Figures 11, 12, and 13 show the manner in which bit error probability PE varies with E_b/N_0 for various rms phase tracking errors and bias error offsets. For PSK referencing with $\Delta \neq 90^0$, a required PE = 10^{-5} requires a phase tracking rms error of no more than about 10°, or a tracking loop SNR such that

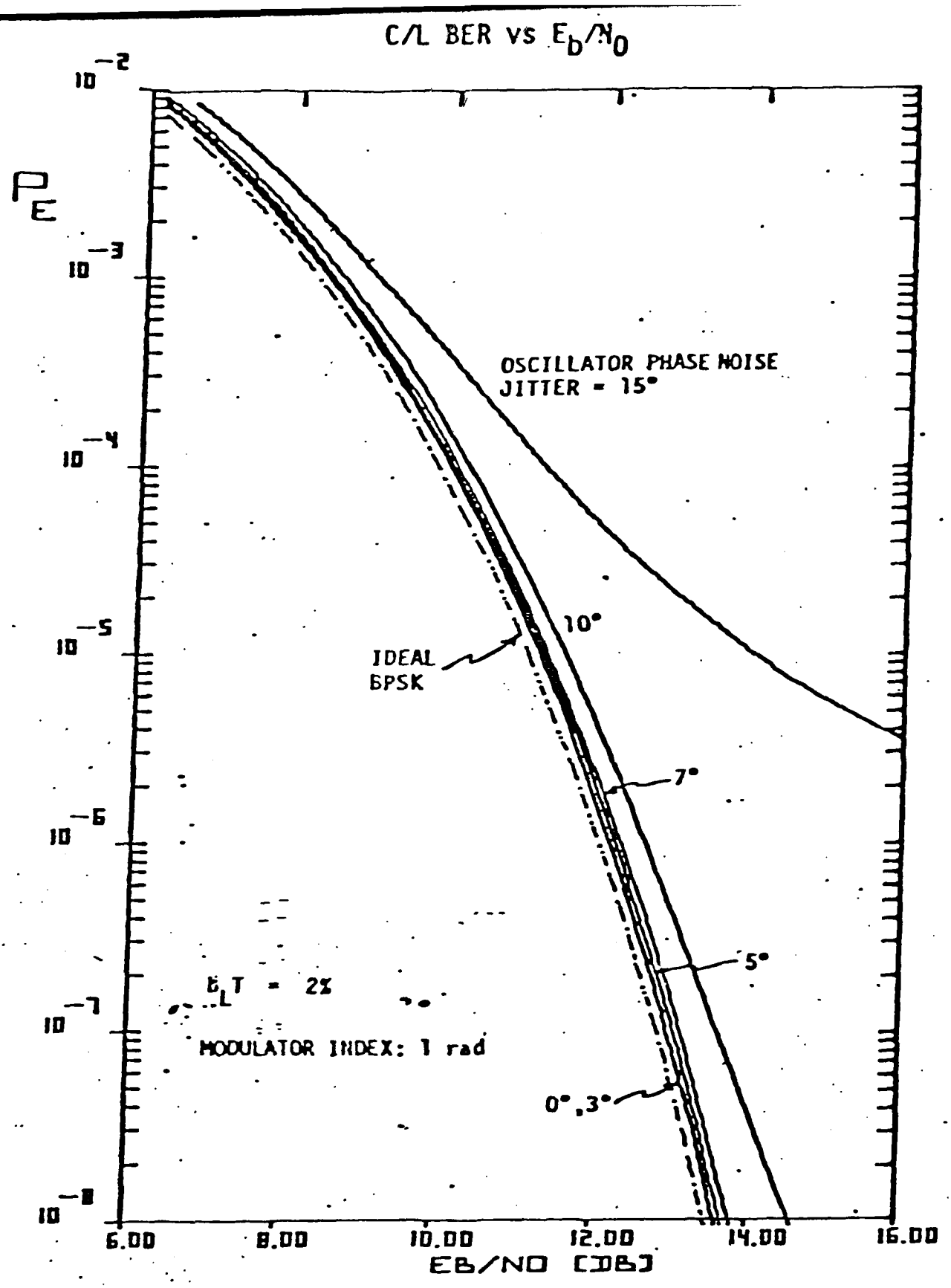

Fig. 11. Effect of Demodulator Phase Offset and Oscillator Phase Jitter on BER (Phase Offset = 10°).

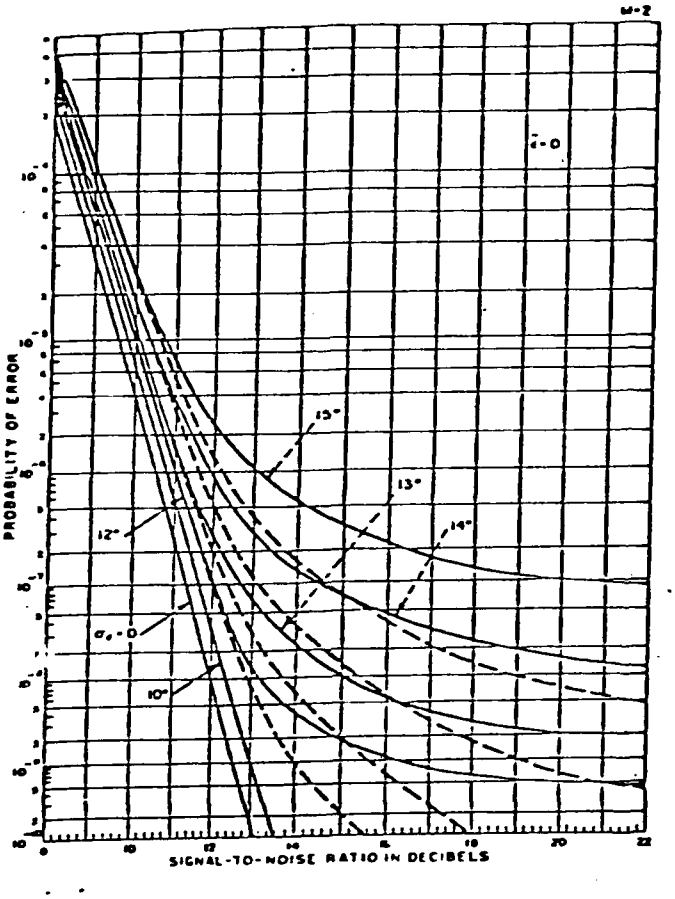

Figure 12. Probability of Bit Error for BPSK

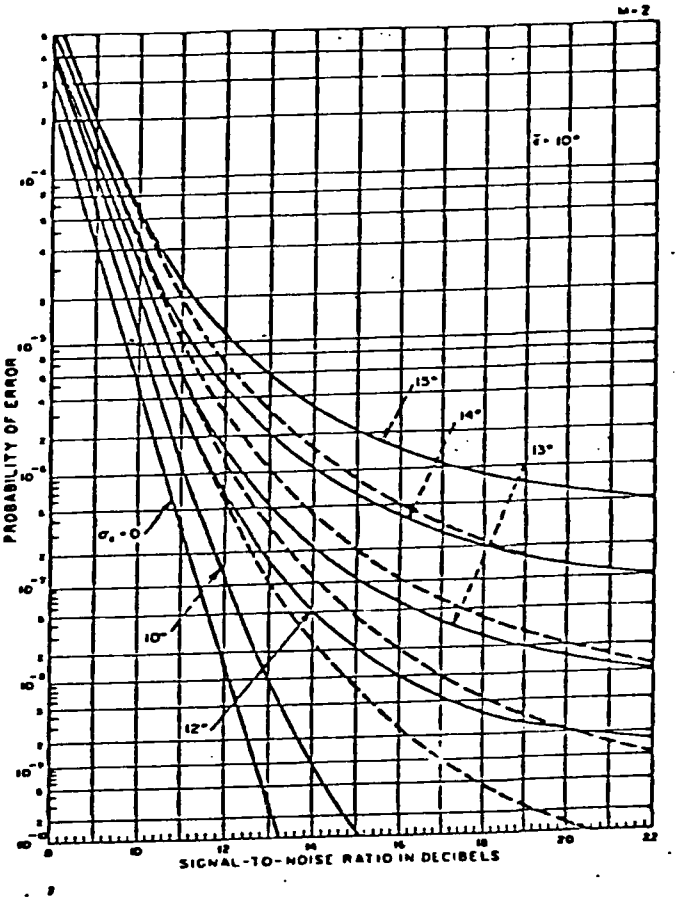

Figure 13. Probability of Bit Error for BPSK.

$$\frac{(E_b/N_0)_c}{B_L T} \cos^2(\Delta) \gtrsim 12 \text{ dB} \qquad (6)$$

Hence as Δ is increased to 90^o, a larger RF E_b/N_0 is needed to prevent the phase referencing from degrading the PE. With Costas loop tracking, the decoding and phase referencing are both accomplished directly within the loop, and the decoding bit error probability is given by

$$PE = \frac{1}{2} \text{erfc}(\Lambda) \qquad (7)$$

where

$$\Lambda^2 = (E_b/N_0)_c [I_1(\rho)/I_0(\rho)]^2 \qquad (8)$$

and

$$\rho = \frac{(E_b/N_0)_c}{B_L T} [1+(E_b/N_0)^{-1}] \qquad (9)$$

At the E_b/N_0 values expected, little degradation to the bit decoding occurs from this phase referencing.

4. Single Channel Error Sources

The single channel error sources are discussed.

4.1 DTTL Bit Jitter

Bit sync for baseband data decoding is achieved by a digital transition tracking loop that time locks on bit transitions (or pulse transitions in the Manchester format). Since this operation sets the bit timing, it therefore becomes a key element in the overall sync operation.

The DTTL has the block diagrams in Figure 14. The input to the DTTL is the baseband waveform demodulated from the RF subsystem and filtered to a bandwidth W. The error detector is a waveform integrator followed by a sampler timed by a count-down counter. The nominal sampling rate is obtained by dividing down the 400 MHz clock to the bit rate of the baseband data. The accumulator sums over a number of error samples to generate the error control voltage and the limiting function can be a hard limiter on a deadband limiter. The hard limiter senses the sign of the error voltage to add or delete a clock tick for timing adjustment. If a deadband limiter is used, allowance for a voltage range where no adjustment is made is present. The error detector operates by effectively integrating over the bit or pulse transition for error magnitudes, and simultaneously integrates over each bit or pulse for sign determination. A full integrator integrates over a complete bit and therefore collects the maximum signal energy. A partial integrator uses only a portion of each bit, but collects less noise.

Consider first the case when the RF filter is wideband enough so as to not distort the pulse shape. The error detector then converts a time error e to a voltage sample with gain 2A, where A is the pulse amplitude. This error sample also contains noise due to the baseband noise in the loop prefilter. The accumulator sums over m voltage

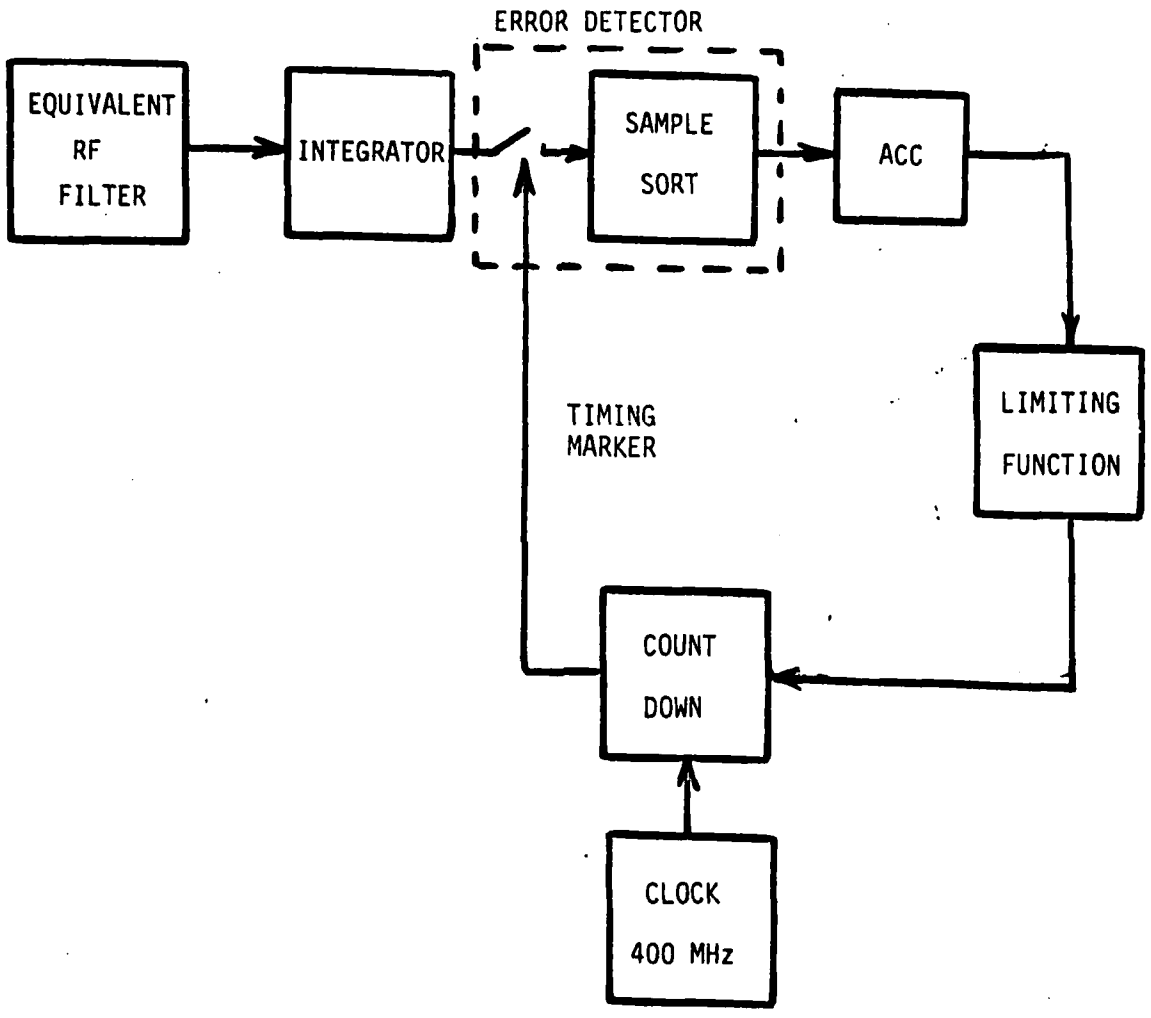

Figure 14. DTTL Block Diagram.

samples to produce the error control signal. The noise enters as random samples with variance $\sigma^2 = N_0B$ where B is the pre-filter bandwidth.

We wish to determine the ability of the DTTL loop to track frequency instabilities, such as offsets due to doppler on the received carrier. The DTTL sampling frequency is 400 MHz/N, and its sampling period is T_s = (N/400) microseconds. Let the input baseband bit stream occur at a period $T_b = T_s + xT_s$, where x is the percentage change caused by a doppler offset due to a velocity V. That is, the bit rate clock frequency is

$$[\frac{1}{T_s} + (\frac{V}{C})\frac{1}{T_s}]^{-1} \tag{10}$$

where C is the speed of light. The bit period is then

$$\begin{aligned} T_b &= \left(\frac{1+(V/C)}{T_s} \right)^{-1} \\ &= T_s(1+\frac{V}{C})^{-1} \\ &\approx T_s(1+x) \quad , \qquad x \ll 1 \end{aligned} \tag{11}$$

where $|x| = V/C$. A difference of periods between the received and local clocks means the timing difference, if uncorrected, will continually slide apart. After i periods the timing error will be

$$\begin{aligned} e &= T_s - T_s(1-ix) \\ &= \pm ixT_s \end{aligned} \tag{12}$$

The build-up in timing error occurring over the accumulator time of the DTTL must be corrected by the loop to prevent loss of lock. The loop will pull-in the offset if the accumulated time error is less than t_0 sec, the maximal amount that can be corrected by the loop in one sample

time. Hence, for the fractional offset x, we require

$$\sum_{i=1}^{m} ixT_s < t_0 \tag{13}$$

or

$$xT_s(m+1)m/2 < t_0 \tag{14}$$

For the given x we therefore require an accumulation of time

$$m < \left(\frac{2t_0}{xT_s}\right)^{1/2} \tag{15}$$

Equation (15) is plotted in Figure 15 as a function of x for the case of $t_0/T_s = 12.5 \times 10^6/400 \times 10^6 = 1/32$. The plot is also shown in terms of velocity V. Note that for velocities on the order of 150 met/sec, accumulations as large as 10^5 can be tolerated.

To determine the effect of noise on the DTTL, we compute the tracking error variance due to the noise samples. Assume the tracking error samples remain constant during the accumulation, while the noise samples n_i at each sample are independent Gaussian variates with the variance in $\sigma^2 = N_0 B_L$. The timing correction in the hard limited DTTL is made according to the limiter output

$$y = \text{sign}[mAe+n] \tag{16}$$

where

$$n = \sum_{i=1}^{m} n_i \tag{17}$$

If the loop is in lock ($|e| \leq t_0/2$), then in the absence of noise, the loop will remain in lock, achieving a steady error of

Figure 15.
Maximum Number of Accumulated Samples as a Function of Velocity.

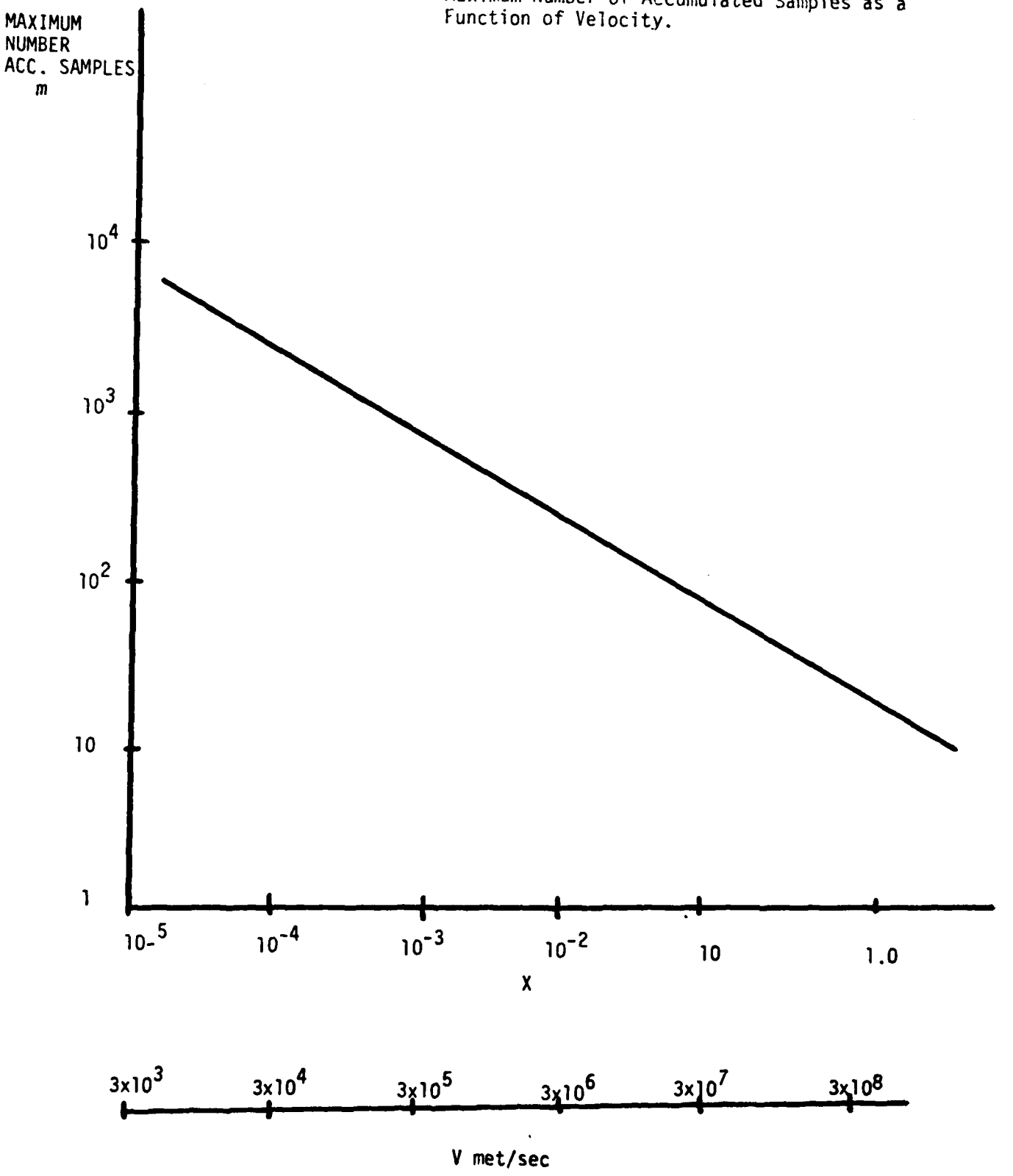

$$e_0 = \pm t_0/2$$

$$= \pm 1.25 \text{ nsec} \qquad (18)$$

With a hard-limiter, the loop will jump between these values, and (18) is the inherent DTTL quantization error. With a deadband limiter, the loop error will stabilize with any error within $\pm t_0/2$.

To determine the effect of noise, we note from Figure 14 that the error will evolve as a random walk process. For a given error the DTTL will correct in the proper direction as long as the accumulated noise n in (16) does not change the sign of e. If the sign changes, the loop will correct in the wrong direction, and the loop error will increase. Assuming an initial timing error of $\pm t_0/2$, the steady state mean squared timing error will evolve as

$$\sigma_t^2 = (\frac{t_0}{2})^2 + (\frac{3t_0}{2})^2 P_1 + (\frac{5t_0}{2})^2 P_1 P_3 \cdots \qquad (19)$$

where P_j is the probability that a change in sign occurs, due to noise, when the loop error e is $jt_0/2$. The probability of this occurring depends on whether a hard-limiter or deadband limiter is used (see Figure 16). It follows that

$$P_j = Q[\sqrt{\rho}]$$

where

$$\rho = \frac{[\sqrt{2}Am(jt_0/T)]^2}{m\sigma^2}$$

$$= m(\frac{A^2}{N_0 B_L})(\frac{jt_0}{T})^2$$

$$= j^2 m(E_b/N_0)(t_0/T)^2(1/B_L T) \qquad (20)$$

SYSTEM EQUATIONS

$$\hat{\delta}(i+1) = \hat{\delta}(i) + F_B - t_0 \, \mathrm{lim}[\textstyle\sum g(e_i) + n_i]$$

$$e(i) = \delta(i) - \hat{\delta}(i)$$

$$e(i+1) = e_i - t_0 \, \mathrm{lim}[mGe_i + mn_i]$$

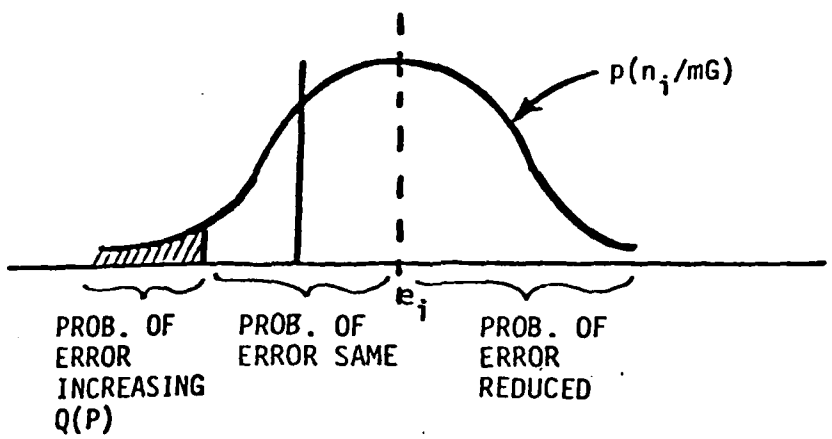

Figure 16.

$$\text{VARIANCE } e \approx \left(\frac{t_0}{2}\right)^2 [1 + 3^2 Q(P) + \ldots]$$

The rms timing error can be approximated from the first two terms of (19). Thus

$$\sigma = \left(\frac{t_0}{2}\right)\left[1+3^2P_1\right]^{1/2}$$

$$= (1.25\text{ns})\left[1+9P_1\right]^{1/2}$$

The above σ is plotted in Figure 17. The result shows that a B_LT no smaller than about 10^{-3} is needed to insure the noise does not increase the tracking error much beyond the inherent quantization error (1.25ns), when E_b/N_0 = 10 dB. This corresponds to a loop noise bandwidth of less than

$$B_L = (10^{-3})(12.5\text{x}10^6)$$

$$= 12.5 \text{ kHz}$$

As the baseband E_b/N_0 is decreased (due to lower RF E_b/N_0 or increased RF phase error) the rms timing error increases. Figure 2-18 shows how σ varies with $(E_b/N_0)_b$. As the latter is incrased a wider DTTL bandwidth can be used.

4.2 Effect of RF Symmetric Filter on DTTL Performance

In this section, we examine the effect of RF bandpass filtering and RF carrier demodulation on the performance of a DTTL timing subsystem used for baseband bit timing. As has been shown earlier, the accuracy of the bit timing effects the overall accuracy of master-slave timing and all distortion effects must be considered in deriving its performance.

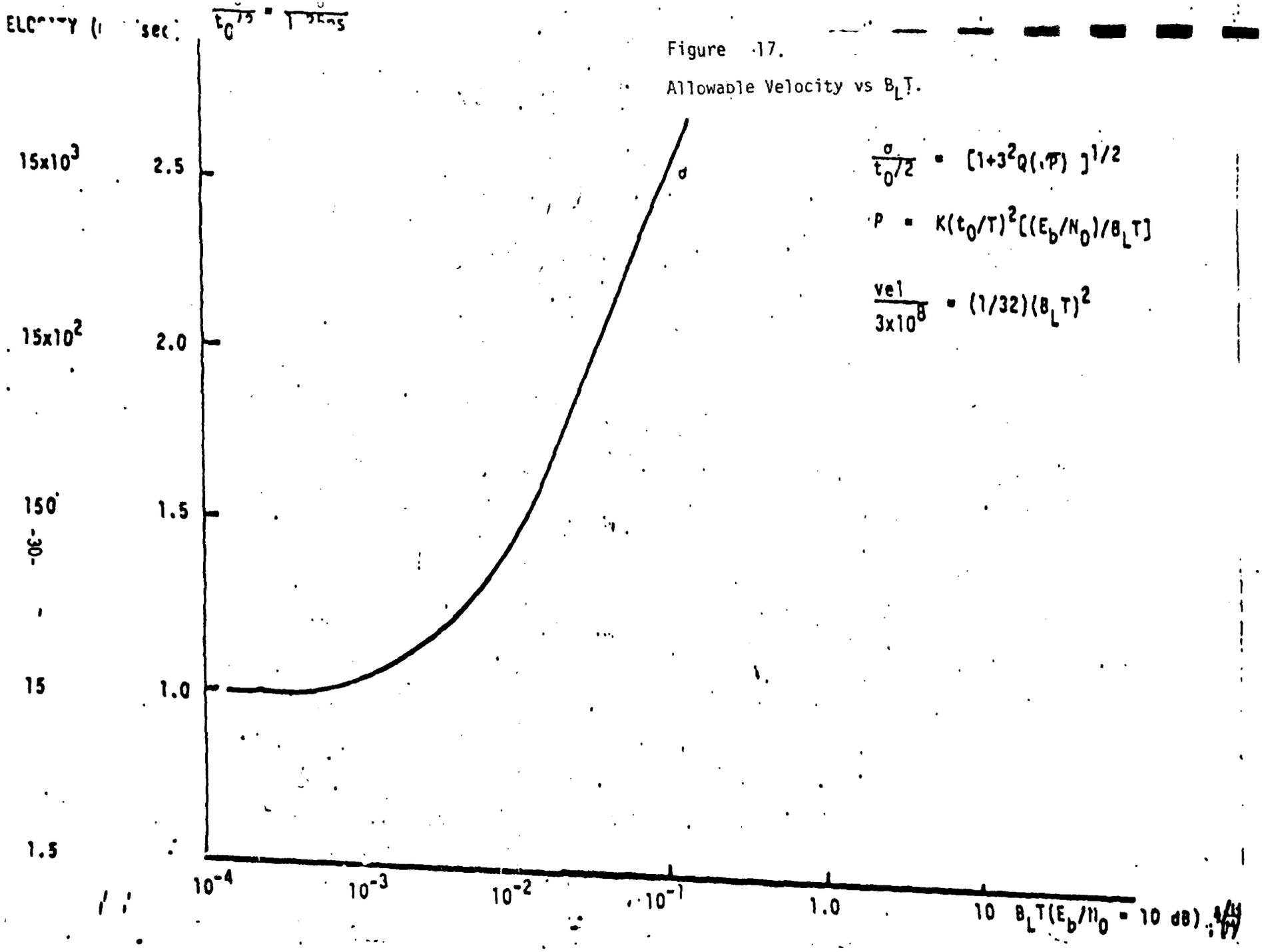

Figure 17.

Allowable Velocity vs $B_L T$.

$$\frac{\sigma}{t_0/2} = [1+3^2 Q(\sqrt{P})]^{1/2}$$

$$P = K(t_0/T)^2[(E_b/N_0)/B_L T]$$

$$\frac{vel}{3\times10^8} = (1/32)(B_L T)^2$$

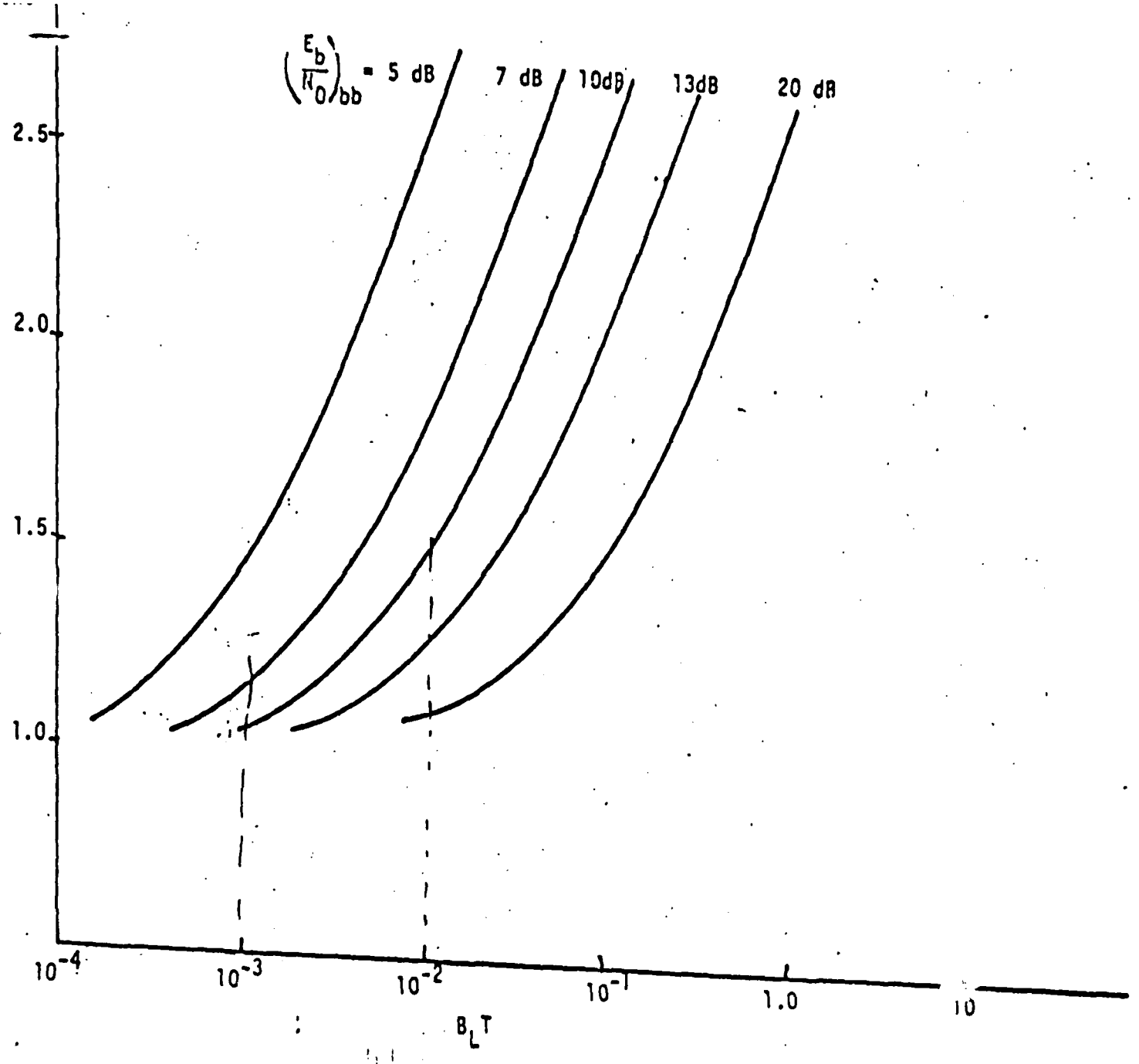

Figure 18. Normalized Error vs $B_L T$.

Consider the system in Figure 19. The demodulated baseband data waveform at x_1 is given by

$$x_1(t) = (A \cos \theta_c) \sum_{j=-\infty}^{\infty} d_j p(t-jT) + \text{noise} \qquad (21)$$

where

$d_j = \pm 1$, sequence of data bits

$p(t)$ = filtered PCM or Manchester waveform

T = bit time $(12.5 \times 10^6)^{-1}$ sec

A = baseband waveform peak amplitude

The noise is white Gaussian with spectral level N_0. The DTTL uses analog baseband pre-filtering, and A-D digital tracking. The pre-filter integrates over a bit time T for bit detection (T/2 for Manchester), and integrates 2T for transition tracking (T for Manchester). The variance of the DTTL timing error is given by

$$\sigma^2 = \frac{B_L \left[N_0 + \frac{\overline{I}_{2T}^2}{2T} \right]}{A^2 \, \text{erf}(\Lambda)^{1/2}} \qquad (22)$$

where

B_L = tracking loop noise bandwidth

$\overline{I}_{2T}^2$ = mean square intersymbol interference over 2T sec intervals

$$= \sum_{\substack{n=-\infty \\ n \neq 0}}^{\infty} \left[\int_0^{2T} p(t-nT)dt \right]^2 \qquad (23)$$

$$\Lambda = \frac{E}{N_0 + \frac{\overline{I}_T^2}{T}} \qquad (24)$$

$$E = (A^2 T) \cos^2(\theta_c) \left[\frac{1}{T} \int_0^T p^2(t)dt \right] \qquad (25)$$

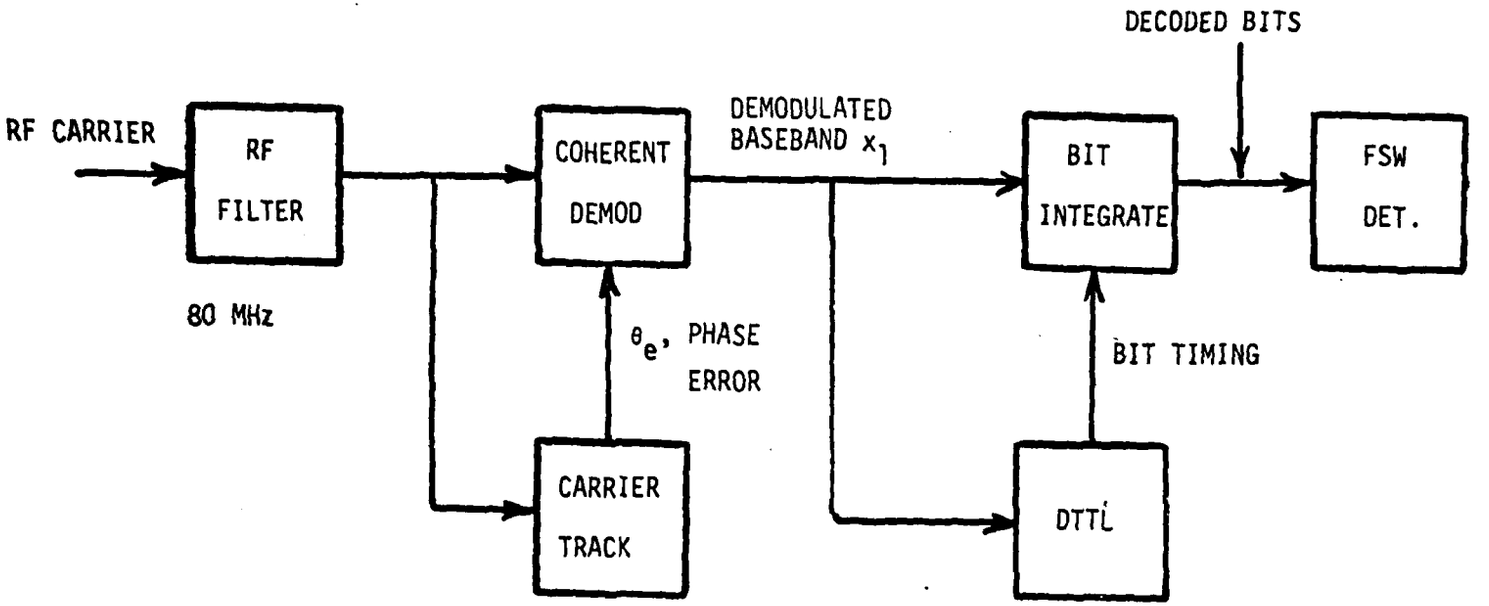

Figure 19. System Overview.

The erf function accounts for bit errors in the DTTL bit detection loop. The parameter σ^2 is the normalized timing variance relative to the bit time T. The variance above is based on a Gaussian intersymbol contribution, and is a worst case value, assuming a least favorable bit sequence.

It is convenient to denote

$$E \triangleq mE_b \tag{26}$$

with

$$E_b = A^2T \tag{27}$$

$$m = (\cos^2\theta_c)\left[\frac{1}{T}\int_0^T p^2(t)dt\right] \tag{28}$$

The term E_b is the pulse energy (bit energy for PCM signals) corresponding to an idealized square pulse. Thus the parameter m accounts for energy degradation due to pulse filtering in the RF and imperfect phase demodulation. We then can write

$$\sigma^2 = \frac{TB_L\left[1 + \frac{\overline{I^2_{2T}}}{2N}\right]}{(E_b/N_0)\mathrm{erf}(\Lambda)^{1/2}} \tag{29}$$

and

$$\Lambda = \frac{mE_b/N_0}{\left[1 + \frac{\overline{I^2_T}}{N}\right]} \tag{30}$$

with $N \triangleq N_0T$ being the integrated noise in T sec. Note for the

$$\frac{I_{2T}^2}{N} = \left(\frac{A^2T^2}{N}\right)\left(\frac{I_{2T}^2}{A^2T^2}\right)$$

$$= \left(\frac{E_b}{N_0}\right)(\hat{I}_{2T})^2 \tag{31}$$

where $\hat{I}_{2T}^2$ is the <u>normalized</u> intersymbol effect given by

$$\hat{I}_{2T}^2 = \frac{A^2}{A^2T^2} \sum_{\substack{n=-\infty \\ n\neq 0}}^{\infty} \left[\int_0^{2T} p(t-nT)dt\right]^2$$

$$= \sum_{\substack{n=-\infty \\ n\neq 0}}^{\infty} \left[\frac{1}{T}\int_0^{2T} p(t-nT)dt\right]^2 \tag{32}$$

Hence, $\hat{I}_{2T}^1$ is the sum of squares consecutive 2T sec integrations over tails of the data awaveform. In essence, $\hat{I}_{2T}$ is the normalized contribution of the intersymbol effect of all previous pulses on to each 2T sec integration of the DTTL. We then have

$$\sigma^2 = \frac{TB_L\left[1+\left(\frac{E_b}{N_0}\right)\hat{I}_{2T}^2\right]}{(E_b/N_0)\,\mathrm{erf}(\Lambda^{1/2})} \tag{33}$$

and

$$\Lambda = \frac{mE_b/N_0}{\left[1+\left(\frac{E_b}{N_0}\right)\hat{I}_T^2\right]} \tag{34}$$

These equations show that timing performance will strongly depend on the amount of intersymbol interference and on the achievable E_b/N_0. If the intersymbol effect is minimal, so that

$$\left(\frac{E_b}{N_0}\right)\hat{I}_{2T}^2 \ll 1 \tag{35a}$$

$$\left(\frac{E_b}{N_0}\right)\hat{I}_T^2 \ll 1 \tag{35b}$$

we have

$$\sigma^2 \simeq \frac{TB_L}{(E_b/N_0)\mathrm{erf}[mE_b/N_0]^{1/2}} \qquad (36)$$

and the DTTL performance depends only on the E_b/N_0 and its degradation through the m parameter. As the intersymbol effect becomes significant (reversing the inequalities in (15)) however

$$\sigma^2 \simeq \frac{TB_L(\hat{I}_{2T})^2}{\mathrm{erf}(m/\hat{I}_T^2)^{1/2}} \qquad (37)$$

The last term represents an inherent, irreducible tracking variance that does not depend on E_b/N_0. This therefore cannot be controlled by signal strength, and is a function of the RF filtering applied to the carrier waveform. As this bandwidth B decreases, $p(t)$ is extended in time, and $\hat{I}_{2T}^2$ is increased. The quantity in Equation (37) is a normalized time variance Figure 20 plots the rms tracking error vs $(\hat{I}^2)$ rms for several loop bandwidths B_L. If the mean square interference $\hat{I}^2$ can be determined, σ^2 can be estimated from the figure. In the following sections this interference is derived from both an analytical (pulse model) and simulation approach.

Analytical Study of Symmetric RF Filtering

We consider the RF filtered pulse

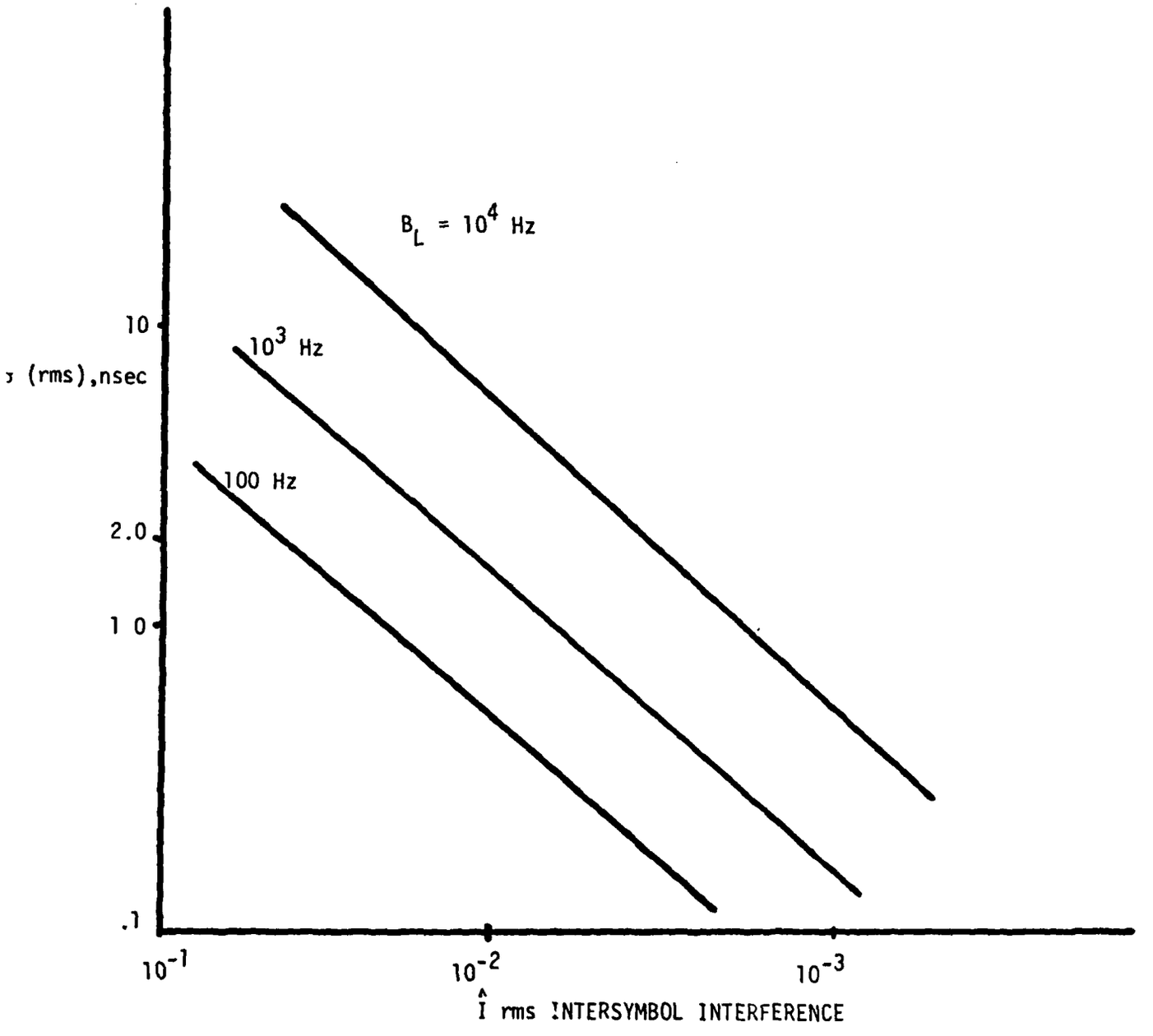

Figure 20. Jitter vs Intersymbol Interference.

$$p(t) = \frac{\sin(2\pi Bt)}{(2\pi Bt)}, \quad t > 0 \tag{39}$$

corresponding to an ideal PCM bandwidth of B Hz. Equation (32) then becomes

$$(\hat{I})^2 = \sum_{n=1}^{\infty} \left[\frac{2}{T\pi} \int_{nT}^{(n+1)T} \frac{\sin(2\pi Bt)}{(2\pi Bt)} \, dt \right]^2 \tag{40}$$

Define

$$S_i(a) = \int_0^a \frac{\sin(a)}{a} \, da$$

Then

$$\hat{I}^2 = \left(\frac{1}{\pi\gamma}\right)^2 \sum_{k=1}^{\infty} [S_i(2\pi\gamma k) - S_i(2\pi\gamma k)]^2$$

with

$$\gamma = BT$$

The intersymbol value can be determined by computing the sum shown above. The results are tabulated in the table below and plotted in Figure 21.

BT	$\sqrt{\hat{I}^2}$
.1	.3369
.5	.38
1.0	.0976
2.0	.022
10.0	9×10^{-5}

Table

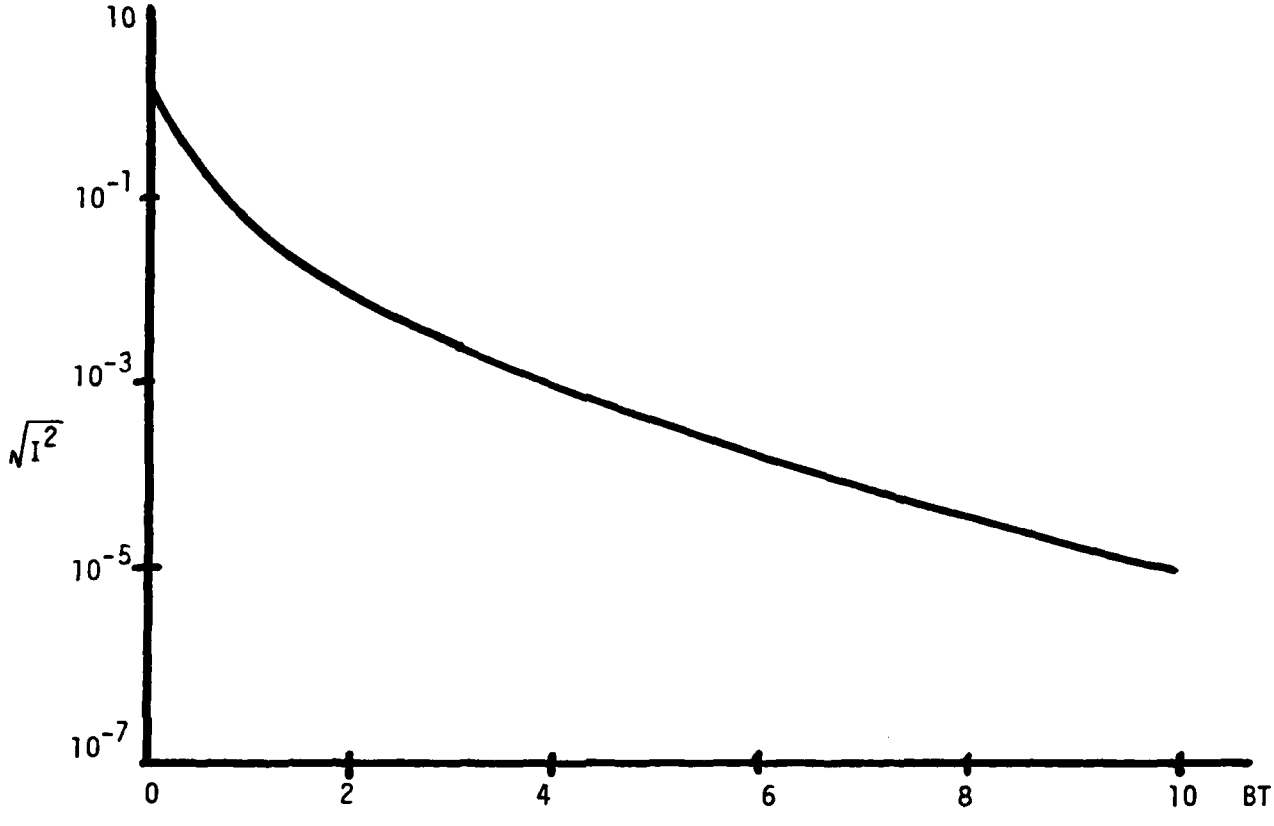

Figure 21. Jitter vs BT.

The results show the intersymbol effect for a PCM baseband waveform with a baseband bandwidth of B. This can be converted to an equivalent RF bandwidth around the carrier frequency. The result is shown in Figure 22 for a 12.5 Mbps bit rate. The bit timing error as a function of RF bandwidth is summarized in Figure 22.

Simulation - Symmetric RF Filtering

A simulation study was implemented to obtain an alternate assessment of symmetric RF filter effects. A more detailed DTTL block diagram is presented in Figure 23. The lower branch of this loop combined with the preceding RC circuit, acts as a mid-bit integrator which integrates the waveform over a bit period. If the loop is in perfect sync , the integration period starts at the middle of each bit. Any timing error in the loop displaces the integration period producing a nonzero error term. The error quantity is accumulated by the digital filter whenever a data transition is detected in the upper branch. The polarity of this error depends on the direction of the associated data transition and is also controlled by the upper branch. Figure 24 illustrates a one-zero bit pattern. The difference between the shaded areas A and B is used as the error term in the loop. A nonzero error will force the loop for automatic correction.

In the case of a nonsymmetric pulse or the presence of ISI, the total shaded area of Figure 24 will not vanish even when the synch is achieved, and thus the loop will incorrectly assume a different timing position with respect to data. In practice, because of limitations of the overall system, ISI will be present. Hence, contribution of waveform distortion to the loop must be considered. Since a typical communication system contains many units or filters with linear

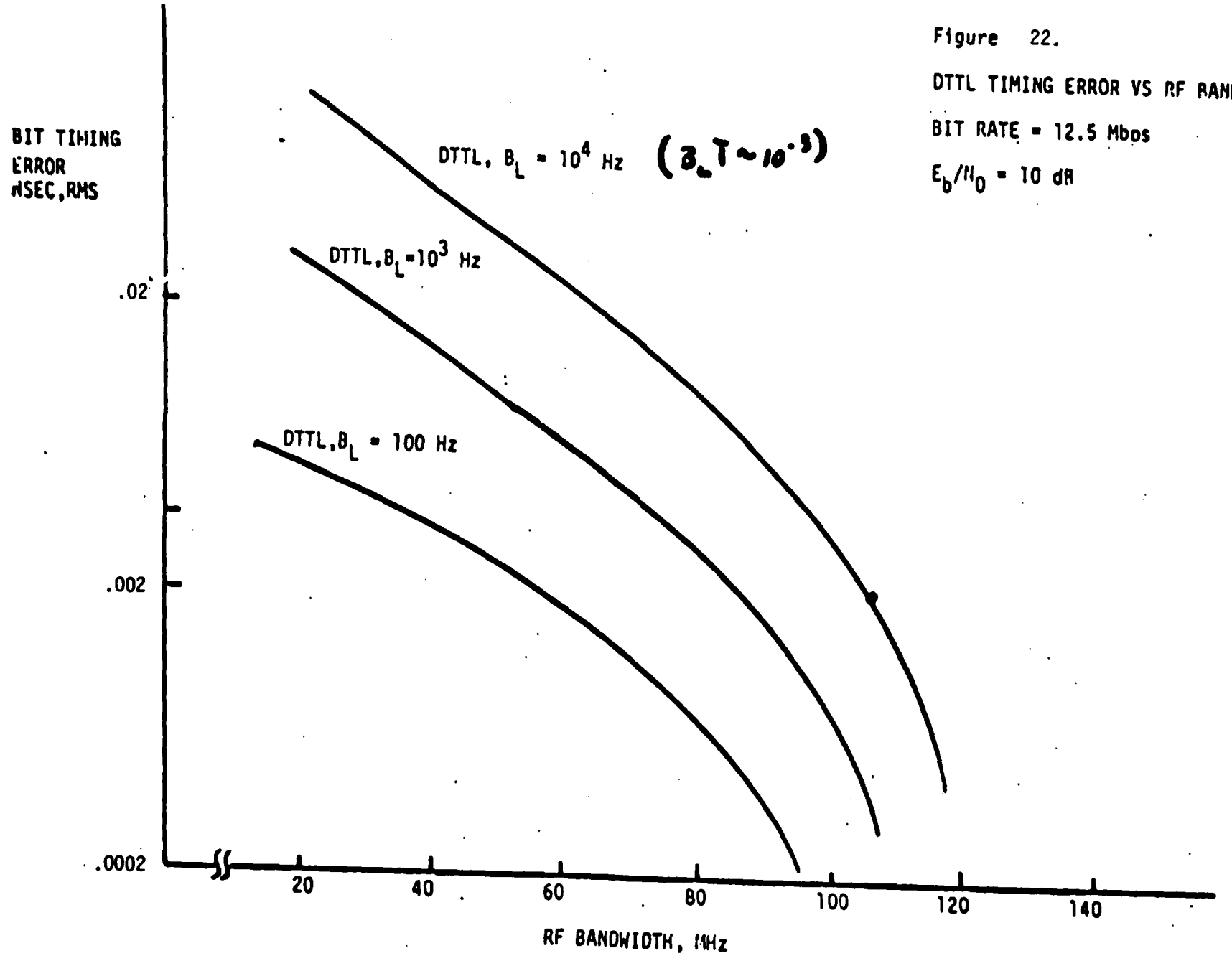

Figure 22.

DTTL TIMING ERROR VS RF BANDWIDTH

BIT RATE = 12.5 Mbps

E_b/N_0 = 10 dB

Figure 23. MODIFICATION TO IMPROVE PERFORMANCE

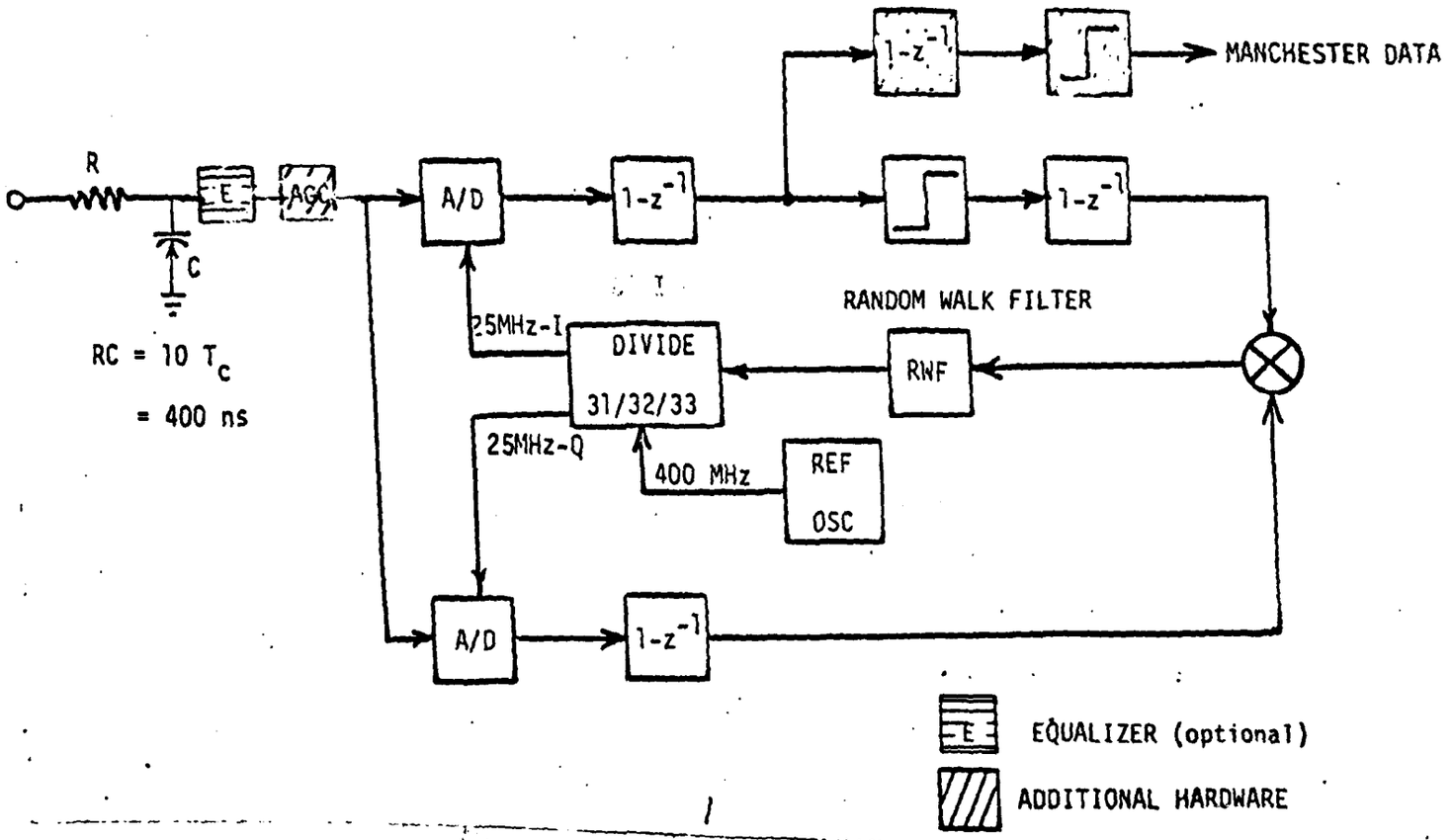

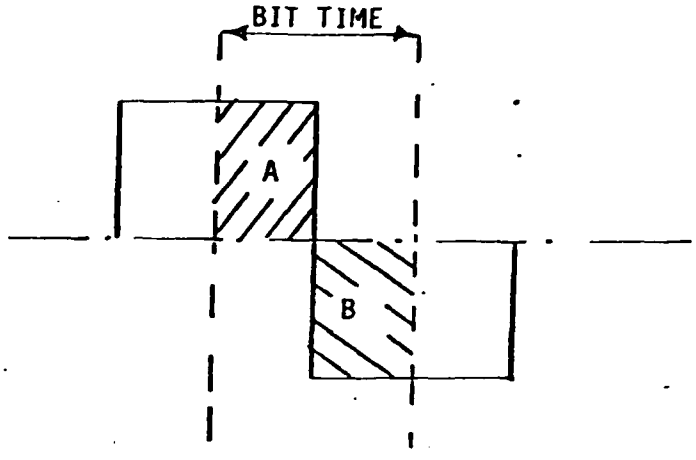

Figure 24 One Zero Bit Pattern with No Distortion.

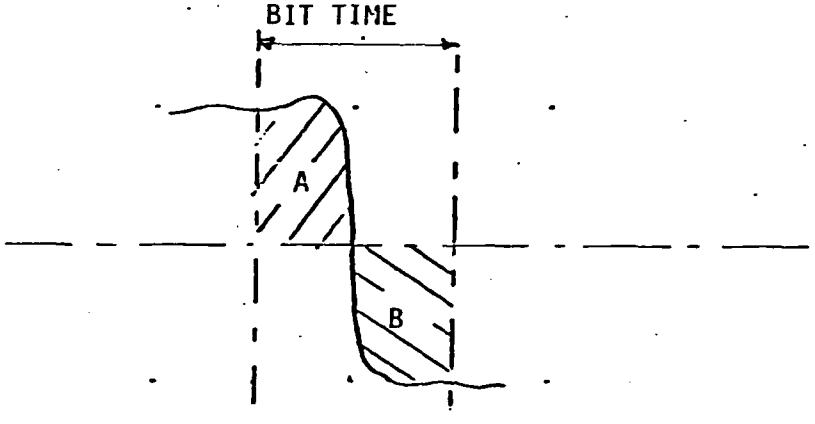

Figure 25. One Zero Bit Pattern After Filtering

behavior, a reasonable approach would be to model the overall system by a linear filter of proper bandwidth and roll off characteristic. Here, it is assumed that the system frequency limitation can be modeled by a 5 pole Butterworth filter, and we would like to specify the RF bandwidth such that the ISI contribution to the loop becomes negligible. The baseband signal under consideration is of NRZ type.

The effects of waveform distortion on bit synchronizer can be viewed as an introduction of a jitter and a DC error in the loop. The DC error is due to asymmetry of a pulse while the jitter is a result of pulse tail contribution of the previous bits to the integration interval. Since only adjacent pulses of different polarity can contribute to the error term in the loop, Figure 25 illustrates a distorted one-zero bit pattern. Quantity |A-B| of this figure is actually the DC timing error in the loop if proper scaling is done. This error can be measured in percent of the bit time, i.e., a 50% error corresponds to the area under one bit.

The jitter in the loop is caused by the decaying, but nonzero, tails of infinite number of pulses transmitted earlier than the bit under consideration. The contribution of these tails to the integration interval is of statistical nature and, in general, is difficult to derive its distribution. However, an upper bound can be established for the timing jitter by summing the absolute values of contributions due to a finite number of pulses.

Figure 26 illustrates a single pulse function after undergoing a five pole Butterworth filter of BT = 2 (B stands for RF bandwidth, T is the bit time). The dotted curve of the same figure corresponds to BT = 200. The ringing phenomena at the edges, BT = 200, is due to limited

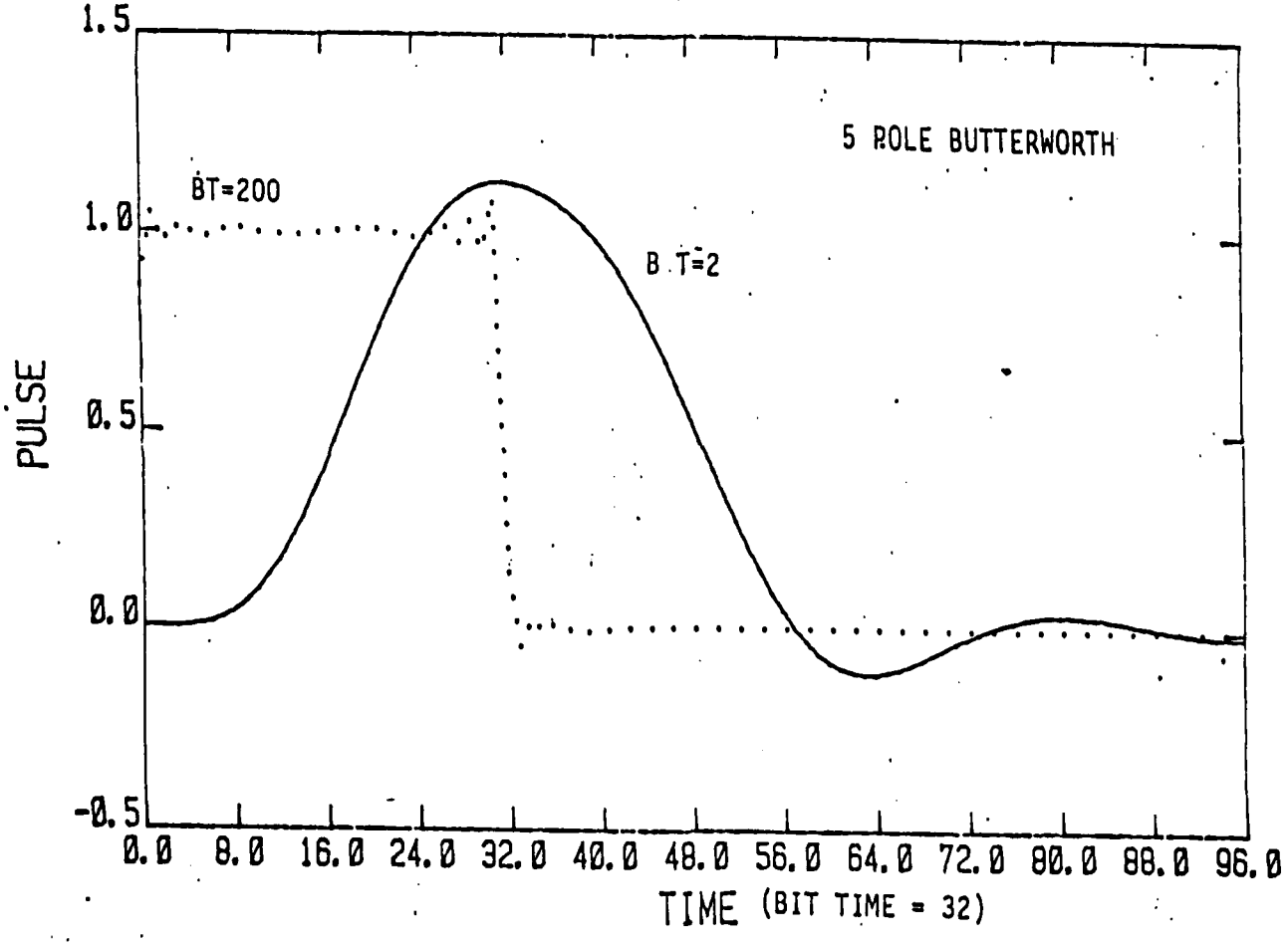

Figure 26 Pulse Shape After Filtering.

resolution of the simulation package. Figure 27 illustrates the case of BT = 10 and BT = 50. Figure 28 shows a one-zero bit pattern for BT = 2 and 10. The shaded area (BT = 10) of this figure corresponds to DC timing error.

Figure 29 illustrates the timing error versus BT (product of bandwidth and bit time). For a PCM baseband waveform, B stands for RF bandwidth while for Manchester code, it represents the baseband bandwidth (multiply by 2 to get RF), and T stands for bit time. For a data rate of 12.5 Mbps, T equals 80 ns. Chip time is also 80 ns for PCM code, but it equals 40 ns for Manchester code. The solid curve indicates the worst case jitter while the dashed curve shows the worst case DC error. It appears that the jitter term vanishes more rapidly than the DC term. Note that the jitter is averaged out by the narrow loop, while the DC error depends on data transition rate and is not averaged out by the loop.

To generate curves of Figure 29, frequency domain filtering was performed with each bit represented by 64 samples with frequency spectrum sampling resolution of 64/2048 or 1/32. The software accuracy is shown in Figure 29 by dotted straight lines. With a spec of 2.5 ns quantization error for the digital oscillator, the rms accuracy of the oscillator is also shown in Figure 29. The dotted straight lines represent this accuracy for a PCM waveform (chip time is 80 ns), and the dashed straight lines illustrate the same accuracy for a Manchester coded waveform (chip time is 40 ns). Incidentially, the software accuracy and oscillator accuracy for PCM case are approximately equal.

To select the desired filter bandwidth, plots of Figure 29 can be

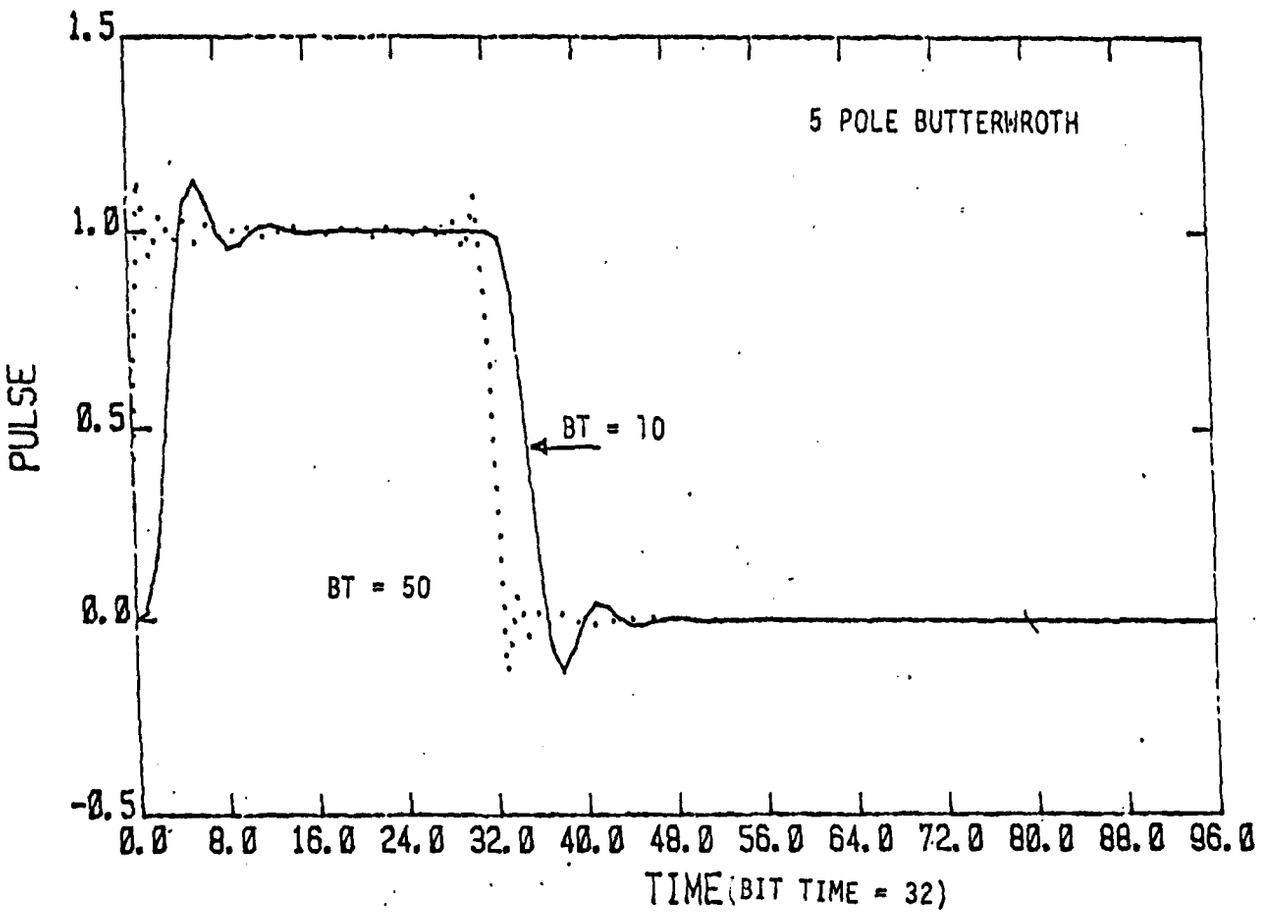

Figure 27.Pulse Shape After Filtering.

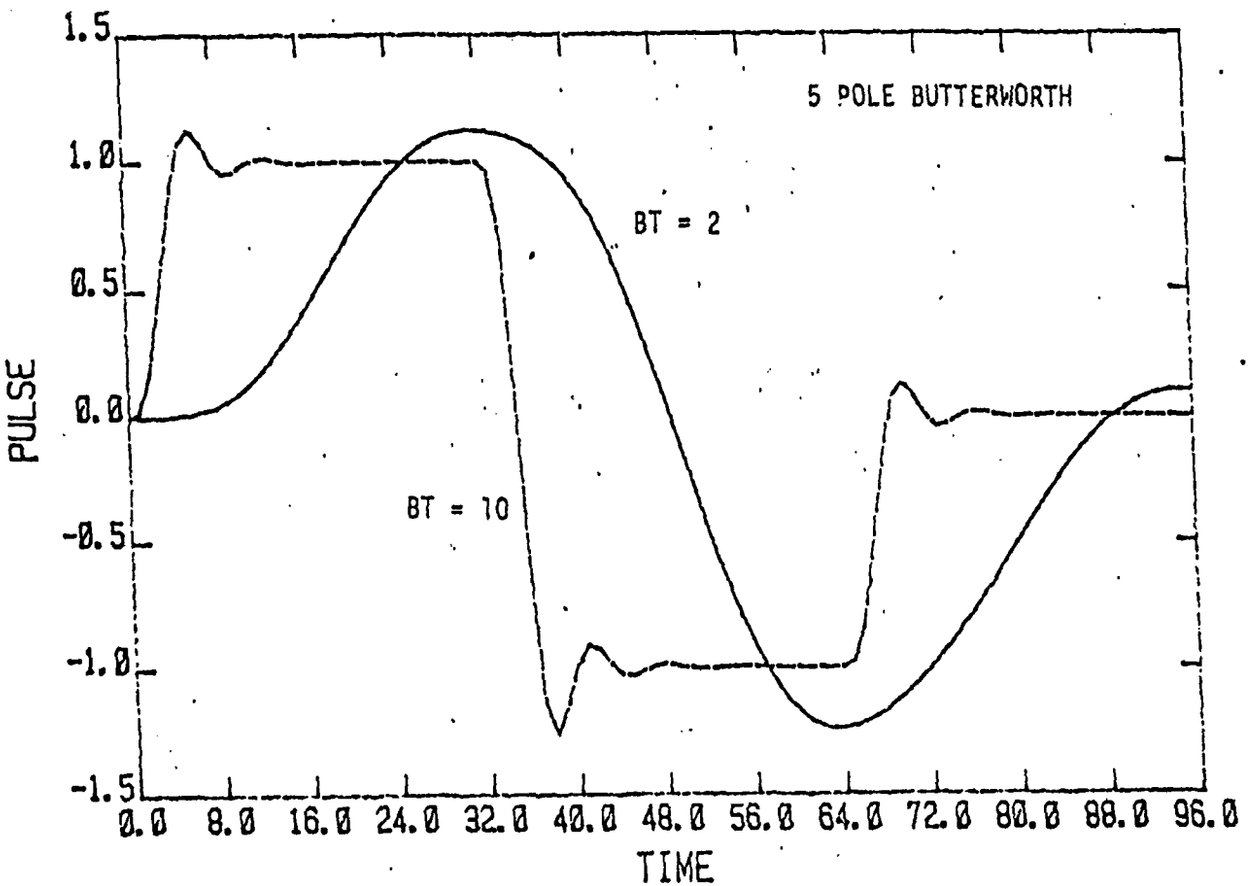

Figure 28. A One Zero Bit Pattern After Filtering.

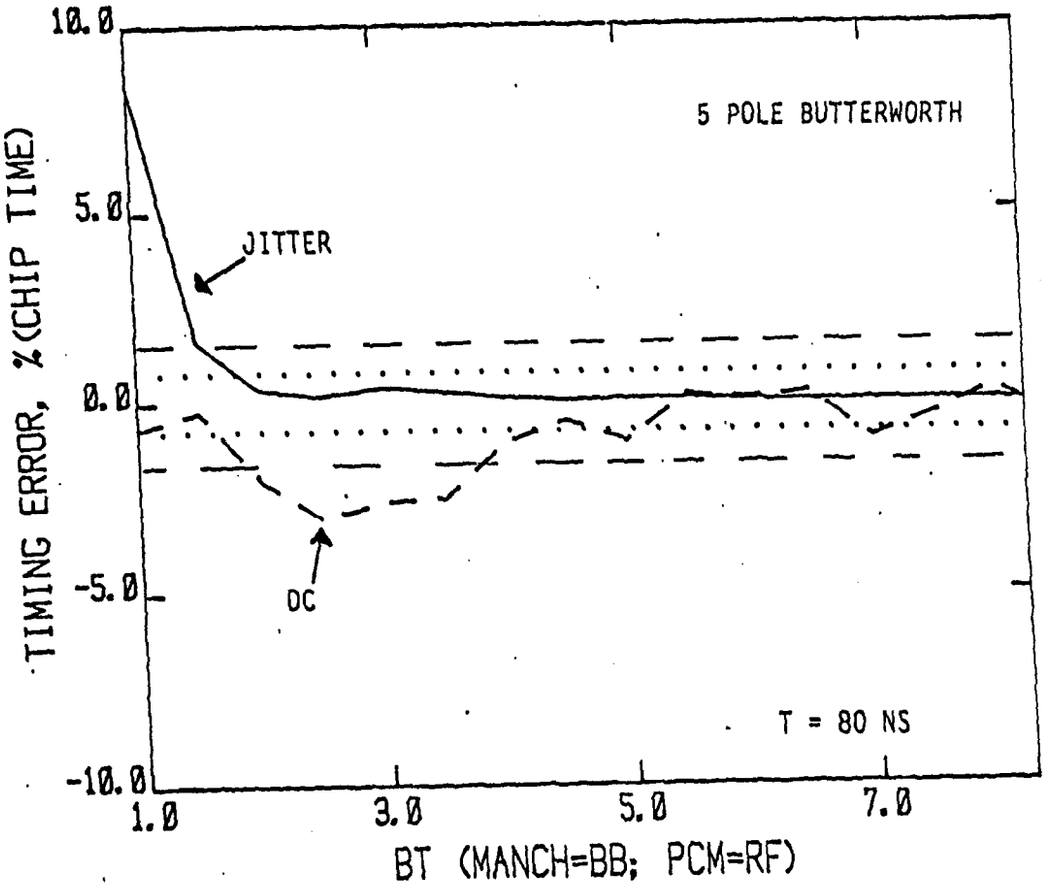

Figure 29. Timing Error in DTTL

utilized. One reasonable criterion to select the bandwidth is to choose a BT value that the DC timing error remains smaller than the rms oscillator accuracy at least by a small margin. Application of this method to Figure 29 reveals that the BT requirement for PCM signal is 7 and for Manchester signal is 10. The equivalent RF bandwidths for the above two cases are 87.5 MHz and 125 MHz, respectively.

Figures 30 and 31 illustrate the timing error due to 3 and 10 pole filters, respectively. The following table summarizes the results for 3, 5 and 10 pole filters.

Figure 32 illustrates the timing error due to a 10-pole phase equalized Butterworth filter. It apears that the DC error is completely diminished and thus the requirements are determined by the jitter term. The required RF bandwidth is approximately 15 MHz for PCM and 30 MHz for Manchester signal: a considerable saving compared to unequalized system.

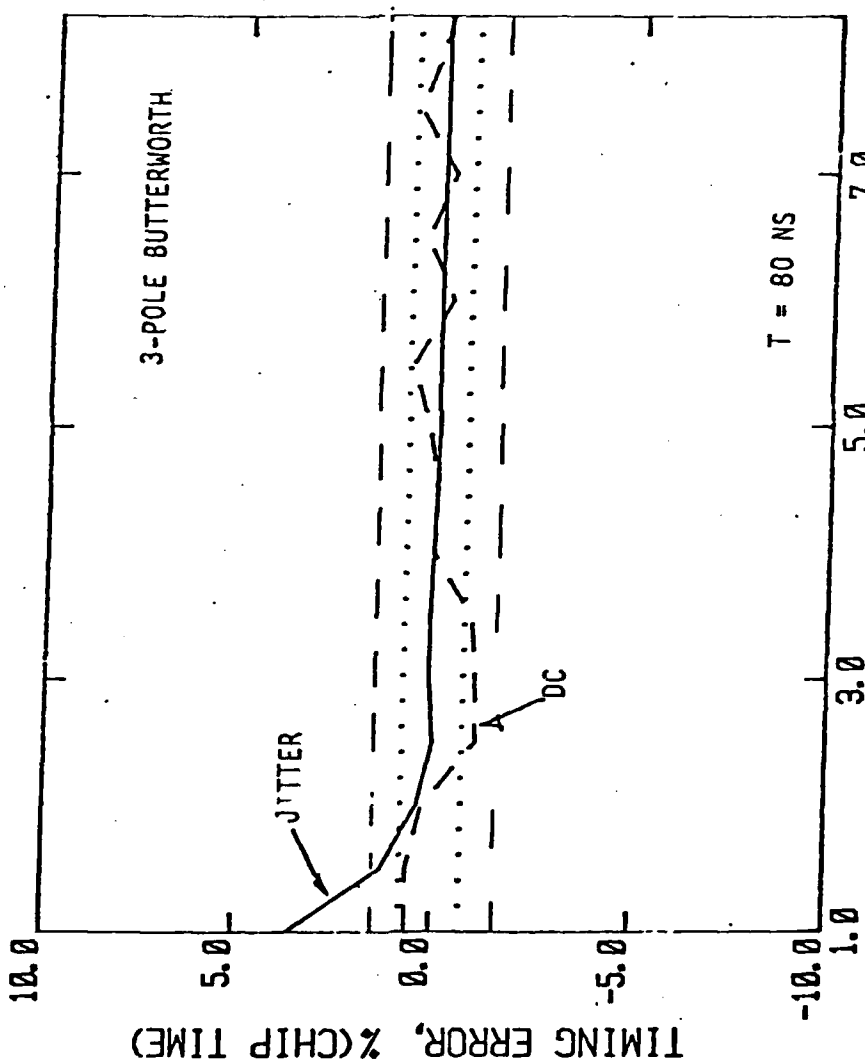

Figure 30. Timing Error in DTTL

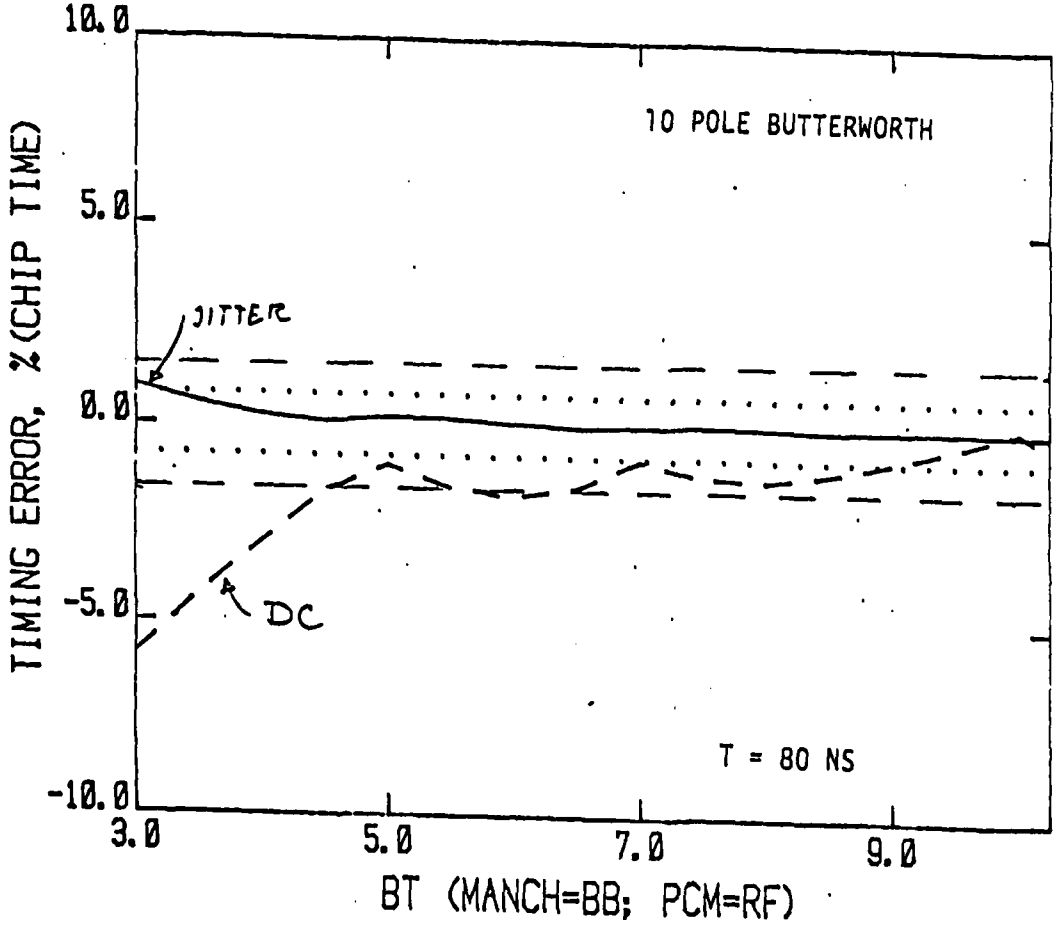

Figure 31. Timing Error in DTTL

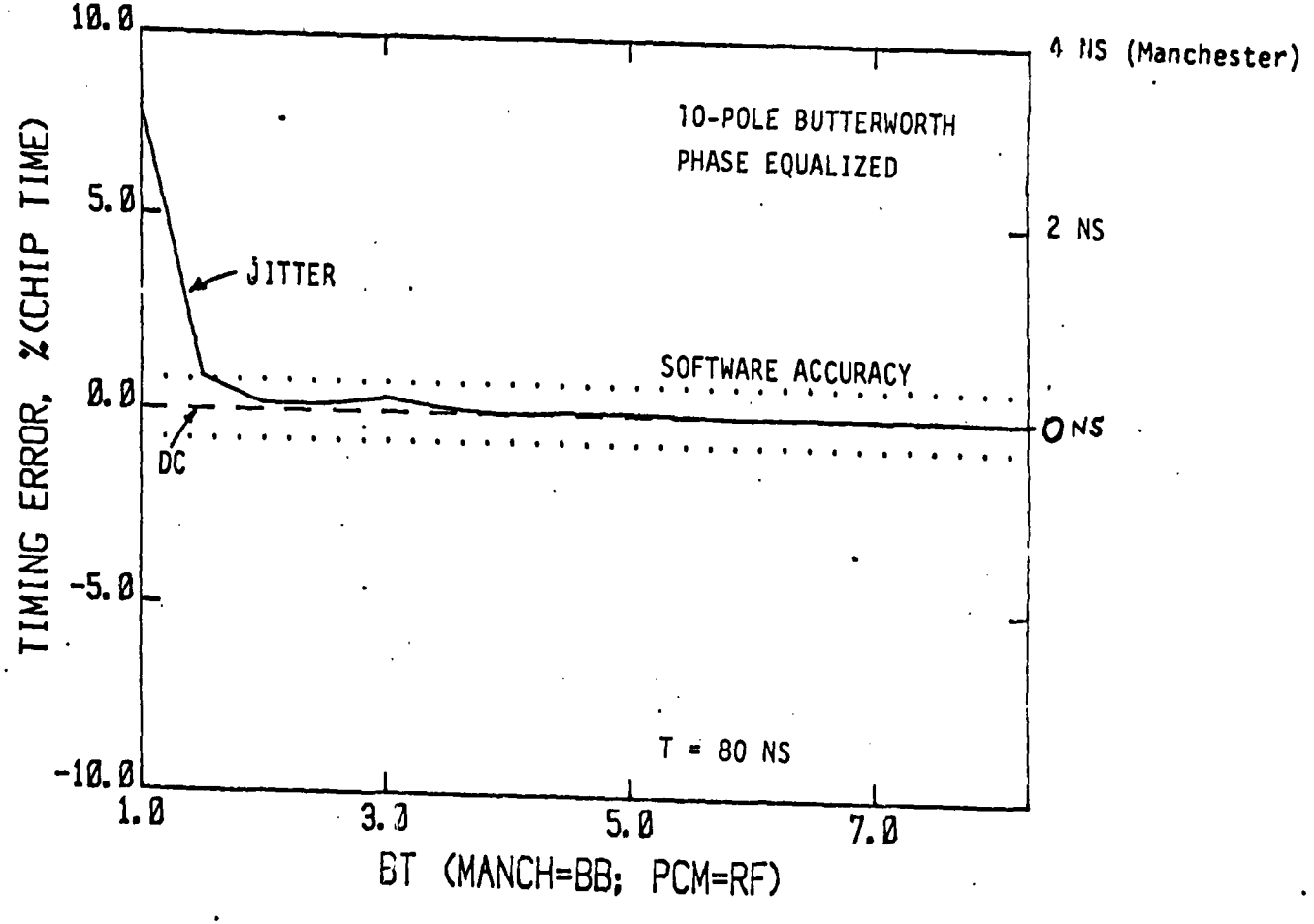

Figure 32. Timing Error in DTTL

4.3 Simulation - Phase Error Processes Caused By Asymmetric RF Filtering

Although phase-locked loop performance evaluation in the presence of thermal noise is very well understood; the effect of intersymbol interference on loop performance has not been fully investigated. In a recent work by Davidov [1], the performance of first order BPSK Costas loop in presence of band limited channel was considered. This work included a study of the phase error process and consequently showed that this process consists of three terms: the noise free, zero seeking error signal, the ISI noise, and the thermal related noise. Because the error process is cyclostationarity, it was possible to derive the equations for all three components of the error process by performing time averaging operation over the bit period T and also utilizing Fourier series expansion.

This work has been extended for the case where the channel filter is asymmetric. The main objective is not to explicitly derive the probability density function (pdf) of the tracking phase error process ϕ, but to examine the problems created by asymmetric RF filtering of data and hence suggest a specification technique for such RF filters in a time transfer system's context.

The Error Process in a First Order Loop

Let s(t) denote the bi-level baseband signal. If a_m can only assume one of the two values $\pm\sqrt{P_s}$ with equal probabilities, this signal can be presented as

$$s(t) = \sum_m a_m p(t-mT) \qquad (41)$$

where p(t) represents a pulse with duration T. After modulation is

performed by the mixer, an RF signal of form $s(t)\cos(\omega_0 t+\phi)$ is generated where ω_0 is the carrier frequency, see the Figure 33 below.

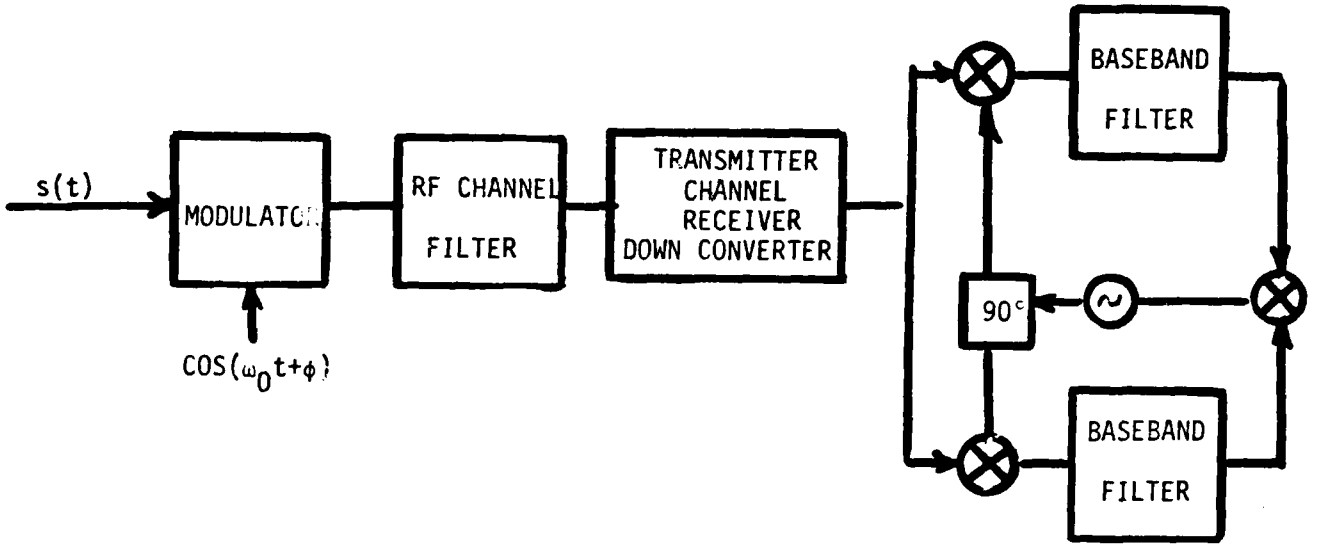

Figure 33. Modem Configuration for Costas Demodulation.

The output of the asymmetric RF filter is no longer a single inphase signal. This output consists of a pair of signals in quadrature. The inphase and quadrature signal components are given as

$$s_I(t) = \sum_m a_m g_I(t-mT)$$

$$s_Q(t) = \sum_m a_m g_Q(t-mT) \qquad (42)$$

where $g_I(t)$ and $g_Q(t)$ are the I and Q filter responses to a pulse of duration T, as shown in the figure below, 34.

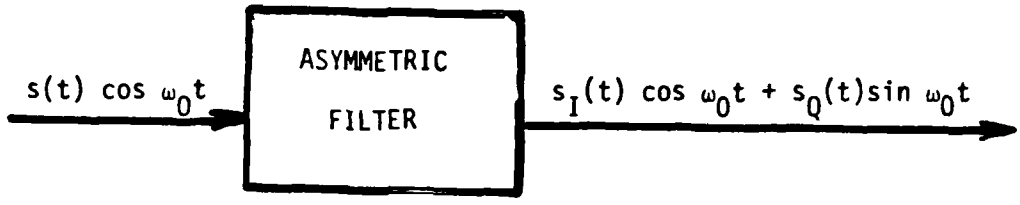

Figure 34. Asymmetric Filtering.

The I and Q filter transfer functions are defined by

$$H_I(f) = \frac{H_1(f)+H_2(f)}{2}$$
$$H_Q(f) = \frac{H_2(f)-H_1(f)}{2j} \qquad (43)$$

where $H_1(f)$ and $H_2(f)$ can be obtained from the asymmetric filter transfer function, $H(f)$, as

$$H_1(f) = H(f-f_0)U(f-f_0)$$
$$H_2(f) = H(f+f_0)U(f_0-f)$$

It can be shown that the tracking error process is given by

$$e(t) = \frac{1}{2}[s_I^2(t)-s_Q^2(t)]\sin 2\phi + s_I(t)s_Q(t) \cos 2\phi + n(t) \qquad (44)$$

where $n(t)$ is the thermal noise related interference. If the RF filter were symmetric, $H_Q(f)$ and consequently $s_Q(t)$ would become identical to

zero. Therefore, in the symmetric filter case, e(t) is given by

$$e(t) = \frac{1}{2} s^2(t) \sin 2\phi + n(t) \tag{45}$$

where s(t) is the symmetric filter response to the signal.

Computation of the ISI Noise

Let's substitute equation (42) in (44)

$$e(t) = \frac{P_s}{2} \{\sum_m [g_I^2(t-mT) - g_Q^2(t-mT)]\} \sin 2\phi$$

$$+ P_s \sum_m g_I(t-mT) g_Q(t-mT) \cos 2\phi + u(t) + n(t) \tag{46}$$

where u(t) is the ISI related noise consisting of three terms $u_1(t)$, $u_2(t)$, and $u_3(t)$ given as

$$u_1(t) = \frac{1}{2} \sum_{m \neq n} a_m a_n g_I(t-mT) g_I(t-nT) \sin 2\phi$$

$$u_2(t) = \frac{1}{2} \sum_{m \neq n} a_m a_n g_Q(t-mT) g_Q(t-nT) \sin 2\phi \tag{47}$$

$$u_3(t) = \sum_{m \neq n} a_m a_n g_I(t-mT) g_Q(t-nT) \cos 2\phi$$

For the cyclostationary process e(t), the noise free zero seeking voltage is given by

$$f(\phi) = K \frac{P_s}{2} \int_0^T \sum_m [g_I^2(t-mT) - g_Q^2(tmT)] \sin 2\phi$$

where K is the loop gain. Since $f(\phi)$ is a periodic signal, it can be

expanded in a Fourier series and using the Poisson summation formula one gets

$$f(\phi) = \frac{K}{T}\frac{P_s}{2}\left[\int |G_I(f)|^2 df - \int |G_Q(f)|^2 df\right]\sin 2\phi \qquad (48)$$

Using the same argument, it can be shown that

$$KP_s \sum_n g_I(t-nT)g_Q(t-nT) = \frac{KP_s}{T}\int G_I(f)G_Q^*(f)df \qquad (49)$$

The quantity in (49) indicates the bias in the loop. Thus, the phase bias ϕ_B is given by

$$\phi_B = \frac{1}{2}\arctan\left(-\frac{2\int G_I(f)G_Q^*(f)df}{\int |G_I(f)|^2 df - \int |G_Q(f)|^2 df}\right) \qquad (50)$$

From the above equation one can see that ϕ_B can vanish only if

$$D = \int G_I(f)G_Q^*(f)df = 0 \qquad (51)$$

If G(f) denotes the Fourier transform of p(t), then

$$\begin{aligned} G_I(f) &= G(f)H_I(f) \\ G_Q(f) &= G(f)H_Q(f) \end{aligned} \qquad (52)$$

Hence,

$$D = \int |G(f)|^2 H_I(f)H_Q^*(f)df \qquad (53)$$

To understand D better, let's write $H_I(f)$ as

$$H_1(f) = a(f) + jb(f) \tag{54}$$

where $a(f)$ and $b(f)$ are two real functions. It can be seen that

$$D = -\frac{1}{2}\int_{-\infty}^{\infty} |G(f)|^2[a(f)b(-f)+a(-f)b(f)]df$$

or (55)

$$D = -\int_{0}^{\infty} |G(f)|^2[a(f)b(-f)+a(-f)b(f)]df$$

Next, we compute the power spectral densities of $u_1(t)$, $u_2(t)$ and $u_3(t)$ at f=0. The results are stated below

$$S_{u_1}(f=0,\phi) = \frac{K^2}{2} P_s^2 \left[\frac{1}{T^2} \sum_m \int |G_I(f)|^2 |G_I(\tfrac{m}{T} - f)|^2 df \right.$$

$$\left. - \frac{1}{T} \left(\int |G_I(f)|^2 df\right)^2 \right] \sin^2 2\phi$$

$$S_{u_2}(f=0,\phi) = \frac{K^2}{2} P_s^2 \left[\frac{1}{T^2} \sum_m \int |G_Q(f)|^2 |G_Q(\tfrac{m}{T} - f)|^2 df \right.$$

$$\left. - \frac{1}{T} \left(\int |G_Q(f)|^2 df\right)^2 \right] \sin^2 2\phi$$

$$S_{u_3}(f=0,\phi) = K^2 P_s^2 \left[\frac{1}{T^2} \sum_m \int G_I(f) G_Q(-f) G_I(\tfrac{m}{T} - f) G_Q(f - \tfrac{m}{T}) df \right.$$

$$- \frac{1}{T} \iint G_I(f) G^*_Q(f) G^*_I(\lambda - f) G_Q(\lambda - f) d\lambda df \Big] \cos^2 2\phi$$

$$\left. + \frac{1}{T^2} \sum_m \int G_Q(f) G_I(-f) G_I(\tfrac{m}{T} - f) G_Q(f - \tfrac{m}{T}) df \right] \cos^2 2\phi$$

(56)

Since three noise terms u_1, u_2, and u_3 are correlated, the cross spectral densities of these noise terms at f=0 are in general nonzero. These cross densities have not been evaluated here to keep this memo brief.

The Demodulated Signal

The demodulated signal M(t) which appears at the I arm of the loop is described by

$$M(t) = s_I(t) \cos \phi + s_Q(t) \sin \phi + n(t) \qquad (57)$$

A nonzero phase error ϕ distorts the demodulated signal in two ways. First, it decreases the signal power proportional to $\cos^2 \phi$, second it introduces an interference term with power proportional to $\sin^2 \phi$. This interfernce can only be eliminated by a symmetric RF filter or the condition that $\sin \phi = 0$. Since the asymmetric filter will generate a bias in ϕ, hence the interference waveform will distort the demodulated signal unless the condition given in (55) is met.

Conclusion and Suggestions

It appears that asymmetric filtering of the signal in the RF domain generates two deleterious effects:

1. Introduction of additional ISI terms in the tracking loop; hence, increased interference power in the loop.
2. Addition of a bias term in the phase noise process.

To eliminate the above stated problems, the RF domain filtering at the front end of the tracking loop symmetrical or it must be avoided. Assuming that the asymmetry in the RF filter is caused by hardware inaccuracies, a practical method of avoiding distortions due to asymmetric filtering would be to perform the filtering task in baseband at the arms of the Costas loop. By utilizing this technique, the ISI distortion in the loop will not totally disappear but it will lessen. The bias error in the loop shown in Figure 33, however, will totally

vanish. A series of illustrative examples are given in Appendix II.

4.4 System Phase Noise Caused by Adjacent Channel Interference

The purpose of this section is to determine the minimum necessary spectrum separation between two adjacent channels in a single communications terminal in order to eliminate the interference (ACI) phenomenon. The signaling format is biphase NRZ. To avoid intersymbol interference (ISI) in each channel both transmitter and receiver filters (Chebyshev) are assumed wideband. The interfering adjacent channel power is given to be 110 dB above the desired signal. It is also assumed that matched filtering technique is employed for detection of the NRZ data.

An approximate analytical approach is first used to select the suitable channel separation $\Delta F'$, where $\Delta F'$ is in units normaalized to the data bandwidth. A computer simulation program is subsequently utilized to obtain the answer more accurately. The two approaches provide similar results.

Assume the symbol rate is unity and that both transmitter and receiver filters are 6-pole with a normalized bandwidth 4. Let's investigate the problem with a frequency separation of $\Delta F = 12$. Observing Figure 35, the adjacent channel is filtered as

$$|H(f)|^{-2} = [2(1+\pi^2 f^2)][1+(.5f)^{12}][1+.5^{12}(f-12)^{12}] \quad (58)$$

In the above equation, the first term corresponds to a matched filter associated with the data rate of unity, the second and third terms correspond to two 6-pole filters centered at F=0 and F=12, respectively. Since the maximum interference power occurs at F=12, it is constructive to compute $|H(f=12)|^{-2}$,

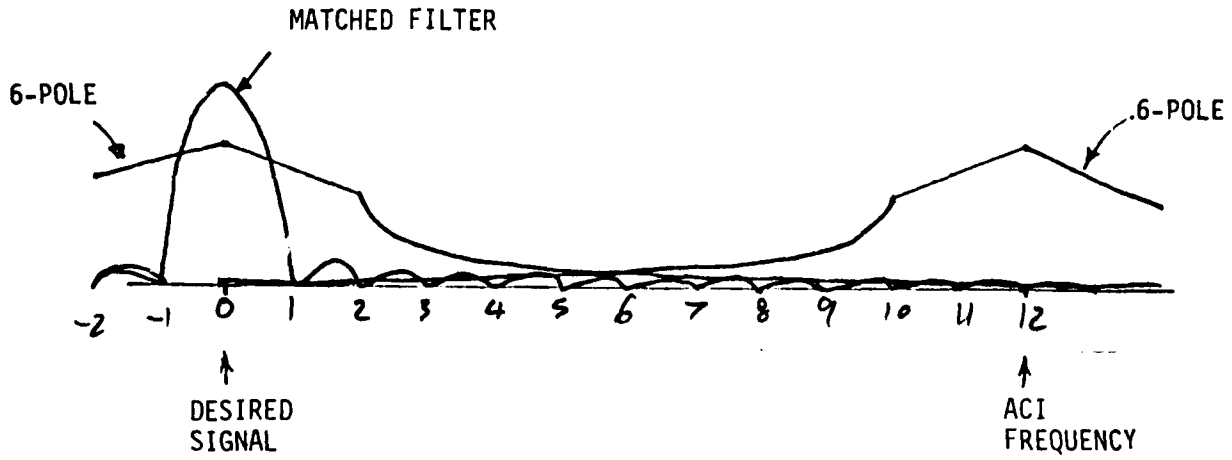

Figure 35.The Desired Signal is Protected From ACI By Two Chebyshev Filters and One Matched Filter.

$$|H(f=12)|^{-2} \simeq 2(1+1440)(1+6^{12}) \simeq 6.3 \times 10^{12}$$

or

$$|H(12)|^{2} \simeq 1.6 \times 10^{-13}$$

Now we may compute the power leakage by multiplying the above term by the power in the adjacent channel. Let P_L denote the power leakage

$$P_L = 10^{11} \times 1.6 \times 10^{-13} P_s = 1.6 \times 10^{-2} P_s$$

where P_s denotes the desired signal power. Thus, the above power in dB is

$$10 \log \frac{P_L}{P_s} \simeq -18 \text{ dB}$$

The computed adjacent channel attenuation seems sufficient to eliminate the interference.

Actually, the above analysis is rather a conservative one. To illustrate this, a computer simulation program is utilized. Here it is assumed that the modulator produces ideal NRZ pulses and also further assumed that the receiver carrier synchronizer and the bit sync circuits are error free. Figure 36 illustrates P_E versus E_b/N_0 for a number of channel separations where the bit rate is 12.5, Chebyshev filters are 50 MHz with .25 dB ripple. It appears that 125 MHz channel separation is sufficient for almost totally eliminating ACI. According to our previous conservative study, a separation of 150 MHz would attenuate the interference to 18 dB below the signal power.

Figure 37 illustrates the same situation with 6-pole Chebyshev filter bandwidth increased to 100 MHz. In this case, a separation of

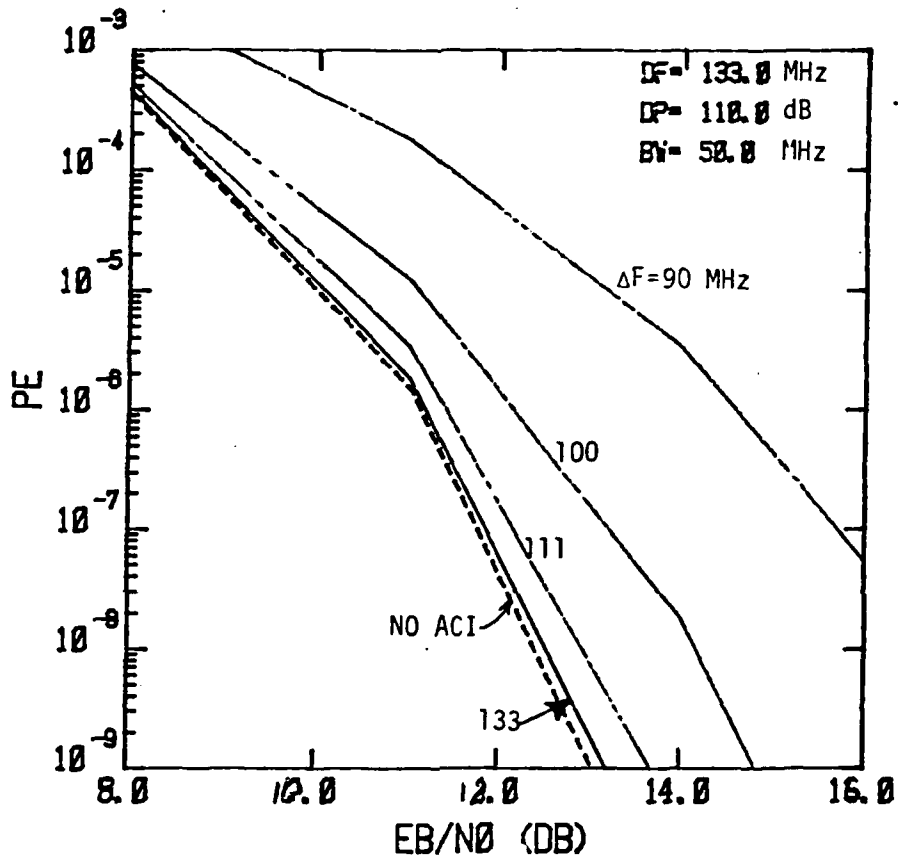

Figure 36 Adjacent Channel Interference and the Error Probability.

- SIGNAL IS BIPHASE NRZ
- BIT RATE IS 12.5 Mbps
- 50 MHz CHEBYSHEV FILTERS WITH .25 dB RIPPLE (6-POLE)

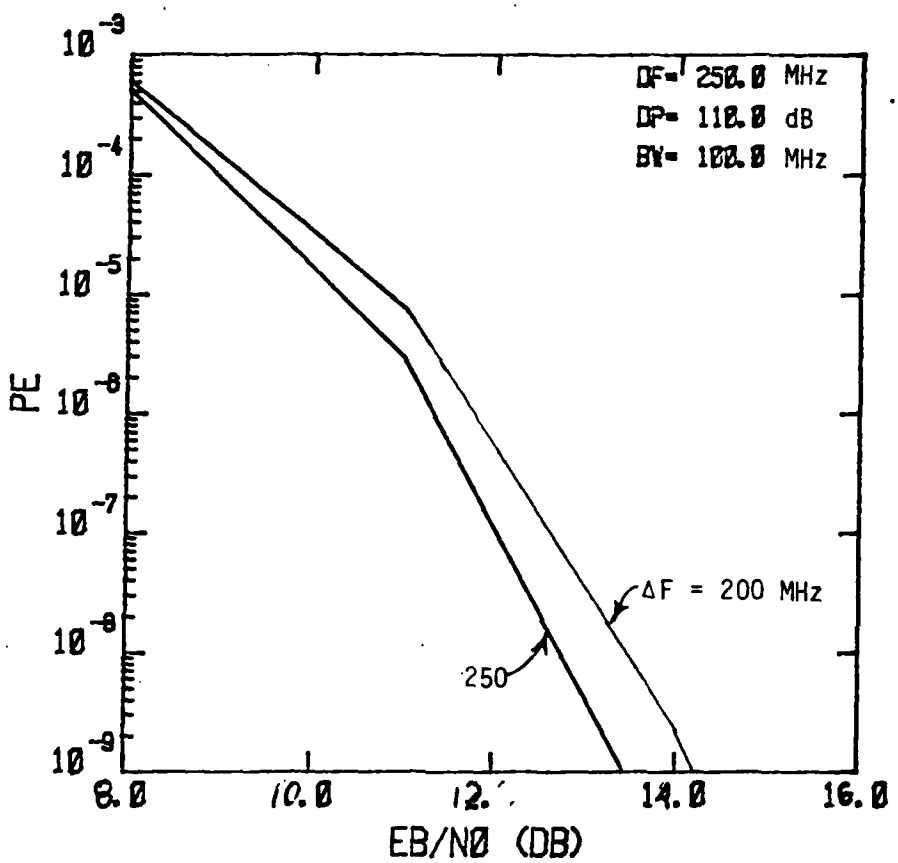

Figure 37. Adjacent Channel Interference and the Error Probability.

- SIGNAL IS BIPHASE NRZ
- 125 Mbps DATA RATE
- 100 MHz CHEBYSHEV FILTERS WITH .25 dB RIPPLE (6-POLE)

250 MHz can totally eliminate the undesired interference.

ACI in Costas Loop

Again we assume that the biphase NRZ data has a normalized rate of 1 and the channel filters are 6-pole with a bandwidth of 4. Further it is assumed that the channel filters prior to the Costas loop are 2-pole with bandwidth 4. The major power leakage in this scenario happens in frequencies between 0 to 2. Observing Figure 38, the following approximate calculation can be performed

$$\frac{P_L}{P} = .25|H_1(10)|^2 \bar{S}(10) + |H_1(12)|^2 \bar{S}(12).*$$

where H_1 denotes the 6-pole transmitter filter, and $\bar{S}$ denotes the interfering signal power average spectrum in the neighborhood of the desired frequency,

$$S(f) = \frac{\sin^2 \pi f}{(\pi f)^2}$$

But

$$\overline{\sin^2 \pi f} = .5$$

Thus

$$\frac{P_L}{P} = |H_1(10)|^2 \frac{.5}{100\pi^2} + |H_1(12)|^2 \frac{.5}{144\pi^2}$$

But

$$|H_1(10)|^2 \simeq \frac{1}{1+5^{12}} \simeq 4 \times 10^{-9}$$

$$|H_1(12)|^2 = \frac{1}{1+6^{12}} \simeq 5 \times 10^{-10}$$

*The factor .25 results from $|H_1(2)|^4$.

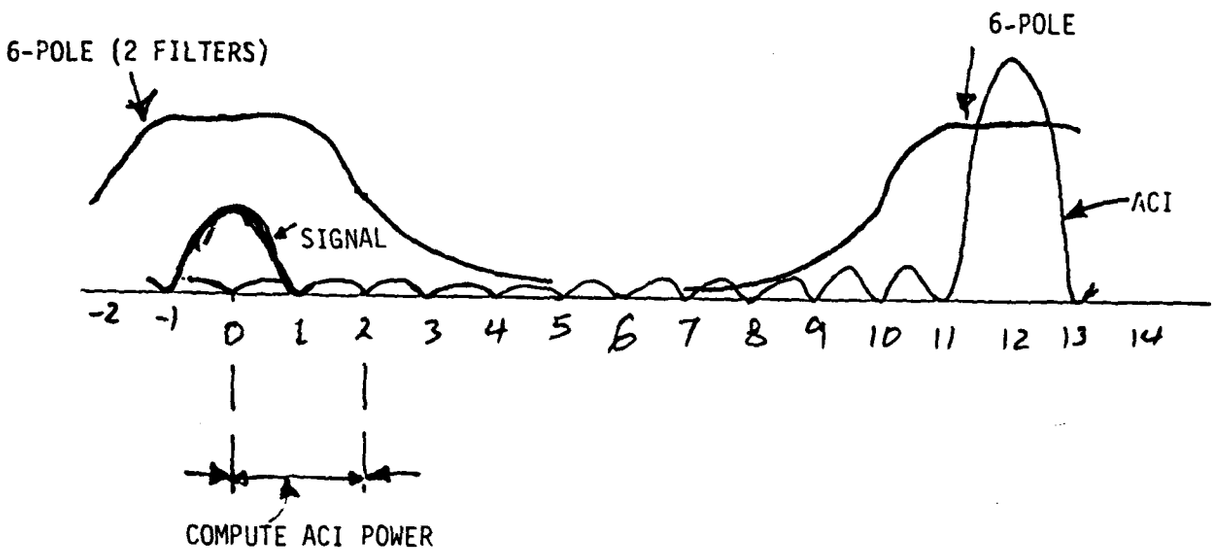

Figure 38 ACI Leakage in Costas Loop.

Thus if $\pi^2 \simeq 10$

$$\frac{P_L}{P} \simeq .25 \times .5 \times 10^{-3} \times 4 \times 10^{-9} + 3.5 \times 10^{-4} \times 5 \times 10^{-10}$$

$$= .5 \times 10^{-12} + 17.5 \times 10^{-14} \simeq 7 \times 10^{-13}$$

Since $P = 10^{11}$ is given

$$P_L = 10^{11} \times 7 \times 10^{-13} = .07$$

The interference power of .07 must be summed with the white noise power to illustrate the true performance of the Costas loop. For example, if the SNR at the front-end of the Costas loop is 10 dB in the absence of ACI, in the presence of ACI the SNR is given as

$$(SNR)_{\text{with ACI}} = \frac{1}{.1+.07} = \frac{1}{.17}$$

$$\simeq 7.7 \text{ in dB}$$

It appears that ACI distortion is equivalent to a loss of 2.3 dB in the input to Costas loop. Since the loop signal-to-noise ratio is much higher than the input SNR, the loss of 2.3 dB can easily be tolerated. In a narrowband loop, loss of 2.3 dB increases the phase jitter by 30%.

ACI in DTTL

Since the DTTL loop acts as an integrate and dump circuit, the matched filtering approach discussed earlier for estimation of the error probability also holds here. To use the result already obtained, we notice that the interference power entering the DTTL is .016 if the

signal power is taken to be 1. The interference power must be added to the thermal noise power to get the correct result. For example, if SNR = 10 dB in absence of ACI, then the new SNR is

$$SNR = \frac{1}{.1+.016} = \frac{1}{.116}$$

$$SNR \text{ in dB} = 9.4 \text{ dB}$$

This figure indicates a power loss of only .6 dB, which considering the narrow DTTL loop bandwidth, is negligible.

5 Summary of Link Specifications

This summary illustrates the communication channel specifications for reliable time and data transfer performance.

5.1 Single Channel Time and Data Transfer Subsystem

The single channel master/slave synchronization is achieved by the balanced technique as summarized below. The balanced system uses timing error control at the slave. The timing errors measured at the master are encoded and transmitted as a digital word in the frame to the slave. The decoded timing error word is then combined with the bit sync error measured at the slave to adjust the slave frame timing derived in the outer loop to derive its frame markers. The latter formats the slave frames, which are returned to the master.

It is shown that the above technique will operate in a stable mode only if the inherent stability error produced by the clocks over a frame period is smaller than the slave clock period t_0 (2.5 ns). It is also important that the master and slave modems are calibrated to avoid timing bias.

Master slave timing analysis has revealed that the performance upper bound of this system is equal to $t_0/2$. In general, depending on the bit sync performance and the E_b/N_0 ratio, the timing jitter may become considerably larger than $t_0/2$. It is shown that accumulation of two or more error samples to control the slave timing is helpful for approaching the above performance upper bound.

Single Channel Time Bandwidth Product BT

In this study channel bandwidth limitation and its effect on the bit sync (DTTL) was considered. An analytical method and a computer simulation were employed to determine channel BT product such that:

First, the DTTL jitter is less than the VCO quantization error; second, the DTTL bias is less than the VCO quantization error--VCO quantization error is about 3% of the bit time T. For the first constraint, the analytical method has selected a hypothetical worst case pulse shape, namely the sinc function. The integrals taken over periods T of the tail of the pulse were computed analytically. The computed values were squared and then summed to form the ISI power in the bit sync. Using a Gaussian model this power is summed with the thermal noise power in the loop and then phase timing jitter is computed.

The simulation has performed a similar technique replacing the sinc function by the response of a Butterworth filter of desired number of poles to a pulse. The integrals of the tail of the filter output over time periods T are computed. Then the sum of absolute values of the computed quantities is determined. Ignoring the thermal noise, the bit sync jitter is computed as a function of the BT product assuming $B_L T = 1$ where B_L is the bit sync loop bandwidth.

Similar answers have been produced by analytical and simulation, both techniques have produced close answers. To reduce the jitter to [illegible] requires that

BT	> 2	NRZ
BT	> 4	Manchester

Simulation has illustrated that the above BT numbers are not sufficient to eliminate bias in the timing loop. For bias controlling, the requirement is

BT	> 7	NRZ
BT	> 10	Manchester

Single Channel Phase and Amplitude Response

Ideally the channel is desired to maintain flat amplitude and linear phase responses throughout the bandwidth of the link spectrum. Any deviation from the ideal response will have adverse effect on the carrier tracking and the timing loops. Analysis has revealed that asymmetric RF channels introduce a DC phase error in the tracking loop. Furthermore, asymmetrically distorted RF channels add a data related interference to the demodulated signal. This interference can cause severe loss of the bit sync performance if not controlled. Clearly, the hardware specification must limit asymmetric channel distortion to an acceptable level.

Channel imperfections have been examined via several examples. Each example is used to determine the system tolerance to a specific type of distortion. The final result is determined such that the timing jitter caused by channel imperfection will be less than the VCO quantization error of .03T or 2.5 ns. The acceptable phase and amplitude distortions with respect to an ideal channel are given as

$$|\text{Phase Distortion}| < 3.5^{o}$$

$$|\text{Normalized Amplitude Distortion}| < .1$$

The above restrictions permit a nonsymmetric phase slope change and a nonlinear amplitude response as long as the inequalities are not violated.

The diagram on the next page outlines the RF channel distortions and their effects on synchronization loops. The channel is modeled by a low thermal noise linear filter where the phase and amplitude responses are considered separately. In the former case (phase alone) a wideband

CHANNEL PHASE AND AMPLITUDE DISTORTION EFFECTS ON CARRIER

AND BIT SYNCHRONIZATION LOOPS

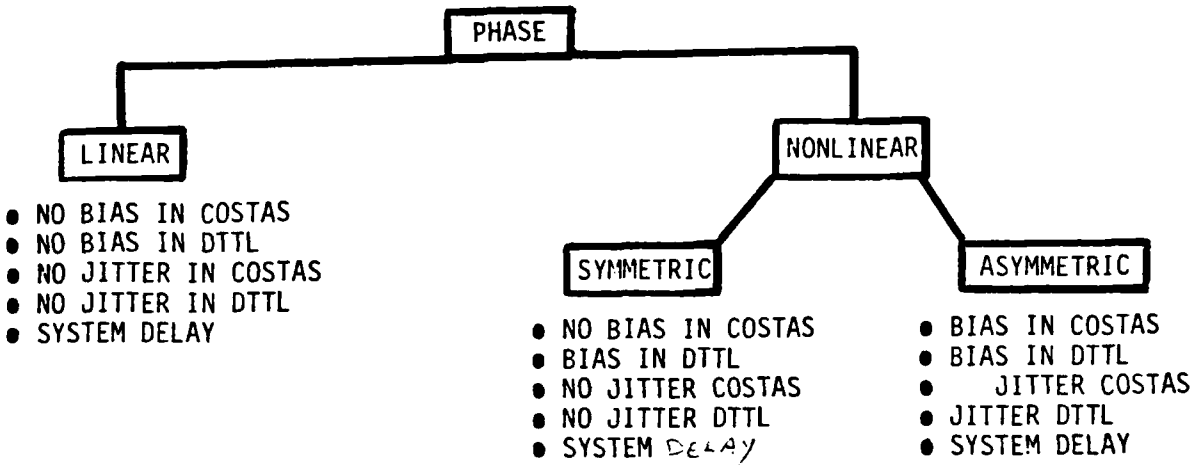

- NO BIAS IN COSTAS
- NO BIAS IN DTTL
- NO JITTER IN COSTAS
- NO JITTER IN DTTL
- SYSTEM DELAY

- NO BIAS IN COSTAS
- BIAS IN DTTL
- NO JITTER COSTAS
- NO JITTER DTTL
- SYSTEM DELAY

- BIAS IN COSTAS
- BIAS IN DTTL
- JITTER COSTAS
- JITTER DTTL
- SYSTEM DELAY

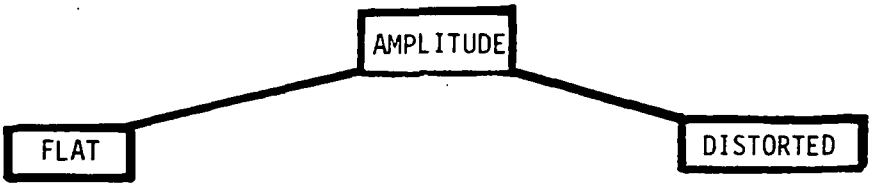

- NO BIAS COSTAS
- NO BIAS DTTL
- NO JITTER COSTAS
- NO JITTER DTTL
- NO SYSTEM DELAY

- NO BIAS COSTAS
- NO BIAS DTTL
- JITTER IN COSTAS
- JITTER IN DTTL
- NO SYSTEM DELAY

channel is assumed and in the latter case (amplitude alone) a phase equalized system is considered.

Each entry of the diagram is briefly explained in the following paragraphs, and whenever necessary each description is illustrated by an example. The case of wideband nonlinear phase channels will be discussed first.

Zero Jitter in Costas Loop

Section 2.4.1 gives the ISI noise power density in the loop as

$$S_{ISI}(f=0) = \frac{P_s^2}{2}\left[\frac{1}{T^2}\sum_m \int|G(f)|^2|G(f-\frac{m}{T})|^2df - \frac{1}{T}\left(\int|G(f)|^2df\right)^2\right]\sin^2 2\phi$$

where T is the bit time, P_s is the bit energy divided by T, G(f) is the distorted pulse spectrum, and ϕ is the tracking phase error.

Notice that the above power spectral density is independent of the channel phase response. In other words, only amplitude distortion occurs in the case of ISI noise in the loop.

DTTL Bias

The DTTL is modeled as a mid-bit to mid-bit integrator. An error term is accumulated whenever a data transition is detected. As a useful example to illustrate timing bias error caused by phase nonlinearity, consider small phase ripple distortion. Therefore, assuming the following channel model

$$H(\omega) = \exp[-j(b_0\omega - b_1 \sin \omega)]$$

and small ripple amplitude b_1, the channel response to a pulse, P(t), with duration T is represented by g(t) as

$$g(t) = P(t) + \frac{b_1}{2}[P(t+c) - P(t-c)]$$

If c = T/2, then

$$g(t) = P(t) + \frac{b_1}{2}[P(t+\frac{T}{2}] - P(t-\frac{T}{2})]$$

The following figure illustrates g(t) as a function of time.

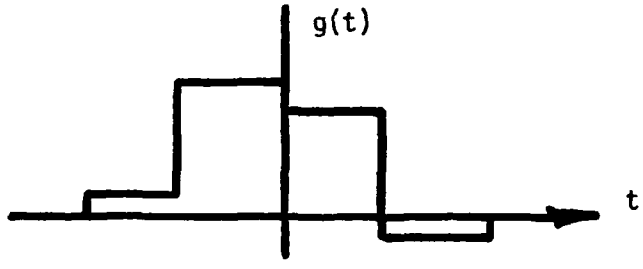

Clearly g(t) is asymmetric, hence the mid-bit to mid-bit integrator is bound to generate a bias error. Notice that for $c \geq T$, the small phase ripple imperfection imposes no distortion on the DTTL (no bias and no jitter).

Zero Costas Loop Bias

As discussed in the text, symmetric channels impose no bias on the carrier tracking loop. This fact can also be seen from the phase noise probability density function. The recovered carrier phase noise probability density function is stated here for convenience

$$P(\phi) \sim \frac{1}{\sqrt{1+R\sin^2 Q}} \left(\frac{\sqrt{1+1/R} + \cos\phi}{\sqrt{1+1/R} - \cos\phi} \right)^{\frac{\alpha}{2R\sqrt{1+1/R}}}$$

where Q is twice the phase error, R is the ratio of the ISI noise to thermal noise power, and α is (E_b/N_0) divided by loop $(B_L T)$.

Notice that $P(\phi)$ is symmetric, hence ϕ is mean zero.

Zero DTTL Filter

Figures 30, 31 and 32 of Section 2.3.3 illustrate that jitter in DTTL is caused byy amplitude distortionwhile bias is caused by phase distortion. Also the small phase ripple example discussed earlier can be used to show that symmetric phase distortion does not cause timing jitter.

System Delay

Unequalized physical channels introduce time delays in general.

Next, the column under asymmetric phase distortion is considered:

Costas Loop Bias

Equation 10 of Section 2.4.2 formulates Costas loop phase bias due to asymmetric signal filtering (RF filter). The phase bias equation is restated here:

$$Q_B = \frac{1}{2} \arctan\left(- \frac{2\int G_I(f)G^*_Q(f)df}{\int|G_I(f)|^2df - \int|G_Q(f)|^2df}\right)$$

$G_I(f)$ and $G_Q(f)$ are the inphase and quadrature channel responses to an input pulse, respectively. It can be shown that the above bias vanishes for channels with linear phase response even if the channel amplitude

response is asymmetrically distorted.

DTTL Bias

It was shown previously that nonlinear phase response is the source of DTTL timing bias. Since asymmetric distortion is a special case of nonlinear phase distortion, therefore the timing bias is also expected for the asymmetric case also.

Costas Loop Jitter

Asymmetric channel hase response causes amplitude distortion in the in-phase and quadrature channel responses. And imperfect amplitude response will in turn produce phase noise jitter in the Costas loop.

DTTL Jitter

Like the previous case, asymmetric channel phase response causes amplitude distortion, and amplitude distortion is a source of DTTL timing jitter.

System Delay

Any unequalized physical channel will introduce time delays.

Now, the case of imperfect amplitude response will be considered.

Zero Costas Loop Bias

Equation (3) can be utilized to illustrate that channels with linear phase and distorted amplitude do nt cuase tracking phase bias error.

Zero DTTL Bias

With symmetric amplitude distortion there is no timing bias since the pulse shape after passing through the channel remains symmetric. However, asymmetric amplitude distortion could cause DTTL timing bias if the tracking phase error is nonzero mean.

Costas Loop Jitter

Equation (1) can be used to determine Costas loop phase jitter due to channel amplitude distortion.

DTTL Jitter

Figure 32 of Section 2.3.3 illustrates the DTTL timing jitter due to a Butterworth phase-equalized filter. The imperfections in channel amplitude response causes pulse spreading. The symmetrically spread pulses interfer with one another giving rise to ISI noise and timing jitter.

No System Delay

Amplitude distortion does not cause system time delay.

Note that if the RF filtering operation in the receiver is performed in baseband rather than RF, the asymmetric column under the nonlinear phase subtitle will disappear. A baseband filter, unlike its RF counterpart, cannot be asymmetric.

Modulation Induced Tracking Error in the Carrier Tracking Loop

Reduced mod index modulation (ΔPSK) does not totally suppress the carrier leaving a residual carrier component for phase referencing in the receiver. The reduced mod index modulated carrier can be tracked by a phase-locked loop. ΔPSK modulation allows one to measure the channel phase and amplitude characteristics to estimate channel quality.

The carrier tracking loop bandwidth and the signaling format determine the amount of ISI related noise in the tracking loop. For Manchester coded signals the ISI related noise is negligible for any loop time bandwidth product ($B_L T$) much less than the dta rate. However, the case of NRZ format is quite different. It is shown that with high signal to noise ratio and NRZ coding, the $B_L T$ must be less than .01 for

acceptable tracking loop performance. For a $B_L T$ of less than .01 it is concluded that the ISI related phase jitter is about 5^o ($\Delta = 60^o$).

The power requirement of the ΔPSK technique is investigated. It is shown that with an index angle of 60^o (versus 90^o for BPSK) the signal power must increase by one dB to maintain the same error probability as the BPSK technique.

5.2 Adjacent Channel Separation for Frequency Multiplexed Links

Whenever a single transponder is used for both reception and transmission of data, separation of the receiver center frequency from the transmitter center frequency must be large enough to avoid a deleterious amount of transmitter power leakage into the receiver. It is assumed that the transmitted power is 110 dB above the received power. Two different techniques resulting in similar answers were used to arrive at the minimum separation requirement.

For an NRZ signal of bit time T when both transmitter and receiver filters are 6-pole Butterworth with BT = 4, it is shown that a diversity separation of 12/T Hz is sufficient for meeting the requirements considered above.

APPENDIX I

PHASE NOISE DENSITY FOR BPSK COSTAS CARRIER TRACKING

Considering a Costas loop utilized for BPSK carrier tracking, we would like to study the effect of intersymbol interference (ISI) on the loop performance. Since the problem of thermal noise interference has already been treated in the literature; hence, the attention is focused on ISI noise alone. Let g(t) denote the BPSK pulse equation after passing through the modulator and channel filters. The noise term associated with the ISI process has been defined by[1]

$$n_I(t) = \frac{1}{2} \sum_{\substack{m \\ m \neq n}} \sum_{n} a_m a_n g(t-nT) g(t-mT) \sin 2\phi$$

where ϕ is the tracking phase error and

$$a_m = \pm\sqrt{P_s} \quad \text{independent and equilikely}$$

To determine contribution of $n_I(t)$ to the loop performance, the power spectral density of $n_I(t)$ must be evaluated. In deriving the phase noise density, it turns out that only the power spectrum of $n_I(t)$ at f = 0 has to be computed. To start, let's determine $R_I(\tau) = \overline{R_I(t,\tau)}$.

$$R_I(t,\tau) = En(t)n(t+\tau)$$

$$R_I(t,\tau) = \frac{1}{4} E \sum_{\substack{m \\ m \neq n}} \sum_{n} \sum_{\substack{p \\ p \neq q}} \sum_{q} \overline{a_m a_n a_p a_q} g(t-nT) g(t+\tau-nT) g(t-mT) g(t+\tau-m) \sin^2 2\phi$$

$$= (P_s^2)/2 \sum_{\substack{m \\ m \neq n}} \sum_{n} v(t-nT) v(t-mT) \sin^2 2\phi$$

where $\nu(t) = g(t)g(t+\tau)$ and $P_s^2 = E(a_m^2 a_n^2)$, then

$$R_I(t,\tau) = \frac{P_s^2}{2}\left[\sum_m \sum_n \nu(t-nT)\nu(t-mT) - \sum_n \nu^2(t-nT)\right] \sin^2 2\phi$$

Let

$$A(t,\tau) = \sum_n \nu^2(t-nT)$$

$$B(t,\tau) = \sum_m \sum_n \nu(t-nT)\nu(t-mT)$$

Using Poisson formula

$$A(t,\tau) = \frac{1}{T}\sum_n F_{\nu^2}\left(\frac{n}{T}\right) e^{-j\frac{2\pi n}{T}t}$$

and the averaging of A requires that in the above equation n = 0

$$A(\tau) = \overline{A(t,\tau)} = \frac{1}{T} F_{\nu^2}(f)\Big|_{f=0}$$

Now let's compute $F_{\nu^2}(f)$

$$F_{\nu^2}(f) = F_\nu(t) * F_\nu(f)$$

where

$$F_\nu(f) = F_g(f) * F_{g_\tau}(f)$$

$$F_\nu(f) = \int G(\lambda)G(f-\lambda)e^{j2\pi\lambda\tau}d\lambda$$

where $G(\lambda)$ is the Fourier transform of $g(t)$

$$F_{\nu^2}(f) = \int [\int G(\lambda)G(\mu-\lambda)e^{j2\pi\lambda\tau}d\lambda][\int G(\alpha)G(f-\Gamma-\alpha)e^{j2\pi\alpha\tau}d\alpha]d\Gamma$$

$$A(\tau) = \frac{1}{T}\iiint G(\lambda)G(\alpha)(\mu-\lambda)G(-\mu-\alpha)e^{j2\pi(\lambda+\alpha)\tau}d\alpha d\lambda d\mu$$

Next let's compute $B(\tau) = \overline{B(t,\tau)}$

$$B(t,\tau) = \frac{1}{T^2}\sum_m\sum_n W\left(\frac{n}{T},\frac{m}{T}\right)e^{\frac{2\pi}{T}(m+n)t} -$$

$$B(\tau) = \overline{B(t,\tau)} = \frac{1}{T^2}\sum_m W\left(\frac{n}{T},-\frac{n}{T}\right)$$

where $W(f_1,f_2) = F_\nu(f_1)F_\nu(f_2)$

$$W\left(\frac{n}{T},-\frac{n}{T}\right) = [\int G(\lambda)G\left(\frac{n}{T}-\lambda\right)e^{j2\pi\lambda T}d\lambda][\int G(\alpha)G\left(-\frac{n}{T}-\lambda\right)e^{j2\pi\alpha\tau}d\alpha]$$

$$B(\tau) = \frac{1}{T^2}\sum_m\iint G(\lambda)G(\alpha)G\left(\frac{n}{T}-\lambda\right)G\left(-\frac{n}{T}-\alpha\right)e^{j2\pi(\alpha+\lambda)\tau}d\alpha d\lambda$$

$$\frac{2}{\sin^2 2\phi\, P_s^2}R_I(\tau) = R_{I\overline{(t,\tau)}} = B(\tau) - A(\tau)$$

$$S_I(f=0) = F(B(\tau)-A(\tau))_{f=0}\cdot\frac{P_s^2}{2}\cdot\sin^2 2\phi$$

$$F[B(\tau)-A(\tau)]_{f=0} = \frac{1}{T^2}\sum_m\int G(\lambda)G(-\lambda)G\left(\frac{n}{T}-\lambda\right)G\left(\lambda-\frac{n}{T}\right)d\lambda$$

$$-\frac{1}{T}\iint G(\lambda)G(-\lambda)G(\Gamma-\lambda)G(\lambda-\Gamma)d\lambda d\Gamma$$

But

$$G(\lambda)G(-\lambda) = G(\lambda)G^*(\lambda) = |G(\lambda)|^2$$

$$S_I(f=0) = \sin^2(2\phi)\,\frac{P_s^2}{2}\left[\frac{1}{T^2}\sum_m \int |G(\lambda)|^2 |G(\tfrac{m}{T}-\lambda)|^2 d\lambda \right.$$

$$\left. - \frac{1}{T}\iint |G(\lambda)|^2 |G(\Gamma-\lambda)|^2 d\lambda d\Gamma\right]$$

Notice that

$$\iint |G(\lambda)|^2 |G(\Gamma-\lambda)|^2 d\lambda\Gamma = \left[\int |G(\lambda)|^2 d\lambda\right]^2$$

$$S_I(0) = \frac{P_s^2}{2}\left[\frac{1}{T^2}\sum_m \int |G(f)|^2 |G(\tfrac{n}{T}-f)|^2 df - \frac{1}{T}\left(\int |G(f)|^2 df\right)^2\right] \sin^2 2\phi$$

Thus the ISI noise spectrum $S_I(0)$ is given by

$$\frac{P_s^2}{2}\left[\frac{1}{T^2}\sum_m \int |G(f)|^2 |G(\tfrac{n}{T}-f)|^2 df - \frac{1}{T}\left[\int |G(f)|^2 df\right]^2\right] \sin^2 2\phi$$

Example 1:

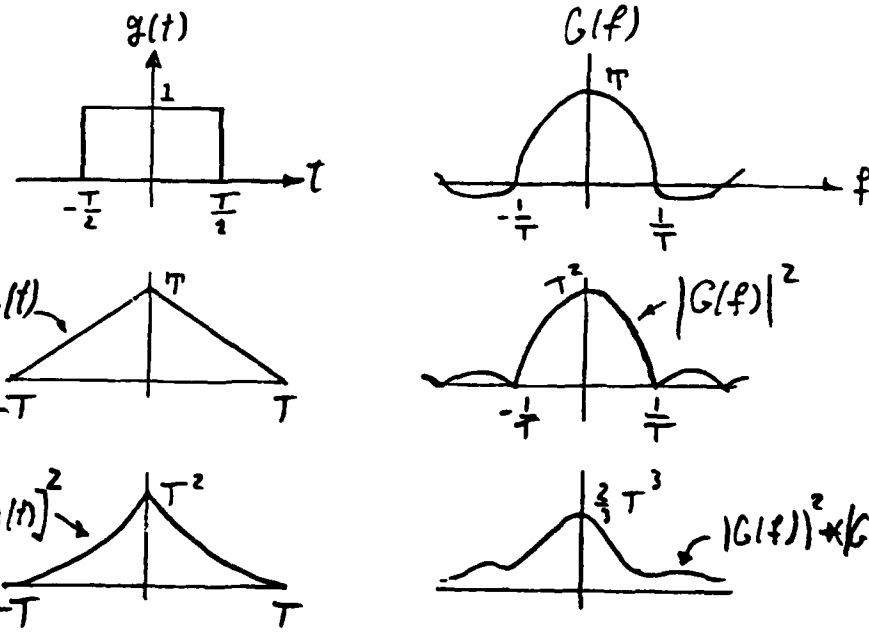

For this example

$$S_I(0) = \frac{P_s^2}{2}\left[\frac{T^3}{T^2} - \frac{T^2}{T}\right] \sin^2 2\phi = 0$$

Example 2

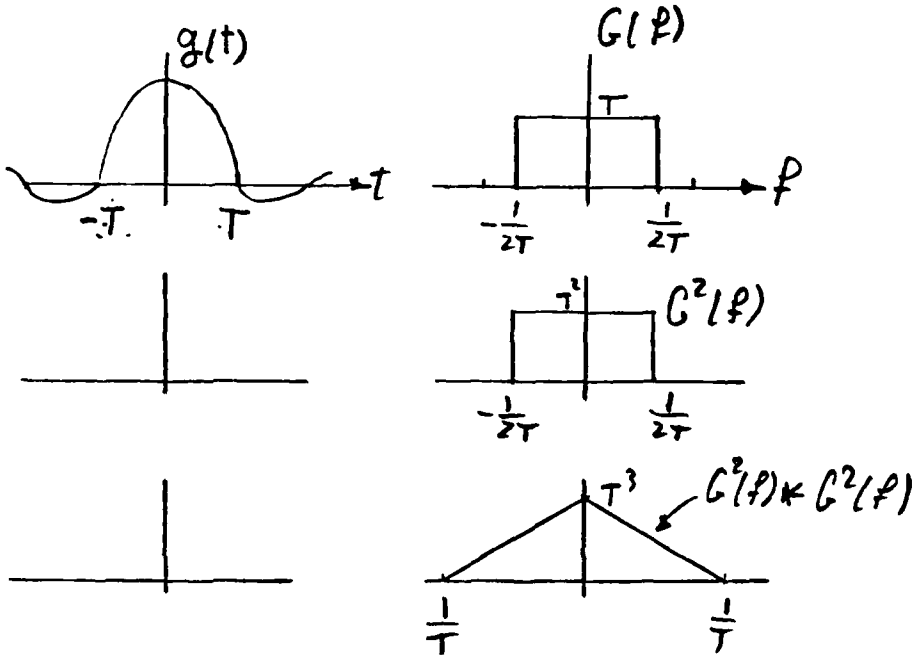

$$(S_I(0)) = \frac{P_s^2}{2}\left[\frac{T^3}{T^2} - \frac{T^2}{T}\right] \sin^2 2\phi = 0$$

Example 3. Assuming T = 1 and the bit energy is unity, the following power spectrum is given

$$S(f) = \frac{1}{T}|G(f)|^2 = \begin{cases} \frac{1}{\varepsilon} & -\frac{\varepsilon}{2} < f < \frac{\varepsilon}{2} \\ 0 & \text{otherwise} \end{cases}$$

Compute

$$N_x = \int_{-\infty}^{\infty} S^2(f)df + 2\sum_{p=1}^{\infty}\int_{-\infty}^{\infty} S(f)S\left(\frac{P}{T} - f\right)df - T\left(\int_{-\infty}^{\infty} S(f)df\right)^2$$

$$\int_{-\infty}^{\infty} S^2(f)df = \frac{1}{\varepsilon}$$

$$\left(\int S(f)df\right)^2 = 1$$

Thus

$$N_x = \frac{1}{\varepsilon} - 1 + \frac{2}{\varepsilon^2}\left[(N-1)\varepsilon - \frac{N(N-1)}{2}\right], \text{ for } N-1<\varepsilon<N$$

We notice that

$$N_x = 0 \quad \text{for } \varepsilon = 1,2,3,\ldots$$

But $N_x = \infty$ for $\varepsilon = 0$. The following figure illustrates N_x as a function of bandwidth ε.

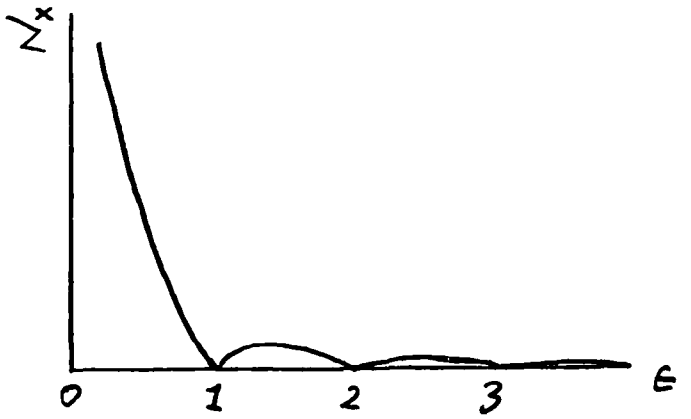

N_x is a maximum for

$$\epsilon_{max} = \frac{2N(N-1)}{2N-1} \quad \text{for } N = 2,3,4,\ldots$$

and

$$N_x|_{\epsilon=\epsilon_{max}} = \frac{1}{4N(N-1)}$$

CARRIER TRACKING LOOP PHASE NOISE RELATED TO ΔPSK MODULATION

Consider the following observed biphase modulated signal when carrier power is not totally suppressed

$$s(t) = \sqrt{2}\,[\sin\Delta \sum_m a_m g(t-mT) + \cos\Delta]\,\sqrt{P_s}\cos(\omega_s t+\phi) + n(t)$$

where g(t) denotes the ΔBPSK pulse equation after passing through the channel, Δ is the modulation phase angle, P_s is the total power, ω_0 is the carrier angular frequency, ϕ_0 is the carrier phase and n(t) is white Guassian noise with one-sided spectral density N_0. To track the carrier, the following phase-locked loop can be used.

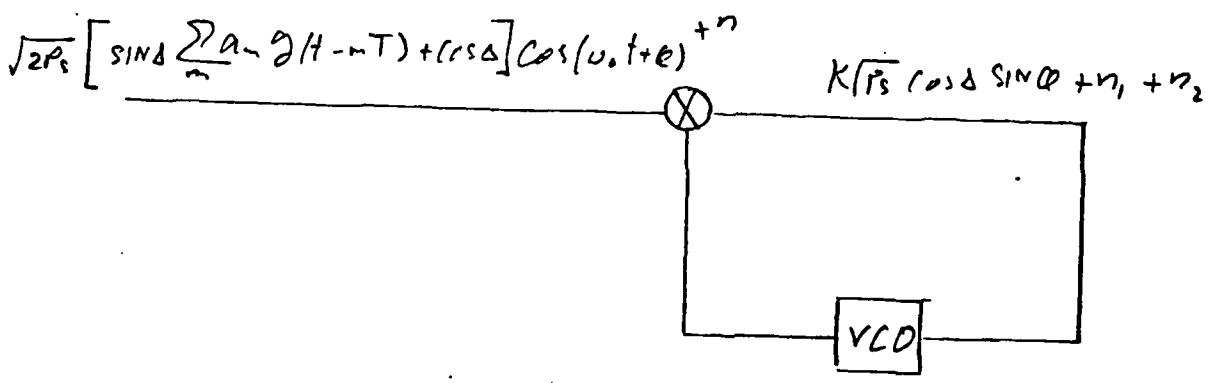

In the following, we will try to determine the density function of the phase noise term $\phi = \phi_0 - \phi_1$ for a first order phase-locked loop. If K denotes the loop gain (phase detector gain), the tracking error can be expressed as

$$e(t) = [\sqrt{P_s} \cos \Delta \sin \phi K + n_1(t) + n_2(t)]$$

where

$$n_1(t) = \sqrt{P_s}\, K \sum_m a_m g(t-mT) \sin \phi \sin \Delta; \quad a_m \pm 1$$

and

$$n_2 = \text{white Gaussian with two-sided spectral density } \frac{N_0 K^2}{4}$$

To apply the results obtained in Reference 1, we must compute $S_n(f=0)$, where $S_n(f)$ is the noise power spectrum. But,

$$S_n(f) = S_{n_1}(f) + S_{n_2}(f)$$

$$R_{n_1}(t,\tau) = K^2 P_s \sum_p \sum_q \overline{a_m a_p}\, g(t-pT)g(t+\tau-pT)\sin^2 \Delta \sin \phi^2$$

$$= K^2 P_s \sum_p g(t-PT)g(t+\tau-PT) \sin^2 \Delta \sin^2 \phi$$

$$R_{n_1}(\tau) = \overline{R_n(t,\tau)} = \frac{P_s}{T} \sum_p H(\tfrac{P}{T})\, e^{j \frac{2\pi}{T} \rho t} K \sin^2 \Delta \sin^2 \phi$$

$$= \frac{P_s}{T} H(0)\, K \sin^2 \Delta \sin^2 \phi$$

where H(f) denotes Fourier transform of $g(t)g(t+\tau)$

$$R_{n_1}(\tau) = \frac{P_s}{T} \int |G(\lambda)|^2 e^{j2\pi\lambda\tau} d\lambda \cdot K \sin^2 \Delta \cdot \sin^2 \phi$$

where it is assumed that g(t) is real. Now Fourier transforming $R_{n_1}(\tau)$,

$$S_{n_1}(f) = \frac{P_s K}{T} \int |G(\lambda)|^2 \, \delta(f-\lambda) d\lambda \sin^2 \Delta \sin^2 \phi$$

$$= \frac{P_s}{T} |G(f)|^2 K^2 \sin^2 \Delta \sin^2 \phi$$

Thus

$$S_{n_1}(f=0) = \frac{P_s}{T} |G(0)|^2 K^2 \sin^2 \Delta \sin^2 \phi$$

Now to be able to use the exact results in the reference, let's introduce quantities N_x and N_0' so that

$$S_n(f=0) = \frac{K^2}{2} N_x \sin^2 \phi + \frac{K^2}{2} N_0'$$

where

$$N_x = 2 \frac{P_s}{T} |G(0)|^2 \sin^2 \Delta$$

But since $G(0) = T$, thus

$$N_x = 2TP_s \sin^2 \Delta$$

N_0' is given by

$$N_0' = 2N_0$$

Now let's define

$$R = \frac{N_x}{N_0'} = \frac{TP_s \sin^2 \Delta}{N_0} = R_b \sin^2 \Delta$$

and compute

$$S_L(0) = \frac{N_0}{N_0'} \frac{1}{T} \int_{-\infty}^{\infty} |G(f)|^2 df = \frac{1}{2}$$

and

$$\alpha = \frac{R_b \cos^2 \Delta}{2B_L T}$$

where $B_L = K/4$ is the loop noise bandwidth. Now using equations (3.3)-(3.5) of Reference 1, the density function of ϕ is given by

$$P(\phi) = C_0 \frac{1}{\sqrt{(1+R \sin^2\phi)}} \left[\frac{\sqrt{(1+\frac{1}{R})}+\cos\phi}{\sqrt{1+\frac{1}{R}}-\cos\phi} \right]^{\alpha/2R[1+\frac{1}{R}]^{1/2}}$$

where C_0 is the normalizing factor

$$\frac{\alpha}{2R} = \frac{1}{4B_L T \tan^2\Delta}$$

and for large R

$$P(\phi) = C_0 \frac{1}{\sqrt{1+R_b \sin^2\Delta \sin^2\phi}} \left[\frac{\sqrt{1+\frac{1}{R_b \sin^2\Delta}}+\cos\phi}{\sqrt{1+\frac{1}{R_b \sin^2\Delta}}-\cos\phi} \right]^{1/4B_L T \tan^2\Delta}$$

It is desirable to have as small jitter on ϕ as possible; hence, $p(\phi)$ is desired to be concentrated around $\phi=0$. To achieve this, the following inequality must hold

$$1 < \frac{1}{4B_L T \tan^2 \Delta}$$

or

$$B_L T < \frac{1}{4 \tan^2 \Delta}$$

For example if $\Delta = 60^o$

$$B_L T < .08$$

We can determine $p(\phi)$ if R_0 is given. Now let's compute $p(\phi)$ for R_b = 10.

AD-A112 669 LINCOM CORP PASADENA CA F/G 17/2.1
PHASE NOISE STUDY, ATTACHMENT II,(U)
OCT 81 R A MAAG, F DAVARIAN N00014-81-C-2338
UNCLASSIFIED TR-1082-0881 NL

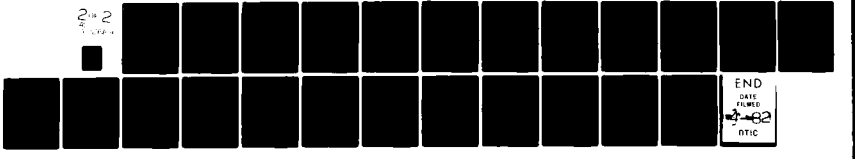

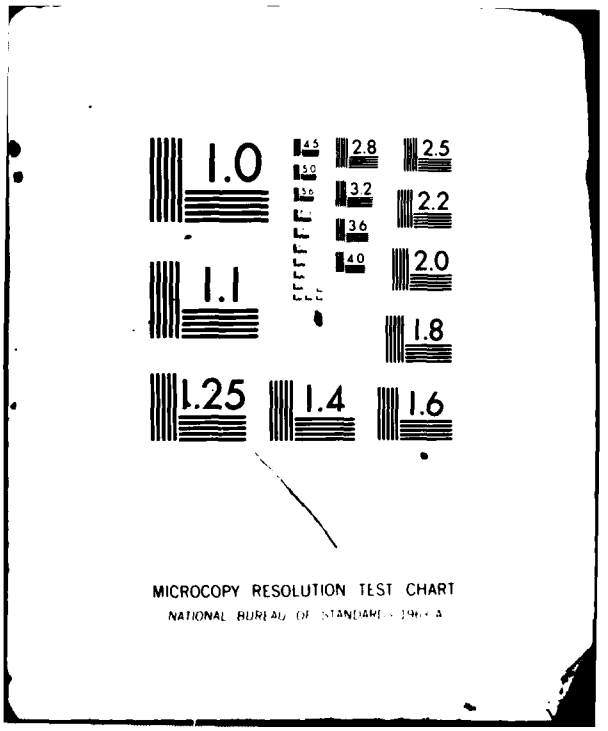
1.0
1.1
1.25
1.4
1.6
1.8
2.0
2.2
2.5
2.8
3.2
3.6
4.0
4.5
5.0
5.6
MICROCOPY RESOLUTION TEST CHART
NATIONAL BUREAU OF STANDARDS - 1963 - A

ϕ	$\frac{\sqrt{1+\frac{1}{R_b \sin^2 \Delta}} + \cos\phi}{\sqrt{1+\frac{1}{R_b \sin^2 \Delta}} - \cos\phi}$	$\frac{1}{\sqrt{1+R_b \sin^2 \Delta \sin^2 \phi}}$	$\frac{1}{C_0} P(\phi)$ $B_L T=.1$	$B_L T=.01$
0	32	1	16	10^{12}
5	30	.97	14.6	$.6\times10^{12}$
10	25	.9	11.8	1.4×10^{11}
15	20	.8	8.8	2×10^{10}
20	15.5	.73	6.5	2.4×10^{9}

As can be observed from the above table, for $B_L T = .1$, $p(\phi)$ drops slowly with ϕ increasing which means a large standard deviation of ϕ. But for $B_L T = .01$, $p(\phi)$ is decreasing rapidly with increasing ϕ.

[1] Davidov, M. A., "ISI Effect on Synchronization Loops," Ph.D. Dissertation, University of Southern California, Los Angeles, 1980.

[2] Papoulis, A., The Fourier Transform and Its Application, McGraw-Hill, New York, 1962, pp. 131-133.

APPENDIX II

ASYMMETRICAL RF FILTERING EFFECTS IN CARRIER AND BIT SYNC TRACKING

Example 1.

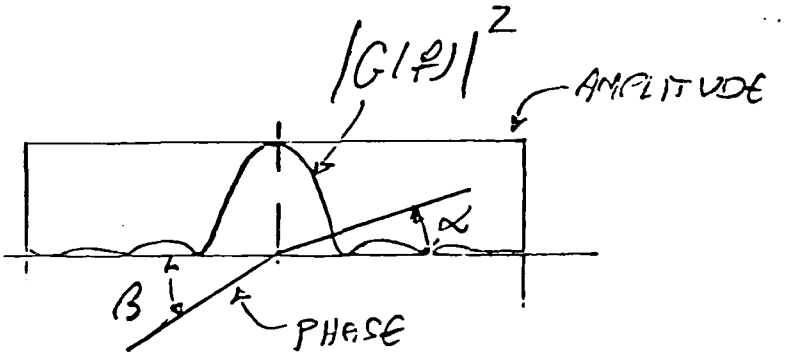

$$H_1(f) = \cos \alpha f + j \sin \alpha f \qquad f > 0$$

$$H_1(f) = \cos \beta f + j \sin \beta f \qquad f < 0$$

$$H_p(f) = \frac{H_1(f)+H_2(f)}{2} = \frac{\cos \alpha f+\cos \beta f}{2} + j \frac{\sin \alpha f+\sin \beta f}{2}$$

$$H_q(f) = \begin{cases} \dfrac{\sin \beta f-\sin \alpha f}{2} - j \dfrac{\cos \beta f-\cos \alpha f}{2} & f>0 \\ -\dfrac{\sin \beta f-\sin \alpha f}{2} + j \dfrac{\cos \beta f-\cos \alpha f}{2} & f<0 \end{cases}$$

$$H_p(f)H_q^*(f) = -\frac{1}{2} \cos \alpha f \, sn \, \alpha f + \frac{1}{2} \cos \beta f \sin \beta f \qquad f>0$$

$$= -[-\frac{1}{2} \alpha f \sin \alpha f + \frac{1}{2} \cos \beta f \sin \beta f) \qquad f<0$$

or

$$H_p(f)H_q^*(f) = \frac{1}{4}\sin(\beta-a)f \qquad f>0$$

$$= -[\cdot] \qquad f<0$$

$$|H_p(f)|^2 - |H_p(f)|^2 = \cos(\alpha-\beta)f$$

$$\int_{-\infty}^{\infty} |G(f)|^2 H_p(f)H_p^*(f)df = \frac{1}{2}\int_0^{\infty}[\sin 2\beta f - \sin 2\alpha f]|G(f)|^2 df$$

$$\int |G(f)|^2[|H_p(f)|^2 - |H_p(f)|^2]df = 2\int_0^{\infty}\cos(\alpha-\beta f)|G(f)|^2 df$$

Hence

$$\phi_B = \frac{1}{2}\arctan\left(\frac{-\int_0^{\infty}|G(f)|^2(\sin\beta\alpha)f}{\int_0^{\infty}|G(f)|^2\cos(\alpha-\beta)fdf}\right)$$

For example if $\beta = -\alpha$

$$\phi_B = \frac{1}{2}\arctan\left(\frac{\int_0^{\infty}|G(f)|^2\sin 2\alpha f df}{\int_0^{\infty}|G(f)|^2\cos 2\alpha df}\right)$$

Let's investigate the bit sync (DTTL) performance in the presence of the channel characteristics defined in Example 1 assuming that $\varepsilon = (\alpha-\beta)/T << 1$. The Q channel transfer function for small phase asymmetry is given by

or

$$H_p(f)H_q^*(f) = \frac{1}{4}\sin(\beta-a)f \qquad f>0$$

$$= -[\cdot] \qquad f<0$$

$$|H_p(f)|^2 - |H_p(f)|^2 = \cos(\alpha-\beta)f$$

$$\int_{-\infty}^{\infty} |G(f)|^2 H_p(f)H_p^*(f)df = \frac{1}{2}\int_0^{\infty}[\sin 2\beta f - \sin 2\alpha f]|G(f)|^2 df$$

$$\int |G(f)|^2[|H_p(f)|^2 - |H_p(f)|^2]df = 2\int_0^{\infty}\cos(\alpha-\beta f)|G(f)|^2 df$$

Hence

$$\phi_B = \frac{1}{2}\arctan\left(\frac{-\int_0^{\infty}|G(f)|^2(\sin\beta\alpha)f}{\int_0^{\infty}|G(f)|^2\cos(\alpha-\beta)fdf}\right)$$

For example if $\beta = -\alpha$

$$\phi_B = \frac{1}{2}\arctan\left(\frac{\int_0^{\infty}|G(f)|^2\sin 2\alpha f df}{\int_0^{\infty}|G(f)|^2\cos 2\alpha df}\right)$$

Let's investigate the bit sync (DTTL) performance in the presence of the channel characteristics defined in Example 1 assuming that $\epsilon = (\alpha-\beta)/T << 1$. The Q channel transfer function for small phase asymmetry is given by

$$H_q(f) = \frac{1}{2} |\alpha-\beta||f|(\cos \frac{\alpha+\beta}{2} f + j \sin \frac{\alpha+\beta}{2} f) \quad f < \frac{1}{T}$$

The input signal to the bit sync has the following structure

$$s(t) = s_I(t) \cos \phi + s_Q(t) \sin \phi$$

where

$$s_I(t) = \sum_m g_I(t-mT)$$

and

$$g_Q(t) = P(t - \frac{\alpha}{2\pi}) + P(t- \frac{\beta}{2\pi})$$

where $P(t)$ is a pulse with duration T. Hence, if ϕ is zero or $s_Q(t)$ is negligible, the perfect sync in absence of thermal noise is achieved. Notice that $s_I(t)$ is symmetric around $\frac{\alpha+\beta}{2\pi}$.

The tracking loop phase bias ϕ_B can be computed from

$$\phi_B = \frac{1}{2} \arctan\left(- \frac{\int_{-\infty}^{\infty} |G(f)|^2 (\sin \beta-\alpha) f}{\int_0^{\infty} |G(f)|^2 \cos(\alpha-\beta) f df}\right)$$

But for $\varepsilon = \frac{\alpha-\beta}{T} \ll 1$, we may write

$$\sin (\beta-\alpha)f \simeq (\beta-\alpha)f, \qquad f < \frac{1}{T}$$

Hence

$$\phi_B \simeq \frac{1}{2} \varepsilon$$

or

$$\sin \phi_B \simeq \frac{1}{2} \varepsilon$$

Signal $S_Q(t)$ is given by

$$S_Q(t) = \sum_m g_Q(t-mT)$$

where

$$g_Q(t) = P(t)*h_q(t)$$

Since $H_q(f)$is linear in phase, hence $g_Q(t)$ is symmetric. Consequently, the bit sync will have no bias error. To compute an upper bound for the jitter, the area under the tail of $g_Q(t)$ must be evaluated. To proceed, let's observe $g_Q(t)$ in the Fourier domain.

$$G_Q(f) = \underbrace{e^{j\frac{\alpha+\beta}{2}f}}_{\text{Delay}} \cdot \underbrace{P(f)f}_{\frac{1}{2\pi j}p'(t)} \cdot \underbrace{\text{sgn}(f)}_{\frac{2j}{t}} \cdot \frac{\alpha-\beta}{2}$$

In the above equation the fact that the signal is band limited has been ignored for simplicity. But

$$p'(t) = \delta(t-\frac{T}{2}) - \delta(t+\frac{T}{2})$$

and

$$\text{sgn}(f) \sim \frac{2j}{t}$$

In case of a practical band limited signal, for example, band limited to 1/T, the function 2j/t must be replaced by $[(1-\cos(2\pi t/T))/jt\pi]$. However, for simplicity the function 2j/t is used here. Hence σ_t is given by

$$\sigma_t < \frac{T\epsilon}{2\pi}\int_{\frac{1}{2}}^{\infty}\left[\frac{1}{t}-\frac{1}{t+1}\right]dt = \frac{T\epsilon}{2\pi}\ln 3 \sin\phi$$

or

$$\frac{\sigma_t}{T} < \frac{\ln 3}{2\pi} \varepsilon^2$$

If $t_A = \alpha - \beta/2\pi$, and $B_L T$ denotes the time loop bandwidth product then

$$\frac{\sigma_t}{T} < \frac{\ln 3}{2\pi} (2\pi)^2 \left(\frac{t_A}{T}\right)^2 = 2\pi \ln 3 \left(\frac{t_0}{T}\right)^2 \sqrt{B_L T}$$

Example 2. ISI Distortion in Costas Loop Due to a Channel with Nonsymmetric Phase Ripple (Small Ripple Amplitude)

$$H(\omega) = 1 \quad b_0 \omega - b_1 \sin(c\omega + \theta)$$

Using the technique in Reference [2] and assuming $\cos[b_1 \sin(c\omega+\theta)] = 1$ and $\sin[b_1 \sin(c\omega+\theta)] = b_1 \sin(c\omega+\theta)$. The two portions of the asymmetric channel are given by

$$H_1(\omega) = b_1 \sin(c\omega+\theta) \sin b_0\omega + \cos b_0\omega + j[\sin b_0\omega - b_1 \sin(c\omega+\theta)\cos b_0\omega]$$

$$H_2(\omega) = b_1 \sin(c\omega-\theta)\sin b_0\omega + \cos b_0\omega + j[\sin b_0\omega - b_1 \sin(c\omega-\theta)\cos b_0\omega]$$

Hence [2],

$$H_p(\omega) = [\cos b_0\omega + j \sin b_0\omega] + b_1 \cos\theta \sin c\omega[\sin b_0\omega - j \cos b_0\omega]$$

$$H_q(\omega) = b_1 \cos c\omega \sin\theta[\cos b_0\omega + j \sin b_0\omega]$$

To compute the phase bias, ϕ_B, let's compute $H_p(\omega)H_q(\omega)$

$$H_p(\omega)H_q^*(\omega) = b_1 \cos c\omega \sin\theta - \frac{1}{4} jb_1^2 \sin 2c\omega \sin 2\theta$$

$$\int_{-\infty}^{\infty} |G(f)|^2 H_p(f)H_q^*(f)df = b_1 \sin\theta \int |G(f)|^2 \cos 2\pi cfdf$$

If we assume

$$\int |G(f)|^2[|H_p(f)|^2 - |H_q(f)|^2]df \simeq \int |G(f)|^2 df$$

$$\phi_B = -b_1 \frac{\int_0^{\infty} |G(f)|^2 \cos 2\pi cfdf}{\int_0^{\infty} |G(f)|^2 df} \sin\theta$$

or

$$|\phi_B| < b_1 \sin\theta \quad \text{if } c \neq 0$$

See the figure below.

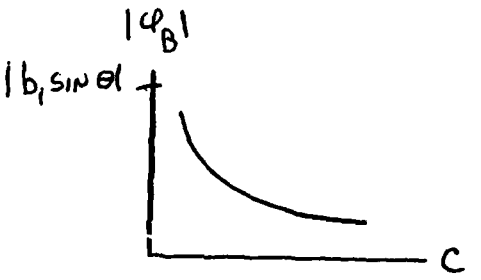

Now, employing a technique similar to the QPSK tracking loop of [1], we may compute the jitter in the loop by computing two independent

jitter terms attributable to the I and Q signals, respectively. Note that in reality these terms are not independent and that there will also be cross terms. However, to simplify the problem the above approximate technique for computation of phase jitter will be used.

Adopting similar terminology as in [1], we compute the spectrum of ISI related noise

$$S_{n_1}(f=0) = B \sin^2 2\phi + C \cos^2 2\phi$$

where

$$C = 2P_s^2 \frac{1}{T^2} \sum_m \int |G(f)|^2 |G(\tfrac{m}{T} - f)|^2 H_p(f) H_q^*(f) H_p(\tfrac{m}{T} - f) H_q^*(\tfrac{m}{T} - f) df$$

For simplicity the following approximation is made

$$C = 2P_s^2 \frac{1}{T^2} \int |G(f)|^4 |H_p(f)|^2 |H_q(f)|^2 df$$

$$C = \frac{2P_s^2}{T^2} [\int |G(f)|^4 \cos^2 c\omega df] b_1^2 \sin^2 \theta$$

But

$$\int |G(f)|^4 = \frac{2}{3} T^3$$

Hence

$$C \simeq \frac{4}{3} P_s^2 T b_1^2 \sin^2 \theta$$

Next, let's find the thermal noise related term

$$S_{n_2}(f=0) = \frac{K^2}{2} N_0'$$

where

$$N_0' = N_0 P_s \left(\frac{1}{T} \int |G(f)|^2 df + \frac{N_0}{2P_s} \int |H(f)|^4 df \right)$$

where

$$\int |H(f)|^4 df = B_w$$

$$N_0' = N_0 P_s \left(\frac{1}{T} \cdot T + \frac{N_0}{2P_s} B_w \right)$$

$$= N_0 P_s + \frac{B_w N_0^2}{2P_s}$$

But

$$R_b = \frac{P_s T}{N_0/2} \qquad N_0' = N_0 P_s + \frac{B_w T N_0}{2R_b}$$

Assuming P_s is unity,

$$N_0' = N_0 \left(1 + \frac{B_w T}{R_b}\right)$$

Hence

$$R_y = \frac{C}{N_0'} = \frac{\frac{4}{3} P_s^2 T}{N_0 \left(1 + \frac{B_w T}{R_b}\right)} b_1^2 \sin^2 \theta = \frac{4}{3} \frac{R_b P_s}{1 + \frac{TB_w}{R_b}} b_1^2 \sin^2 \theta$$

$$R_y = \frac{4}{3} \frac{R_b}{1 + TB_w} b_1^2 \sin^2 \theta$$

Now assuming R_x=0 (R_x represents the inphase signal distortion), we may compute the jitter due to the Q signal

$$S_L(0) = \frac{N_0}{N_0'} = \frac{1}{1 + \frac{B_w T}{R_b}}$$

$$\alpha = \frac{R_b}{B_L T} S_L(0) = \frac{R_b}{B_L T} \frac{1}{(1+\frac{TB_w}{R_b})}$$

But for small R_y and $R_x=0$,

$$p(2\phi) \simeq \exp\left(\frac{\alpha}{\sqrt{R_y}} \sqrt{R_y} \cos\theta\right)$$

or

$$p(2\phi) \simeq \exp[\alpha(1-\frac{\phi^2}{2})]$$

$$p(2\phi) = e^{\alpha\sqrt{R_y}} e^{-[\phi^2/2(1/\alpha)]}$$

This is a Gaussian function and hence the standard deviation is

$$\sigma_{2\phi} = \frac{1}{\sqrt{\alpha}}$$

or

$$\sigma_{2\phi} = \frac{\sqrt{1+\frac{TB_w}{R_b}}}{\sqrt{R_b/B_L T}} \quad \text{or} \quad \sigma_\phi = \frac{1}{2} \frac{\sqrt{1+\frac{TB_w}{R_b}}}{\sqrt{R_b/B_L T}}$$

For example if $TB_w=5$, $R_b=10$, $B_L T=.1$

$$\sigma_\phi = \frac{1}{2} \frac{\sqrt{1+.5}}{\sqrt{100}} \simeq .06 \text{ radian} \quad \text{or} \quad 3.5^o$$

Note that for small phase ripple the above jitter does not depend on the ripple amplitude.

It will be shown that the ISI distortion in the in-phase channel for this example is relatively small, and hence, the phase jitter due to thermal noise is the main non-DC distortion component in the loop. The ISI related term is computed as [2]

$$N_x = P_s^2\left[\frac{1}{T^2}\sum_{m=1}^{\infty}\int |G(f)|^2|G(\frac{m}{T}-f)|^2df - \frac{1}{T}\left(\int_{-\infty}^{\infty}|G(f)|^2df\right)^2\right]$$

Also,

$$G(f) = |P(f)|^2|H_p(f)|^2$$

where P(f) is the spectrum of a pulse with width T, and

$$|H_p(f)|^2 = 1 + 2b_1 \sin c\omega \sin 2b_0\omega$$

Since the exact computation of N_x requires a computer, the following bound can be obtained by observation

$$N_x < 2b_1P_s^2T$$

Next the thermal noise related term is obtained

$$N_0' = N_0P_s(1 + \frac{N_0}{2P_s}B_w) = N_0(1+\frac{TB_w}{R_b})$$

The following ratio illustrates the ISI power relative to the Gaussian noise power

$$R = \frac{N_x}{N_0'} < \frac{b_1R_b}{1+\frac{TB_w}{2R_b}}$$

where

$$R_b = \frac{P_sT}{\frac{N_0}{2}}$$

For moderate values of R_b and small b_1, R is a ratio smaller than 1. Hence for the sake of simplicity, ISI contribution to phase jitter is

ignored at this point and the thermal noise related jitter is computed using the Gaussian model,

$$2\sigma_\phi = \sqrt{\frac{B_L T}{R_b}}$$

i.e. for $R_b = 10$, $B_L T = .1$

$$2\sigma_\phi \simeq .1 \text{ rad or } \sigma_\phi = 3 \text{ deg}$$

Previously we had computed σ_ϕ to be 3.5^o. In practice, however, due to ISI and also Q-signal interference, jitter will be more than 3.5 degrees.

In summary, for a phase ripple amplitude of 6 degrees, $R_b = 10$, $B_L T = .1$, and $B_w T = 5$, we have

$$\sigma_\phi > 3.5 \text{ degrees}$$

$$\phi_B < 6 \text{ degrees}$$

Let's investigate the bit sync performance in presence of phase ripple of form given in Example 2.

The waveform s(t) entering the bit sync (DTTL) has the following from

$$s(t) = s_I(t) \cos \phi + s_Q(t) \sin \phi$$

where

$$s_I(t) = \sum_m g_I(t-mT)$$

$$s_Q(t) = \sum_m g_Q(t-mT)$$

and

$$g_I(t) = p(t)*h_p(t)$$

$$g_Q(t) = p(t)*h_q(t)$$

where p(t) is a pulse with duration T. Further, let h_p and h_q be the inphase and quadrature channel impulse responses, respectively.

To observe the bit sync performance for the two extreme cases of $\theta = 0$ (symmetric channel) and $\theta = \pi/2$. For case of $\theta = 0$, the I and Q signals are given as

$$\text{I} \begin{cases} g_I(t) = p(t) + \frac{b_1}{2}[p(t+c) - p(t-c)] \\ g_Q(t) = 0 \end{cases}$$

and for the second case of $\theta = \pi/2$

$$\text{II} \begin{cases} g_I(t) = p(t) \\ g_Q(t) = \frac{b_1}{2}[p(t+c) + p(t-c)] \end{cases}$$

Case I will cause no jitter at the DTTL (phase distortion). The jitter attributed to Case II is found from the following integration

$$\frac{1}{2}\int_0^T [\frac{1}{2}|b_1| + \frac{1}{2}|b_1|]dt = \frac{1}{2}b_1T$$

If B_LT denotes the time bandwidth product of the loop and $\sin\phi = b_1$, the normalized jitter is given by

$$\left(\frac{\sigma_t}{T}\right)_{II} < \frac{1}{2} b_1 \sqrt{B_L T}$$

Let

$$\sigma_t < .02T$$

Then

$$\frac{1}{2} b_1^2 \sqrt{B_L T}\, T < .02T$$

or

$$b_1 < \frac{.2}{\sqrt{B_L T}}$$

Since $B_L T < 1$ therefore the above bound does not imose any serious restriction on b_1. The worst case bias at DTTL occurs when $\theta = 0$. In this case the bias equals $1/2\ b_1 T$. To draw a bound on b_1 the above bias must be less than .03T

$$1/2\ B_1 T < .03T$$

$$b_1 < .06 \text{ rad}$$

or

$$b_1 < 3.5^{o}$$

Example 3: Suppose the channel amplitude response contains a slight asymmetry of the form given in the following figure:

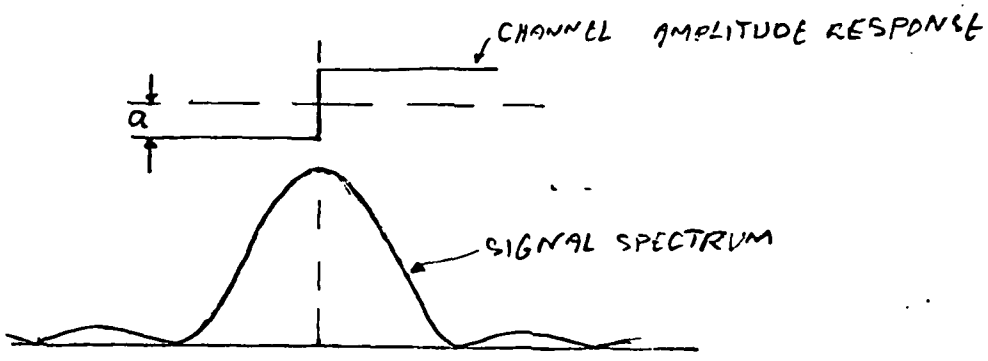

The objective is to compute the inphase and quadrature signal componets in order to investigate the resulting ISI effect in a first order Costas loop. The signal format is NRZ, and modulation format is BPSK.

To compute the inphase and quadrature channel transfer functions, let's apply the method used earlier

$$H_1(f) = 1 + a\ \mathrm{sgn}(f)$$
$$H_2(f) = 1 - a\ \mathrm{sgn}(f) \qquad \text{(E1)}$$

Hence

$$H_p(f) = \frac{H_1(f)+H_2(f)}{2} = 1$$
$$H_q(f) = \frac{H_2(f)-H_1(f)}{2j} = a\,j\ \mathrm{sgn}(f) \qquad \text{(E2)}$$

Since the product $H_p(f)H_q^*(f) = j\ \mathrm{sgn}(f)$ has odd symmetry, the tracking loop will have no channel DC related phase error. This observation implies that the channel effect on the bit sync (DTTL) can be assumed

negligible if the tracking loop phase noise can be kept under control. Here we wish to specify distortion parameter a such that the ISI contribution to the phase noise be smaller than the phase noise due to the thermal noise with moderate E_b/N_0 values.

From Equations E2 it is clear that $H_p(f)$ does not distort the signal in any way. Hence, the inphase component of the signal cannot cause ISI related noise in the loop. Now, referring to Equations 16, $s_{u_1}(f=0) = 0$ and $s_{u_3}(f)$ is proportional to a^2 where s_{u_2} is proportional to a^4. Since $\alpha << 1$, s_{u_2} can be ignored. Employing the QPSK technique of Reference 1 we may determine the phase noise by first computing parameters R_x and R_y. Since $s_{u_1}(f=0) = 0$, thus $R_x = 0$ and R_y can be computed from $s_{u_3}(f=0)$.

$$s_{u_3}(f=0) = P_s^2\left[\frac{2}{T^2}\sum_m \int |G(f)|^2 |G(\tfrac{n}{T}-f)|^2 H_p(f) H_q^*(f) H_p(\tfrac{n}{T}-f) H_q^*(\tfrac{n}{T}-f)\,df\right.$$

Since $H_p(f) = 1$ and $H_q(fg) = aj\ \mathrm{sgn}(f)$

$$s_{u_3}(f=0) = \frac{2P_s^2\alpha^2}{T^2}\sum_m \int |G(f)|^2 |G(\tfrac{m}{T}-f)|^2 \mathrm{sgn}(f)\,\mathrm{sgn}(f-\tfrac{m}{T})\,df$$

$$< \frac{2P_s^2 a^2}{T^2} T^3 = 2P_s^2 T a^2$$

and

$$N_0' = N_0 P_s\left[1+\frac{BT}{R_b}\right]$$

$$R_b = \frac{P_s T}{N_0/2}$$

Thus

$$R_y < a^2 \frac{R_b}{1+\frac{BT}{R_b}}$$

and

$$\alpha = \frac{R_b}{B_L T} \frac{1}{1+\frac{BT}{R_b}}$$

The phase noise density function is given in [1] and is written here

$$p(\phi) \sim \frac{1}{\sqrt{1+R_y \cos^2 2\phi}} \exp\left[\frac{\alpha \tan^{-1}(\sqrt{R_y} \cos 2\phi)}{\sqrt{R_y}}\right]$$

But for small R_y, $\tan^{-1}(\sqrt{R_y} \cos^2 \phi) \tilde{=} \sqrt{R_y} \cos 2\phi$ and assuming $2\phi < 20^0$

$$p(\phi) \sim \exp \alpha \cos 2\phi \sim \exp - \alpha \frac{4\phi^2}{2}$$

$$p(\phi) \sim \exp\left(-\frac{\phi^2}{2\frac{\alpha}{4}}\right)$$

Hence

$$\sigma_\phi \approx \frac{1}{2\sqrt{\alpha}}$$

For example if $R_b = 10$, $BT = 5$, $B_L T = .1$, $a = .1$

$$R_y < .01 \frac{10}{1+.5} = \frac{1}{15} = .067$$

$$\alpha = \frac{10}{.1} \frac{1}{1+.5} = \frac{1000}{15} = 67$$

since $R_y < 1$. Thus

$$\sigma_\phi = \frac{1}{2\sqrt{67}} = .6 \text{ rad}$$

or

$$\sigma_\phi = 3.5^0$$

The conclusion here is that for a = .1. The ISI distortion in the loop can be ignored. This assumption is true, in general, if the following approximation could hold

$$\tan^{-1}\sqrt{y} \approx \sqrt{y}$$

To check the validity of the above condition, let's write tan (x) in its expanded form $x < 1$

$$\tan^{-1} x = x - \frac{x^3}{3}$$

Thus if $x^3/3x = x^2/3 << 1$, then the above approximation is valid, i.e.

$$\frac{(\sqrt{R_y})^3}{3\sqrt{R_y}} = \frac{R_y}{3} << 1$$

or

$$R_y << 3$$

or

$$\frac{a^2 R_b}{1+\frac{BT}{R_b}} << 3$$

$$a^2 << 3\,\frac{1+\frac{BT}{R_b}}{R_b}$$

Let's plot $f(Rb) = \frac{3}{R_b}\left(1+\frac{BT}{R_b}\right)$ for BT = 5

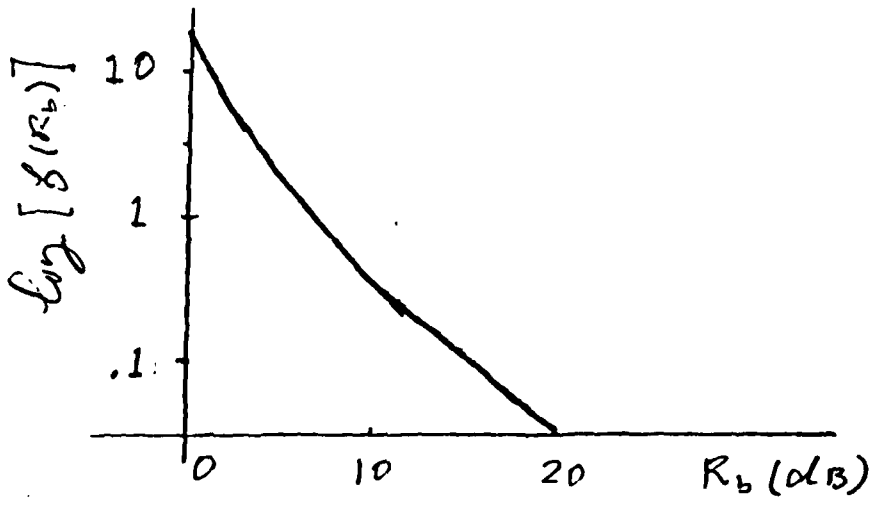

The above curve can aid us in determining an upper bound for a. If R_b = 10 dB is used, the following upper bound on a can be asserted.

As another example let's consider a symmetric channel with small amplitude ripple and equalized phase. passage of a pulse through a channel with small amplitude ripple introduces the paired echo phenomenon. To formulate the ISI contribution to the first order loop, let's rewrite the noise power spectrum given in the appendix

$$s_I(f=0) = \frac{1}{2} P_s^2 \sin^2 2\phi \left[\frac{1}{T^2} \sum_m \int |G(f)|^2 |G(\tfrac{m}{T} - f)|^2 df \right.$$

$$\left. - \frac{1}{T} \iint |G(f)|^2 |G(\lambda - f)|^2 df d\lambda \right.$$

Let $z(f) = |G(f)|^2 * |G(f)|^2$. Hence

$$N_x = \frac{2S_I(f=0)}{k^2 \sin^2 2\phi} = \frac{P_s^2}{T^2} \sum_m z(\tfrac{m}{T}) - \frac{P_s^2}{T} \int z(f) df$$

But if $z(t) = F^{-1}\{z(f)\}$, then

$$\sum_m z\left(\frac{m}{T}\right) < T \sum_m z(mT)$$

Thus

$$N_x < \frac{p_s^2}{T}\left[\sum_m z(mT) - z(0)\right]$$

But if amplitude ripple period is equal to 1/T, then the following pairs of transform figures hold.

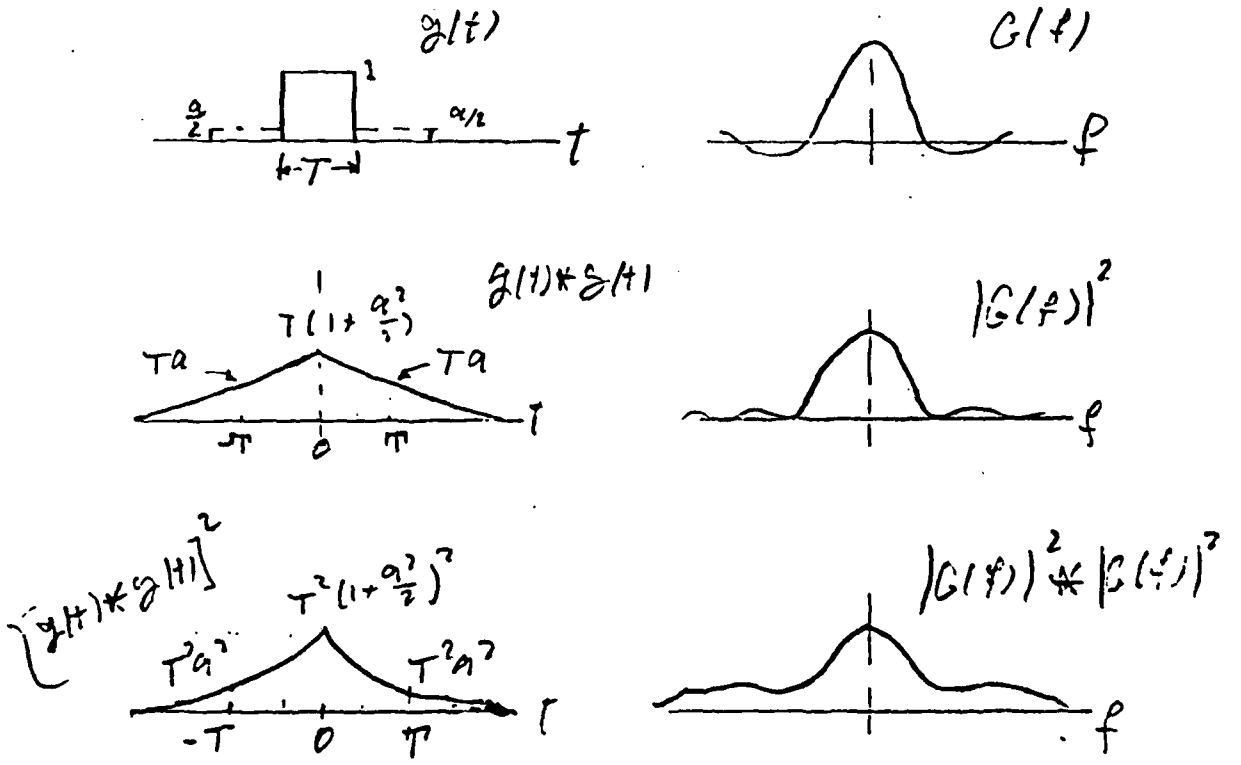

$$N_x < \frac{P_s^2}{T}\left[T^2\left(1+\frac{a^2}{2}\right)^2 + 2a^2T^2 - T^2\left(1+\frac{a^2}{2}\right)\right]$$

$$= \frac{P_s^2}{T}\left[2a^2T^2\right] = 2Ta^2P_s^2$$

Also from [1]

$$N_0' = N_0P_s\left[1+\frac{N_0B}{2P_s}\right]$$

If

$$R_b = \frac{P_sT}{N_0/2}$$

$$N_0' = N_0P_s\left[1+\frac{BT}{R_b}\right]$$

and

$$R = \frac{N_x}{N_0'} < \frac{2Ta^2P_s^2}{N_0P_s\left[1+\frac{BT}{R_b}\right]} = \frac{R_ba^2}{1+\frac{BT}{R_b}}$$

$$\alpha = \frac{R_b}{B_LT}S_L(0) = \frac{R_b}{B_LT}\frac{1}{1+\frac{BT}{R_b}}$$

For example if $R_b = 10$, $B_LT = .1$, $BT = 5$, $a = .1$

$$R < \frac{10x.01}{1+.5} = \frac{.1}{1.5} = \frac{1}{15}$$

$$\alpha = \frac{10}{.1}\frac{1}{1+.5} = \frac{100}{1.5} = \frac{1000}{15}$$

and

$$\frac{\alpha}{R}\frac{1}{2\sqrt{1+\frac{1}{R}}} = 1000\frac{1}{2\sqrt{1+15}} = \frac{500}{4} = 125$$

The phase noise probability density function for small ϕ is given by [1]

$$p(\phi) = \left(\frac{4+\cos\phi}{4-\cos\phi}\right)^{125}$$

Letting $\cos\phi = 1 - \phi^2/2$ and setting the second derivative to zero

$$\cos 2\phi_0 > .988$$

$$2\phi_0 < 9^0$$

Hence the jitter is less than 4.5 degrees.

This jitter will reduce the DTTL power by a small amount. If $B_L T$ were one hundred times smaller, i.e. $B_L T = .001$, thus

$$\alpha = \frac{10^5}{15}$$

and

$$\frac{\alpha}{R}\frac{1}{2\sqrt{1+\frac{1}{R}}} = \frac{10^5}{2\cdot 4} = \frac{10^5}{8} = 12500$$

Hence

$$\cos 2\phi_0 = .999$$

and

$$2\phi_0 = 1 \text{ deg}$$

For $B_L T = .01$ $2\phi_0 = 3.2$.

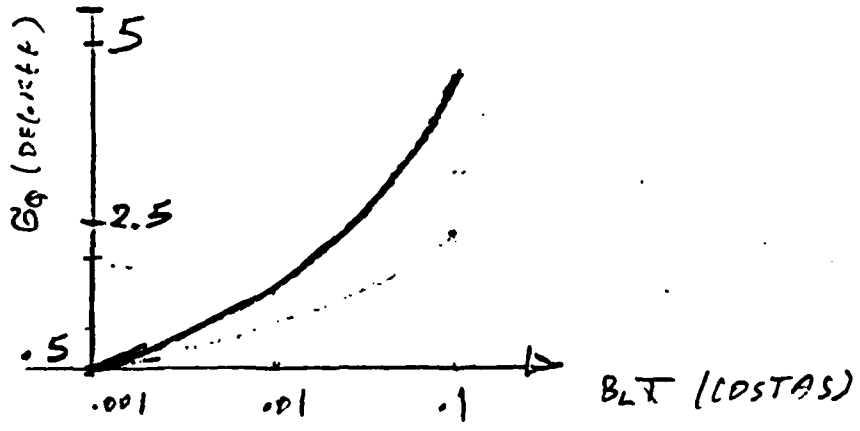

The ISI in the bit sync can be approximately computed by computing the ISI contribution to one bit (worst case)

$$\int_0^T \left[\frac{1}{2}|a| + \frac{1}{2}|a|\right]dt = aT$$

with $B_L T$ as the time bandwidth product of the bit sync

$$\sigma_t < aT\sqrt{B_L T}$$

or

$$\frac{\sigma_t}{T} < a\sqrt{B_L T}$$

If $a = .1$ and $B_L T = .01$, then

$$\frac{\sigma_t}{T} < .01$$

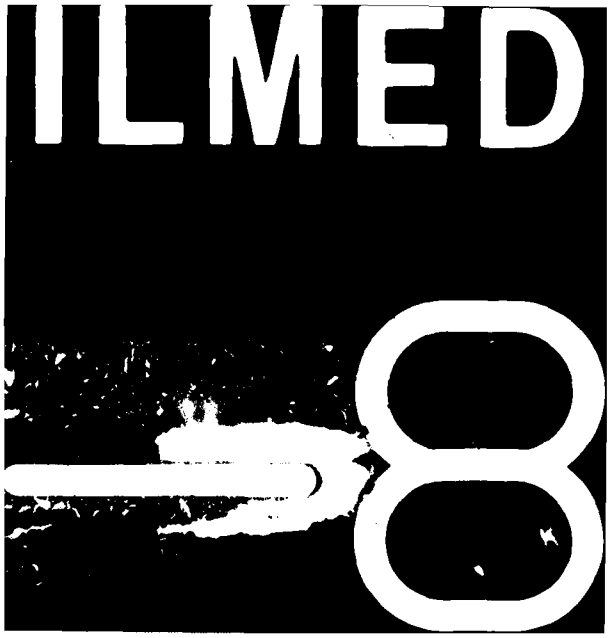
ILMED
8